

**TENSILE PROPERTIES AND RHEOTROPIC BEHAVIOR
OF TITANIUM ALLOYS AND MOLYBDENUM**

E. J. RIPLING

CASE INSTITUTE OF TECHNOLOGY

MAY 1955

MATERIALS LABORATORY
CONTRACT No. AF 33(616)-2223
PROJECT No. 7351

WRIGHT AIR DEVELOPMENT CENTER
AIR RESEARCH AND DEVELOPMENT COMMAND
UNITED STATES AIR FORCE
WRIGHT-PATTERSON AIR FORCE BASE, OHIO

Contrails

FOREWORD

This report was prepared by Case Institute of Technology on USAF Contract AF 33(616)-2223. The contract was initiated under Project No. 7351, "Metallic Materials", Task No. 73510, "Titanium Metal and Alloys", formerly RDO No. 615-11, Titanium Metal and Alloys, and was administered under the direction of the Materials Laboratory, Directorate of Research, Wright Air Development Center, with Lt. G. T. Hahn acting as project engineer.

This report covers work conducted from August 1953 to February 1955.

WADC TR 55-5

ABSTRACT

The unnotched and notched tensile properties are described as a function of testing temperature for a series of titanium-nitrogen, and titanium-manganese binary alloys as well as for the commercial alloy, TI 140A, and the experimental 3 Mn-complex alloy.

It was shown that the nitrogen embrittles alpha titanium by elevating its transition temperature. This brittleness, can be partially eliminated by taking advantage of a rheotropic recovery.

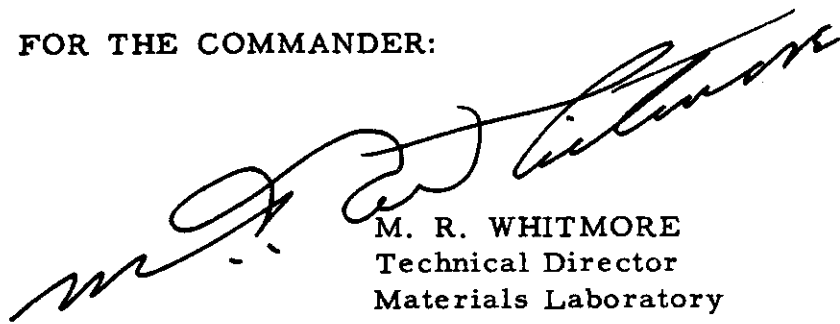
The Ti 140A alloy in the "as-received" condition was high in hydrogen so that a brief investigation of the effect of hydrogen in this alloy was also conducted.

Recrystallization embrittlement in commercial unalloyed molybdenum was found to be a manifestation of rheotropic embrittlement.

PUBLICATION REVIEW

This report has been reviewed and is approved.

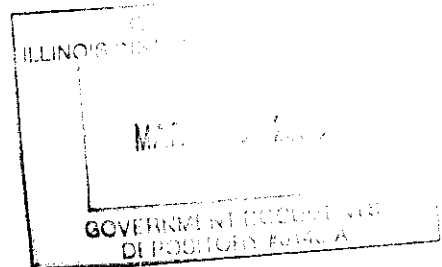
FOR THE COMMANDER:



M. R. WHITMORE
Technical Director
Materials Laboratory
Directorate of Research

WADC TR 55-5

iii



Continental
TABLE OF CONTENTS

	<u>Page</u>
PART I TENSILE AND RHEOTROPIC BEHAVIORS OF TITANIUM-NITROGEN ALLOYS	1
Introduction	1
Material and Procedure	5
Results and Discussion.	8
Unnotched Tensile Properties vs. Testing Temperature	8
Notch Properties vs. Testing Temperature	16
Rheotropic Brittleness in Unnotched Test Bars.	22
Rheotropic Brittleness in Notched Test Bars	27
Rheotropic Recovery Produced by Extruding	28
Conclusions	31
PART II TENSILE AND RHEOTROPIC BEHAVIORS OF TITANIUM-MANGANESE ALLOYS	74
Introduction	74
Material and Procedure	75
Results and Discussion.	76
Conclusions	77
PART III TENSILE AND RHEOTROPIC BEHAVIOR OF A COMMERCIAL AND AN EXPERIMENTAL ALLOY.	88
Introduction	88
Material and Procedure	88
Results and Discussion.	90
Ti 140A Alloy.	90
3 Mn Complex Alloy	96
Conclusions	97

Continued
TABLE OF CONTENTS

(Continued)

	<u>Page</u>
PART IV TENSILE AND RHEOTROPIC BEHAVIOR OF COMMERCIAL UNALLOYED MOLYBDENUM. . .	111
Introduction	111
Material and Procedure	112
Results and Discussion.	112
Conclusions	114
BIBLIOGRAPHY	121

LIST OF TABLES

	<u>Page</u>
Table I Nitrogen Content of Alloys	5
Table II Manganese Content and Annealing Temperatures of Alloys	76
Table III Nominal Compositions of the Commercial and Experimental Alloys, Percent.	89

LIST OF ILLUSTRATIONS

<u>Fig. No.</u>	<u>Page</u>
Figure 1. Test Specimens	32
Figure 2. Microstructure of Vacuum Annealed Titanium- Nitrogen Alloys (Specimen and Applied Stress Axis Vertical)	33
Figure 3. Conventional Stress vs. Contraction in Area for a Variety of Titanium-Nitrogen Alloys	34
Figure 4. Unnotched Tensile Properties vs. Testing Temperature for Unalloyed Titanium	35

Continued
LIST OF ILLUSTRATIONS
(Continued)

<u>Fig. No.</u>		<u>Page</u>
Figure 5.	Unnotched Tensile Properties vs. Testing Temperature for the Titanium - 0.085 Percent Nitrogen Alloy.	36
Figure 6.	Unnotched Tensile Properties vs. Testing Temperature for the Titanium - 0.17 Percent Nitrogen Alloy.	37
Figure 7.	Unnotched Tensile Properties vs. Testing Temperature for the Titanium-0.25 Percent Nitrogen Alloy.	38
Figure 8.	Unnotched Tensile Properties vs. Testing Temperature for the Titanium - 0.33 Percent Nitrogen Alloy.	39
Figure 9.	Unnotched Tensile Properties vs. Testing Temperature for the Titanium - 0.41 Percent Nitrogen Alloy.	40
Figure 10.	Summary of Unnotched Tensile Properties vs. Testing Temperature	41
Figure 11.	Effect of Nitrogen Content on the Transition Temperature.	42
Figure 12.	Cracks Formed in the Vicinity of Fracture on Testing at Room Temperature and +200°F (Specimen and Applied Stress Axis Vertical).	43
Figure 13.	Cracks Formed in Vicinity of Fracture on Testing at Temperatures of +400°F and Above (Specimen and Applied Stress Axis Vertical).	44
Figure 14.	Ductility vs. Nitrogen Content at a Variety of Testing Temperatures	45
Figure 15.	Comparison of Previously Reported Room Temperature Tensile Properties with Those Obtained in the Present Investigation.	46

Continued
LIST OF ILLUSTRATIONS

(Continued)

<u>Fig. No.</u>		<u>Page</u>
Figure 16.	Unnotched Tensile Properties vs. Testing Temperature Curves as Reported by Luster, Wentz, and Catlin	47
Figure 17.	Anisotropy (Ratio of Maximum to Minimum Transverse Strains) of Fractured Specimens vs. Testing Temperature	48
Figure 18.	Appearance of Broken Test Bar of the Titanium - 0.17 Percent Nitrogen Alloy	49
Figure 19.	Notched Tensile Properties vs. Testing Temperature for the Titanium - 0.17 Percent Nitrogen Alloy	50
Figure 20.	Notched Tensile Properties vs. Testing Temperature for the Titanium - 0.25 Percent Nitrogen Alloy	51
Figure 21.	Notched Tensile Properties vs. Testing Temperature for the Titanium - 0.33 Percent Nitrogen Alloy	52
Figure 22.	Notched Tensile Properties vs. Testing Temperature for the Titanium - 0.41 Percent Nitrogen Alloy	53
Figure 23.	Unnotched and Notched Tensile Properties vs. Testing Temperature for Quenched and Tempered SAE 1340 Steel.	54
Figure 24.	Dependence of Heel of Transition on Notch Depth and Nitrogen Content	55
Figure 25.	Notch Ductility and Notch Strength vs Nitrogen Content at a Variety of Temperatures	56
Figure 26.	Notch Strength and Notch Ductility vs. Notch Depth at Room Temperature and -175°F for the Unalloyed Titanium	57

Continued
LIST OF ILLUSTRATIONS
(Continued)

<u>Fig. No.</u>		<u>Page</u>
Figure 27.	Notch Strength and Notch Ductility vs. Notch Depth at Room Temperature for the Titanium - 0.085 Percent Nitrogen Alloy.	58
Figure 28.	Notch Strength and Notch Ductility vs. Notch Depth at Room Temperature for the Titanium - 0.17 Percent Nitrogen Alloy.	59
Figure 29.	Notch Strength and Notch Ductility vs. Notch Depth at Room Temperature, -110°F and -200°F for the Titanium - 0.25 Percent Nitrogen Alloy. . .	60
Figure 30.	Notch Strength and Notch Ductility vs. Notch Depth at Room Temperature, -110°F and -200°F for the Titanium - 0.33 Percent Nitrogen Alloy. . .	61
Figure 31.	Notch Strength and Notch Ductility vs. Notch Depth at +200, Room Temperature and -110°F for the Titanium - 0.41 Percent Nitrogen Alloy. . .	62
Figure 32.	Room Temperature Notch Sensitivity vs. Nitrogen Content	63
Figure 33.	Arrhenius Type Plot of Log b (b [′]) vs. $\frac{1}{T_a}$	64
Figure 34.	Rheotropic Behavior of the Titanium - 0.17 Percent Nitrogen Alloy.	65
Figure 35.	Rheotropic Behavior of the Titanium - 0.25 Percent Nitrogen Alloy.	66
Figure 36.	Schematic Representation Showing the Characteristics and Nomenclatures Applied to Rheotropic Brittleness	67
Figure 37.	Rheotropic Behavior of the Titanium - 0.33 Percent Nitrogen Alloy.	68
Figure 38.	Rheotropic Behavior of the Titanium - 0.41 Percent Nitrogen Alloy.	69

LIST OF ILLUSTRATIONS
(Continued)

<u>Fig. No.</u>		<u>Page</u>
Figure 39.	Rheotropic Behavior of the Titanium - 0.41 Percent Nitrogen Alloy, Prestrained in the Unnotched Condition and Tested in the Notched (35%) Condition.	70
Figure 40.	Rheotropic Behavior of the Titanium - 0.33 Percent Nitrogen Alloy, Prestrained in the Unnotched Condition and Tested in the Notched (35%) Condition.	71
Figure 41.	Rheotropic Recovery Produced in the Titanium - 0.33 Percent Nitrogen Alloy by Extruding	72
Figure 42.	Rheotropic Recovery Produced in the Titanium - 0.41 Percent Nitrogen Alloy by Extruding	73
Figure 43.	Microstructure of Vacuum Annealed Titanium - Mn Alloys	78
Figure 44.	Unnotched Tensile Properties vs. Testing Temperature for Unalloyed Titanium	79
Figure 45.	Unnotched Tensile Properties vs. Testing Temperature for the Titanium - 1.69 Percent Manganese Alloy.	80
Figure 46.	Unnotched Tensile Properties vs. Testing Temperature for the Titanium - 4.68 Percent Manganese Alloy.	81
Figure 47.	Unnotched Tensile Properties vs. Testing Temperature for the Titanium - 5.40 Percent Manganese Alloy.	82
Figure 48.	Unnotched Tensile Properties vs. Testing Temperature for the Titanium - 5.75 Percent Manganese Alloy.	83
Figure 49.	Unnotched Tensile Properties vs. Testing Temperature for the Titanium - 8.0 Percent Manganese Alloy.	84

LIST OF ILLUSTRATIONS

(Continued)

<u>Fig. No.</u>		<u>Page</u>
Figure 50.	Rheotropic Behavior of the Titanium - 5.40 Percent Manganese Alloy.	85
Figure 51.	Rheotropic Behavior of the Titanium - 5.75 Percent Manganese Alloy.	86
Figure 52.	Rheotropic Behavior for Titanium - 8.0 Percent Manganese Alloy.	87
Figure 53.	Microstructure of Vacuum Annealed Ti 140A and 3 Mn Complex Alloys.	98
Figure 54.	Effect of Hydrogen Level on the Tensile Properties of Ti 140A at a Strain Rate of 0.05 in/min.	99
Figure 55.	Effect of Strain Rate on the Ductility of Ti 140A with 310 ppm. Hydrogen	100
Figure 56.	Effect of Strain Rate on the Ductility of Vacuum Annealed Ti 140A	101
Figure 57.	Effect of Strain Rate on the Ductility of Ti 140A with 270 ppm. of Hydrogen.	102
Figure 58.	Fracture Strain of Spherodized SAE 1020 Steel With and Without Hydrogen Embrittlement as a Function of Temperature and Strain Rate (Brown and Baldwin (21))	103
Figure 59.	Ductility of Ti 140A in the As Received (310 ppm of Hydrogen) and Vacuum Annealed Condition vs. Testing Temperature and Strain Rate.	104
Figure 60.	Ductility of Ti 140A in the As Received (270 ppm of Hydrogen) and Vacuum Annealed Condition vs. Testing Temperature and Strain Rate.	105
Figure 61.	Effect of Hydrogen Level on the Ductility of 3 Mn-Complex Alloy at a Variety of Testing Temperatures and Strain Rates (Kotfila and Erbin) (25).	106

Continued
LIST OF ILLUSTRATIONS
(Continued)

<u>Fig. No.</u>		<u>Page</u>
Figure 62.	Room Temperature Notch Properties of Ti 140A With a High and Low Hydrogen Content.	107
Figure 63.	Rheotropic Behavior of the Ti 140A Alloy	108
Figure 64.	Unnotched Tensile Properties vs. Testing Temperature for the 3 Mn-Complex Alloy.	109
Figure 65.	Rheotropic Behavior of the 3 Mn-Complex Alloy . .	110
Figure 66.	Microstructure of Unalloyed Molybdenum.	115
Figure 67.	Unnotched Tensile Properties vs. Testing Temperature for Unalloyed Molybdenum	116
Figure 68.	Unnotched Tensile Properties vs. Testing Temperature for Equiaxed Recrystallized (Fine Grain) Unalloyed Molybdenum.	117
Figure 69.	Unnotched Tensile Properties vs. Testing Temperature for Equiaxed Recrystallized (Coarse Grain) Unalloyed Molybdenum.	118
Figure 70.	Rheotropic Behavior of Equiaxed Recrystallized (Fine Grain) Unalloyed Molybdenum.	119
Figure 71.	Rheotropic Behavior of Equiaxed Recrystallized (Fine Grain) Unalloyed Molybdenum Prestrained at a Variety of Temperatures and Tested at Room Temperature.	120

Contrails

TENSILE AND RHEOTROPIC BEHAVIOR OF
TITANIUM-NITROGEN ALLOYS

INTRODUCTION

One of the major obstacles to a faster growth of the titanium industry results from the deterioration of mechanical properties that is thought to be produced in the titanium base alloys by the interstitial impurities, carbon, nitrogen and oxygen. Because it is difficult to eliminate these harmful contaminants in the processes that presently are being used in titanium production, a considerable amount of research has been undertaken in an attempt to define the influence of these impurities on mechanical behaviors in order to establish safe limits for these interstitials. Jaffee and Campbell (1)*, Finlay and Snyder (2), Jaffee, Ogden and Maykuth (3), as well as Luster, Wentz, and Catlin (4) collectively have described the room temperature static tensile properties, and to a limited extent the sub-room temperature tensile and Charpy impact properties, of sponge and iodide titanium containing carbon, nitrogen and oxygen. These investigators all agreed that the interstitial elements improve the properties which depend on deformation resistance such as hardness, tensile strength, etc. while the ductility dependent properties, elongation and contraction in area in tensile specimens, and toughness

* Numbers in parentheses pertain to the references at the end of this paper.

Continuity

in Charpy specimens were severely harmed. None of these studies however, were sufficiently intensive to describe the manner in which the impurities depressed the ductility. One cannot ascertain from the published literature whether the poor room temperature ductility and toughness associated with the presence of these contaminants result from an elevation of the transition temperature, as is the case for steels, or whether the ductility and toughness levels are lowered under all testing conditions by these interstitials. This question of the mode of embrittlement is one of more than academic interest. The poor sub-transition temperature performance of a number of other metals has been shown to be amenable to a ductility and toughness recovery by properly cold working the metal (5) (6) (7). Consequently, if impurities produce ductility damage by raising the transition temperature in titanium, the allowable impurity limits presently placed on commercial titanium alloys might be increased by overcoming the strain-curable, or rheotropic, brittleness.

The study reported upon herein, consequently, was undertaken in order to: first, determine whether or not the poor ductility produced in titanium by interstitial contaminants is the result of an elevation of the transition temperature of the pure metal which is brought about by the impurities; second, to define how the transition temperature is affected by other mechanical embrittling agents; and finally, to establish whether or not poor sub-transition temperature

Continued
behaviors in these alloys are rheotropic, or strain sensitive.

Of the three common, similar-acting, interstitial impurities -- carbon, nitrogen and oxygen -- nitrogen was used as a prototype of interstitial contamination in this investigation both because of its continuing commercial importance and because of the ease with which it can be alloyed and analyzed for, in titanium.

The three common mechanical embrittling variables, testing temperature, notch severity and strain rate, are usually thought to be related so far as their effects on ductility and toughness are concerned. Those materials that are excessively sensitive to one of these agents are generally sensitive to the other two as well. Since temperature is the most readily controlled of these variables, the tensile properties of the various titanium-nitrogen alloys were defined first as a function of testing temperature. Notch tests were then made on these alloys, in order to correlate room temperature notch and low temperature unnotched behaviors.

Those alloys which exhibited a transition temperature were then further studied in order to detect whether or not sub-transition temperature embrittlement in nitrogen bearing alpha titanium alloys is amenable to a rheotropic recovery. The characteristics of the rheotropic behavior (effect of testing temperature, etc.) were also examined, but primarily in the single alloy whose transition temperature was sufficiently high to allow such a study. In order to

Contrails

determine whether or not cold deformation could be used to overcome notch brittleness, a rheotropic embrittled condition produced by notches, as well as one produced by low temperatures, was also investigated.

Since deformation methods, or stress-states, whose mean stress is compressive, sacrifice ductility at a much slower rate than tensile-stress-state deformations, prestretching was also compared with preextrusion as methods for overcoming rheotropic brittleness.

Controls
MATERIAL AND PROCEDURE

The six titanium-nitrogen binary alloys whose compositions are shown in Table I were prepared as six pound heats by the Battelle Memorial Institute. The sponge base alloys were double melted in an arc furnace under an argon-helium atmosphere. The additions for the nitrogen alloys were made with a master alloy of 2.5 percent nitrogen. After the first melting operation, the ingots were forged at 1450°F, rolled at 1600°F to one-tenth inch sheet, grit blasted, pickled, sheared and remelted. The remelted ingots were forged at 1450°F to 3/4 inch square bar stock, grit blasted, pickled and vacuum annealed to insure a low hydrogen content. After annealing, the stock was rolled to one-half inch rounds at 1600°F. The nitrogen analyses obtained on the rods as supplied by Battelle were checked by an independent laboratory on broken test bars as shown below:*

TABLE I

NITROGEN CONTENT OF ALLOYS

Nitrogen Content As Determined By Alloy Supplier	Nitrogen Content Determined In Check Analysis	
Unalloyed	0.022	0.01
0.085	0.100	0.08
0.17	0.180	0.16
0.25	0.245	0.25
0.33	0.30	0.36
0.41	0.37	0.39

* The alloys are subsequently referred to by their Battelle analysis.

The supplied rods were rough machined to the shapes shown in Fig. 1 (approx. 0.05 inch oversize) after which the specimens were vacuum annealed* at 800°C (1470°F)** for two hours and furnace cooled to insure homogeneity before final machining to the dimensions shown in Fig. 1.

The microstructures of the heads of a number of the broken test bars were examined to determine the structure of the alloys, Fig. 2. Although, in general, the grain size of the alloys decreased as the nitrogen content was increased, the grain size varied considerably within any one alloy. This grain size variation within a single alloy did not noticeably affect the mechanical properties of the alloys.

The microstructures of the two highest nitrogen alloys, 0.33 and 0.41 percent nitrogen, showed some structure that might be a second phase. A diffraction pattern was made on the specimen whose microstructure is shown in Fig. 2f. All the lines in the pattern however could be associated with the alpha titanium. An examination of this specimen under polarized light showed the small globular phase to be optically sensitive indicating that it was not beta.

All tests were made with the aid of a specially designed loading fixture which yielded an eccentricity of less than 0.001 inch. This

* Less than 5×10^{-5} mm. mercury.

** This is well within the all-alpha region.

Contrails

equipment and the straining procedure have been previously described (8). Ductility values were calculated on cylindrical specimens by determining gage lengths and specimen diameters on an optical comparator. The ductility of notched specimens was determined from diameter measurements of the notch bottom before and after testing.

Unnotched Tensile Properties vs. Testing Temperature

The stress-strain characteristics of the alloys were determined only on unnotched specimens tested at room temperature, Fig. 3. Only the unalloyed titanium showed a smooth dependence of conventional stress on strain. All of the other alloys showed at least one jog in its stress-strain curve, and the magnitude of the jog increased as the nitrogen content increased until eventually the 0.41 percent nitrogen alloy showed an upper and lower yield point.

The dependence of unnotched tensile strength, elongation and contraction in area on testing temperature are shown in Figs. 4 to 9 for the binary titanium-nitrogen alloys whose nitrogen contents varied from 0.0 to 0.41 weight percent. These curves are replotted in Fig. 10, in order to facilitate a comparison. A number of striking behaviors are to be seen in these curves, not the least of which is the ability of the alloys to maintain a large portion of the high ductility (both contraction in area and elongation) exhibited by the unalloyed titanium, over a wide temperature range, even in the presence of large amounts of nitrogen.*

- - - - -
* Although this is a sponge base material, the very low room temperature tensile strength (about 52,000 psi) and the very high ductility (60 percent elongation and 76 percent contraction in area) of the unalloyed titanium suggest that this sponge was practically impurity free. Consequently, the added nitrogen in these alloys can be considered as the only contaminant.

Continued

The tensile strength of the alloys behaved in a rather simple fashion, increasing both as the testing temperature was decreased and as the nitrogen content increased. This, of course, is in keeping with previously reported data. Even the highest nitrogen alloy showed an increasing tensile strength with decreasing temperatures in the range of liquid air temperatures, suggesting that the unnotched ductility never becomes appreciably less than the unnotched necking strain.

The ductility, on the other hand, showed a rather complex dependence on both testing temperature and nitrogen content. An unnotched transition temperature became apparent above the temperature of boiling nitrogen in this hexagonal titanium when the nitrogen content was sufficiently high (0.25 weight percent 0.86 atomic percent).* Increasing the nitrogen content from 0.25 to 0.33 percent (an 0.08 weight percent increase) produced an elevation of the transition from -320 to -270°F, Fig. 11. A further nitrogen addition of 0.08 weight percent, increasing the total nitrogen content to 0.41 percent, produced a somewhat larger transition temperature rise, from -270 to -150°F.

- - - - -

* The transition temperature is defined as the heel of the ductility-testing temperature curve throughout this report. This temperature value is chosen as the intersection of the sub-transition branch and the branch of the ductility-testing temperature curve with the most positive slope. The heel rather than the more commonly used knee of the curve is used because the knee was frequently difficult to define as will be shown in a later section. The trends herein reported are independent of the manner in which the transition temperatures are defined.

In addition to the transition temperature embrittlement, which would be expected in this hexagonal metal, a second embrittlement displayed itself, generally at mildly elevated temperatures, as a ductility minimum in both the contraction in area and elongation vs. testing temperature curves, see Figs. 4 to 9.

The occurrence of a ductility minimum at mildly elevated temperatures is not uncommon in metals. This type of behavior has been reported for copper, armco iron, nickel, tungsten, molybdenum, aluminum, lead, zinc, stainless steel, an aluminum-copper alloy, tin, a number of magnesium base alloys, vitalium and even titanium* (6), (9), (10), (11), (12), (13), (14). In spite of the fact that this embrittlement frequently occurs at temperatures at which metals are formed and used, investigations of this ductility depression, especially in non-ferrous metals, are indeed rare. The very limited available data indicate that possibly there are two different mechanisms operative to produce the embrittlement, depending on the metal and the temperature at which the embrittlement is found. All metals, regardless of both the system in which they crystallize, and the presence or absence of alloying elements or impurities, appear to undergo an embrittlement at temperatures just below that at which they recrystallize or flow viscously during testing (15). This behavior is thought to occur because the deformation is restricted to

- - - - -
* Parker reported an embrittlement in titanium at 800°F. (12).

Continued

viscous flow of the grain boundary material at temperatures just below those at which the entire body flows viscously, and above that at which all the material is still in a plastic state. This embrittlement is frequently referred to as "one-half the absolute temperature brittleness" although it may occur over a rather wide range of temperatures depending on the testing condition, grain size of the metal, etc. Strength data are seldom given with these ductility data, but because of the grain boundary fracturing, it seems safe to assume that the embrittlement here is not reflected in strength peaks.* The 800°F embrittlement reported by Parker may be of this type.

Other metals, and in particular steels which showed blue brittleness, also undergo a second type of embrittlement at mildly elevated temperatures. This second type of ductility depression is accompanied by higher-than-normal strength values, and the fractured specimens do not show a high density of intergranular cracks which is thought to be characteristic of the embrittlement described above. This latter embrittlement is considered to be a result of some precipitation phenomenon which accounts for the strength increases. The precipitation is strain accelerated during the test or use of these metals at elevated temperatures.

- - - - -

* In many of these metals, such as zinc, where tensile strength data might be available, the elevated temperature and the transition temperature embrittlement are superimposed so that it is not possible to determine what the strength might "normally" be as a function of testing temperature.

Continued

The embrittlement found at +200°F in the titanium-nitrogen alloys appears to fall into this latter class so far as mechanical behaviors are concerned. The ductility depressions in Figs. 5 to 10 are generally accompanied by higher strength values than would be obtained by extrapolating the tensile strength-testing temperature curves from higher and lower temperatures to the embrittled range*. Further, the embrittlement in these alloys is at too low a temperature to suggest plastic-viscous flow.

The data in Figs. 4 to 10 suggest that there are two types of embrittlement active to produce these curves. The low nitrogen alloys, unalloyed and 0.085 weight percent nitrogen, are embrittled at +400°F in the absence of a strength rise. The higher-nitrogen alloys as well as the 0.085 percent nitrogen alloy, may or may not be continuing to undergo this embrittlement; but in any event, they show a pronounced brittleness with a mild strength rise at about +200°F. Because of the concurrent ductility deficiency and strength peak, this latter embrittlement appears to be a precipitation phenomenon. This implies that stable ϵ must be forming during deformation of alloys with nitrogen contents as low as 0.085 weight percent. As described

- - - - -

* Although the strength increases in the temperature range of the embrittlement are mild, they appear to be sufficiently consistent in all the alloys to indicate their existence. The anticipated tensile strength-testing temperature curves in the absence of the +200°F embrittlement are shown by the thin curves in Figs. 5 to 9.

above, a second phase was found microscopically in the 0.33 and the 0.41 percent nitrogen alloy specimens, see Fig. 2-e and -f, but the second phase could not be identified.

Because this +200°F brittleness occurred at a temperature range in which specimens would normally be prestrained for the rheotropic study, the microstructures of a few specimens tested in this temperature range were examined. As shown in Fig. 12, fracturing at room temperature and at +200°F is accompanied by an enormous number of intergranular cracks, suggesting that the fracturing is almost entirely restricted to the grain boundaries. The density of these one-grain-long cracks is enormous in the region of the main separation, indicating that fractures are readily nucleated in this temperature range. The ductility in this region (see Fig. 10) is depressed to a value less than one-half of that which would be expected in the absence of the embrittlement suggesting that the cracks do not grow any easier at this temperature than they do above or below the embrittling temperature.

At temperatures above that of the ductility depression (+400°F and above) the method of crack formation was different from that described above. At these elevated temperatures, voids, whose major axes were parallel with the specimen axes, appeared to form around small volumes of metal. These voids grew into spheres until they isolated the enclosed volumes from the applied stress,

Fig. 13. It is difficult to rationalize the occurrence of this type of void, especially since the cracks appear to form and grow in a direction parallel to that of the applied load, see Fig. 13.

Also above the +200°F embrittled range, the contraction in area increased with temperature while the elongation decreased. A behavior of this type requires a drop in strain hardening exponent with increasing temperatures. Rosi, Perkins and Seigle (16) have shown that the deformation mechanism for titanium is a function of the straining temperature, and further suggest that the deformation mechanism is not affected by the nitrogen or oxygen content. A change in deformation mechanism above and below +400°F could account for the change in strain hardening exponent.

It is interesting to note that although increasing nitrogen contents in titanium alloys are considered detrimental to ductility, there was only a limited testing temperature range (at low temperatures) where this appeared to be valid. As shown in Fig. 14, any nitrogen increase was harmful at -321°F. At temperatures of room temperature and above, nitrogen additions were desirable within the range of 0.1 to 0.3 percent nitrogen in respect to both strength and ductility. An 0.25 percent nitrogen alloy had an elongation of about 50 percent and a contraction in area of about 60 percent with a tensile strength of about 60,000 psi at +400°F while at this temperature the unalloyed titanium had an elongation of about 40 percent, a

contraction in area of about 55 percent, and a tensile strength of 30,000 psi.

The data obtained on this project are compared with that previously reported by other investigators on titanium-nitrogen alloys in Figs. 15 and 16. The continuous ductility drop with increasing nitrogen content on room temperature tensile testing previously reported on iodide titanium is different from that found here, see Fig. 15. These earlier investigations presumably did not include sufficiently high nitrogen contents to find the ductility recovery. The transition just below room temperature, Fig. 16, found by Luster, Wentz and Catlin (4) on an 0.2 percent nitrogen alloy is higher than that which would be expected on the basis of the present data. However, the unalloyed sponge used by these authors had a tensile strength of 65,000 psi indicating that nitrogen was probably not the only contaminant in their alloy.

The specimens tested in these alloy series showed a rather large amount of flow anisotropy. The magnitude of the anisotropy (measured as the ratio of the maximum and minimum transverse strains) is shown as a function of the testing temperature for the alloys in Fig. 17. Only the unalloyed and 0.085 percent nitrogen alloys were found to show an unambiguous dependence of anisotropy on the testing temperature.

The anisotropy displayed itself in two different fashions. Some

of the specimens, whose cross-section was initially circular, deformed to form ellipses while others deformed to diamond shapes as shown by the photograph of fractured specimens in Fig. 18. The open circles labeled two-fold symmetry in Fig. 17 formed ellipses on straining while the closed circles, labeled four-fold symmetry, formed diamonds.

Notch Properties vs. Testing Temperature

Notched tests were also conducted at a variety of testing temperatures on those alloys for which the ductility-testing temperature curve had a positive slope at -321°F as shown in Figs. 19, 20, 21 and 22. The introduction of a notch elevated the transition temperature in these alloys somewhat less than that which might be expected in a steel. SAE 1340 quenched and tempered at 700°F showed a smooth specimen contraction in area-testing temperature curve much like that presented above for the 0.25 percent nitrogen alloy, compare Figs. 23 (17), and 20. The introduction of a ten percent notch to these steel specimens elevated the temperature of the heel of the transition curve from approximately -300°F to $+450^{\circ}\text{F}$, as compared with an elevation from -320°F to about $+170^{\circ}\text{F}$ for the 0.25 percent nitrogen titanium alloy. The dependence of the transition temperature on notch severity for these hexagonal alpha titanium alloys is compared with that for body centered-cubic steel in

Fig. 24a. Since body-centered-cubic chromium (18) is also excessively notch sensitive compared with hexagonal zinc (19) and magnesium (14), it is suggested that this latter class of metals, in spite of frequent high unnotched transition temperatures, is in a class between that of body-centered-cubic and face-centered-cubic metals so far as notch sensitivity is concerned.

The elevation of the transition temperature produced by the introduction of a notch is shown as a function of the nitrogen content in Fig. 24b. The higher the nitrogen content (and hence the higher the unnotched transition temperature, see Fig. 11) the less the transition temperature was moved on notching the specimen.

One other striking feature of these notch curves, Figs. 19 to 22, is the very slow rate at which the notch ductility decreases with decreasing temperatures in the sub-transition range. Although the 0.25 percent nitrogen alloy shows ten and thirty-five percent notch transition temperatures at about $+200^{\circ}\text{F}$, the ductility is not excessively low, even at -321°F .

The notch strength* is also shown as a function of the testing temperature in Figs. 19, 20, 21 and 22. Notch strength is frequently used as a criterion of notch sensitivity in place of ductility, because it is more readily measured, and under certain conditions reflects the notch ductility behavior.

- - - - -
* Notch strength is defined as the ratio of the maximum load to the original cross-sectional area at the notch bottom.

Since the necking strain is thought to be independent of the tri-axiality,* the notch strength can be written as:

$$\text{Notch Strength} = \text{Unnotched Tensile Strength} \left[1 + 0.01 \left(\frac{\text{notch depth}}{\text{in percent}} \right) \right]$$

- - - - - [1]

so long as the notch ductility exceeds the necking strain of the material. It is only when the notch ductility becomes less than the necking strain, and no longer obeys the above equation that the notch strength reflects ductility and can be used as a notch sensitivity criterion. The calculated notch strength curves based on the above equation are shown in Figs. 19 to 22 along with the data points. So long as the ductility is high, the data points fall very close to the calculated curve, Fig. 19 and 20. Only for the two highest nitrogen alloys does the ductility loss influence the notch strength behaviors. The shaded area has been added to these charts between the experimental and calculated curves in order to represent the loss in strength due to notch ductility deficiencies. Because of the very gentle ductility drop below the transition temperature for the 0.25 percent nitrogen alloy, the data points for notch strength continue to fall on the calculated curve even at -321°F. The 0.33 percent alloy shows somewhat lower sub-transition ductility than the 0.25 percent nitrogen alloy so that a mild degree of notch strength lowering is

- - - - -
 * Which appears to be the case for steel at least.

Contrails

found in the 35 percent notches at sub-room temperatures. Only for the 0.41 percent nitrogen alloy were the sub-transition temperature ductilities sufficiently low to produce a severe lowering of the notch strength, Fig. 22.

The notch strength and notch ductility (35 percent notch) are shown as a function of the nitrogen content in Fig. 25 for a variety of testing temperatures. The continuous depression of unnotched ductility produced by nitrogen additions found at a testing temperature of -321°F (see Fig. 14) persists in the notched ductility--nitrogen content curves to testing temperatures even as high as $+200^{\circ}\text{F}$. This is not surprising since high nitrogen additions produced the poor unnotched ductilities at -321°F by the development of a transition temperature. Notching the specimens elevates the transition temperature so that the unnotched behavior found at liquid air temperatures is similar to notched behaviors in the vicinity of room temperature or slightly above.

In other investigations on the notch properties of metals by the author, it was shown that the notch ductility vs. notch depth curves for metals all belong to a single family of hyperbolae (20).* The family

* In the following discussion of notch property-notch depth curves, only the effect of notch depth on notch ductility is discussed because the notch strength is a simple function of the notch depth as given by eq. [1]. The calculated notch strengths are added to Figs. 26 to 31 as thin straight lines.

is described by the equation:

$$\text{Notch Ductility} = \frac{(b) (\text{unnotched ductility in percent})}{(b) + (\text{notch depth in percent})} \text{ --- [2]}$$

"b" in the above equation is a constant for a given material. Graphically it is a measure of the distance between the experimental ordinate axis, (zero notch depth) and some ordinate axis in the second quadrant (negative notch depths) that the experimental hyperbola approaches. As shown in the earlier study, the logarithm of b, which will be referred to a b', is not only an excellent measure of notch insensitivity* but also seems to be simply related to other inherent properties of metals.**

Curves relating the notch ductility to the notch depth for a variety of testing temperatures are shown for these alloys in Figs. 26 to 31. For those curves in Figs. 26 to 31 for which sufficient data were available, the b values were calculated from the data points. For those curves in which only a few data points were available the values of b were calculated from the shape of the curve itself. These values of b were converted to b' values in order to

* Physically "b" measures the loss in unnotched ductility produced by the introduction of the notch. Small values of b mean the vertical branch of the hyperbola relating notch ductility and notch depth is slightly to the left of the ordinate while large values of b represent hyperbolae whose vertical branch is far into the second quadrant. Consequently, notch insensitivity increases as b' increases.

** For example b' was found to be a linear function of the unnotched strain hardening exponent for face-centered-cubic metals.

determine the dependence of room temperature notch sensitivity on nitrogen content, Fig. 32, and the notch sensitivity testing temperature relationship for all of the alloys, Fig. 33. The room temperature notch sensitivity increases linearly with nitrogen content, see Fig. 32, so that the dependence of notch sensitivity on nitrogen content can be written as:

$$b' = 1.3 - 2.4 (\text{nitrogen content in percent}) \dots \dots \dots [3]$$

The plot of log b vs. 1/T curves for each of the alloys also resulted in one or two straight lines, see Fig. 33. These linear relationships considerably simplify the description of the dependence of notch sensitivity on testing temperature. It was surprising to find that increasing the testing temperature above ambient values increased the notch sensitivity for all the titanium-nitrogen alloys as well as the steels whose properties are shown in Fig. 23, at about the same rate. This relationship between notch insensitivity and testing temperature is described by the equation:

$$b' = C + \frac{M}{T_a} \dots \dots \dots [4]$$

- where b' = notch insensitivity
- C = Constant
- M = Constant
- T_a = Absolute Temperature

These are hyperbolae with asymptotes at the (b' -c) and T_a axes.

Above room temperature, "M" is equal to approximately -8 x 10⁻²

while C is a function of the composition. Below room temperature, both "M" and "C" are highly material dependent. Notch properties are harmed by low testing temperatures at a rate that increases as the nitrogen content is increased. The 0.17 percent nitrogen alloy has a notch ductility that is not affected by testing temperature below ambient values while the unalloyed titanium actually becomes more notch insensitive as the testing temperature is lowered in this testing range.

Rheotropic Brittleness in Unnotched Bars

After having established the effect of testing temperature and notch severity on the tensile properties of the alloys, it became possible to study their rheotropic behaviors. Since only the two lowest nitrogen alloys (unalloyed and 0.085 percent) did not show ductility testing temperature curves with a positive slope at low temperatures, rheotropic studies were conducted on all of the alloys except these.

In spite of the fact that the 0.17 percent nitrogen alloy lost ductility as the testing temperature was lowered, it never underwent an abrupt ductility loss as the temperature decreased, see Fig. 19, so that it cannot be considered as showing a transition temperature above the temperature of boiling nitrogen. This ductility drop was nevertheless investigated by prestretching a few unnotched specimens at room temperature after which the specimens were further strained

in tension to failure at -321°F. As shown in Fig. 34, the prestrain vs. retained ductility relationship for this alloy can be described by the equation:

$$\left(\frac{\epsilon_r}{\epsilon_B}\right)^m + \left(\frac{\epsilon_p}{\epsilon_A}\right)^n = 1 \text{ * } \text{-----} [5]$$

- where ϵ_r = retained ductility in second straining operation
- ϵ_p = prestrain
- ϵ_B = fracture ductility at the temperature of second strain
- ϵ_A = fracture ductility at the temperature of first strain
- m and n = exponents which are thought to have a value of unity in the absence of strain aging and other second order effects

An adherence to this equation indicates an absence of rheotropic brittleness (5). Since ductility deficiencies resulting from transition temperature behaviors are thought to be strain curable, or rheotropic, the mechanism which produces the ductility loss in this alloy at low temperatures must be different from that which is effective at the transition temperature.

* Earlier investigations of the rheotropic behavior of other metals have shown the behaviors to be best described by defining the ductility in terms of natural or logarithmic strain which is defined as:

$$\epsilon = \ln \frac{A_0}{A_f}$$

- A_0 = cross sectional area before straining
- A_f = cross sectional after fracturing

The natural strain can be derived directly from contraction in area measurements by use of the relation:

$$\epsilon = \ln (1-q)$$

q = contraction in area divided by 100

Prestretching the 0.25 percent nitrogen alloy at room temperature followed by a tensile test at -321°F produced a rheotropic recovery. The retained ductility vs. prestrain curve was made up of three branches, the metastable, transition, and stable branches, Fig. 35, similar to the behavior normally found in rheotropically embrittled metals.*

* On the basis of studies on rheotropic brittleness in steels and zinc, the following characteristics of retained ductility vs. prestrain (tension) curves of the type schematically shown in Fig. 36 might be listed.

1. The metal at a sub-transition temperature suffers some impediment which is stable at small prestrains so that the retained ductility decreases with small prestrains in a normal fashion over this metastable range.
2. Prestrains beyond those in the metastable range partially overcome the impediment so that the ductility increases with prestrain over some range of strains. This branch of the ϵ_r vs. ϵ_p curve has been labeled the transition branch.
3. Prestraining beyond the transition branch again results in a decreasing retained ductility with prestrain. This is thought to be a stable behavior. In the absence of secondary effects, such as aging, the stable curve is described by eq. [5] with exponents of unity, and a value of ϵ_B equal to the unimpeded ductility at the testing, or second straining temperature.
4. The magnitude of prestrains over which the metastable and transition branches of the curve exist, are a function of the second straining temperature only. The lower this temperature, in relationship to the transition temperature, the longer are these branches.
5. The metastable and transition branches of the ϵ_r vs. ϵ_p curves are independent of the prestraining temperature while the stable branch of the curve is a function of the prestraining and testing temperature as described in footnote 3 above.

An extrapolation of the stable portion of the curve in Fig. 35 to zero prestrain yielded a value for unimpeded ductility equal to that which would have been obtained if the ductile branch of the ductility-testing temperature curve had been extrapolated to this same temperature, see Fig. 7. This behavior of course, is also consistent with that previously reported for other metals.

Tensile prestraining at room temperature also produced a rheotropic recovery at -321°F in the 0.33 percent nitrogen alloy, Fig. 37. The magnitude of the prestrain necessary to produce the stable behavior, however, was close to the prestrain ductility of the metal, see Fig. 8, so that the magnitude of the recovery was small. In order to make larger prestrains possible, another group of specimens were stretched at $+400^{\circ}\text{F}$ before testing them at -321°F . As shown in Fig. 37, elevating the prestraining temperature produced much larger values of retained ductility at -321°F . The metastable and transition branches of curves of the type shown in Fig. 37 are thought to be independent of the prestraining temperature (so long as the metal is cold worked). The 0.33 percent nitrogen alloy showed rheotropic recovery at much smaller strains at elevated temperature than at room temperature. This unexpected behavior could result from either the different type of micro-cracks formed on stretching at room temperature as compared with those formed at $+400^{\circ}\text{F}$ as discussed above, or from the apparent difference in deformation

mechanisms at the two prestraining temperatures. Nevertheless, pre-stretching at +400°F doubled the ductility at -321°F while the tensile strength was increased approximately ten percent. The -321°F tensile strength of the specimens prestrained at +400°F is considerably lower than those prestrained at room temperature. This would imply that at least a portion of the higher ductility developed on +400°F prestraining resulted from an overaging effect.

The 0.41 percent nitrogen alloy exhibited an unnotched sub-transition temperature behavior even at room temperature, and probably at +200°F as well.* Consequently, specimens of this alloy were prestrained at +400°F and subsequently tested at room temperature and at +200°F. As shown in Fig. 38 prestraining at +400°F and testing at either of these temperatures yielded a rheotropic recovery. The unimpeded ductility at zero prestrain, obtained from the extrapolation of the stable branch of these curves to zero prestrain, is higher for the +200°F data than for the room temperature testing data. Further, these extrapolated values are sufficiently high to indicate that the +200°F embrittlement shown in Fig. 9 is not apparent in these tests. Although the scattering in room temperature test data is rather severe, it does not appear to require more prestraining to produce a stable behavior at room temperature than it does at +200°F.

- - - - -

* As stated above, it was not possible to detect the minimum super transition temperature in this alloy because of the superimposed +200°F brittleness.

Contrails

Actually the opposite appears to be the case here.

Rheotropic Brittleness in Notched Test Bars

It was shown above that the introduction of a notch to these tensile bars produces notch embrittlement by raising the transition temperature of the metal. Consequently poor static notched tensile performance should be amenable to an improvement by prestraining in the unnotched state before testing in the notch condition. By the use of an unnotched specimen in prestraining and a notch bar in testing the transition temperature can be crossed between the first and second straining operations, even though both of these straining operations are conducted at the same temperature.

Only the 0.41 percent nitrogen alloy became excessively brittle at room temperature with notches whose depth was 35 percent. Consequently, most of the attempts to eliminate rheotropic brittleness in notched bars were conducted on this alloy.

Prestretching smooth tensile bars at room temperature followed by room temperature notch testing did produce a rheotropic recovery in this alloy as shown in Fig. 39. The unworked ductility of about $\epsilon_r = 0.008$ was almost tripled by unnotched prestretching to an $\epsilon_p = 0.06$. Along with this ductility improvement there was, of course, an appreciable notch strength increase. The strength increase would be expected, of course, both because of strain hardening in prestraining,

Contrails

and because the ductility is increased.

The magnitude of the maximum possible prestrain at room temperature was rather small (about $\epsilon_p = 0.26$, see Fig. 9). Consequently other groups of specimens were prestretched at +400 and +600°F. The notch ductility after prestraining at +400°F was quite low. Presumably this was an aging effect. Prestretching at +600°F again yielded high values of notch ductility. At this higher prestraining temperature, the material apparently overaged.

A few unnotched specimens of the 0.33 percent nitrogen alloy were also prestretched at +600°F followed by room temperature notch testing, Fig. 40. Here again, the material showed a ductility recovery, but because the magnitude of prestrains were rather closely bunched, the shape of the retained ductility-prestrain curves could not be determined accurately.

Rheotropic Recovery Produced by Extruding

Unfortunately, increasing tensile prestrains continuously exhaust the ductility of metals even in the absence of rheotropic embrittlement. Because the ductility sacrifice on prestraining is proportional to the metal's ductility under the prestraining conditions, as described by equation [5], prestraining under a stress state whose mean stress is compression can produce large deformations with only slight ductility sacrifices. Consequently, rods of the type shown in

Fig. 1 of the 0.33 and 0.41 percent nitrogen alloy were extruded at +600°F through a small angle conical die (7° one-half die angle) to approximately a 56 percent reduction. The extruded rods were then stress-relieved at 800°F for one hour, after which test pieces were machined from the extruded bars. Because the rod diameters before extruding were limited to somewhat under one-half inch, these test bars had to be made quite small, see Fig. 1.

The unnotched properties of the extruded 0.33 percent nitrogen alloy are shown as a function of testing temperature in Fig. 41, along with the curves obtained on the annealed material. Extruding did not appreciably change the contraction in area on subsequent testing at super transition temperatures, but the elongation was considerably reduced while the tensile strength was raised at these temperatures. At sub-transition testing temperatures, the contraction in area was appreciably raised, the elongation unchanged, and the tensile strength increased.

As discussed above, only the 0.41 percent nitrogen alloy exhibited an unnotched sub-transition behavior at room temperature. Extruding this alloy about 56 percent at +600°F produced remarkable ductility (contraction in area) improvements in the alloy between -110°F and +400°F, Fig. 42. These high contraction in area values were accompanied by depressed values of elongation and high tensile strengths.

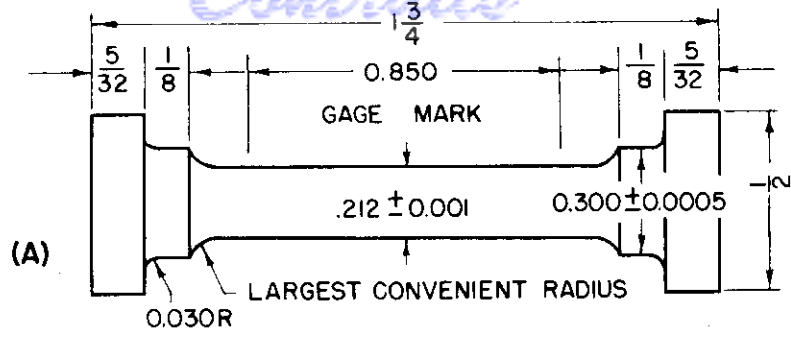
Contrails

A few notched tests were also conducted on extruded 0.33 percent and 0.41 percent nitrogen bars, but the ductility recovery here was small.

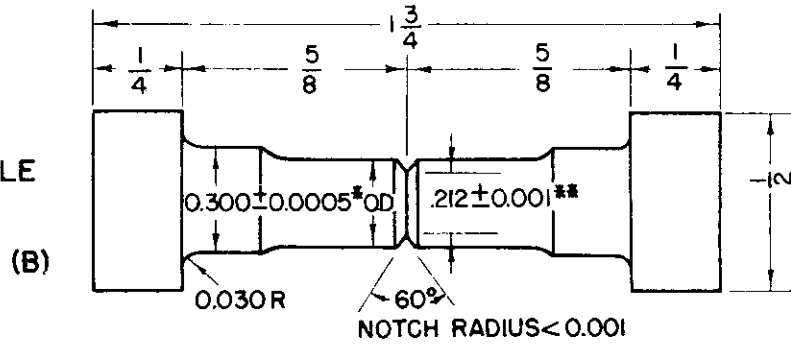
Continuity
CONCLUSIONS

1. The poor ductility associated with nitrogen contamination in alpha titanium is a result of an elevation of the transition temperature of the titanium by the introduction of the contaminant.
2. In addition to the transition temperature embrittlement, a second elevated temperature brittleness displayed itself at about +200°F.
3. Increasing nitrogen contents do not continuously lower the unnotched tensile ductility of titanium except at very low testing temperatures.
4. Notch embrittlement is a result of an elevation of the transition temperature by the introduction of the notch.
5. Sub-transition temperature embrittlement is amenable to a rheotropic recovery whether the embrittlement is produced by low temperatures or notches.
6. A prestrain stress state whose mean stress is compression is most effective in relieving rheotropic brittleness.

BUTTON-HEAD UNNOTCHED SPECIMEN

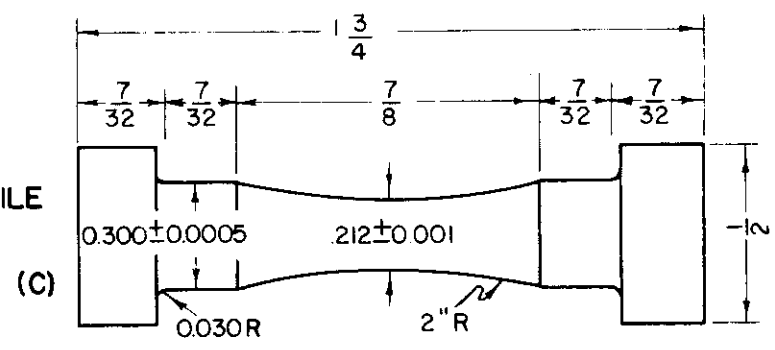


NOTCHED TENSILE SPECIMEN

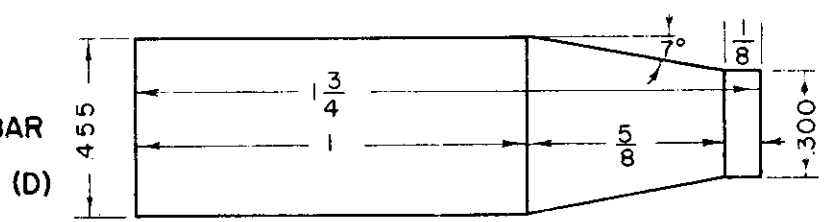


* O.D. VARIABLE
 ** THIS DIMENSION SMALLER ON PRESTRAIN BARS

PRESTRAIN TENSILE SPECIMEN



EXTRUSION BAR



TEST SPECIMEN

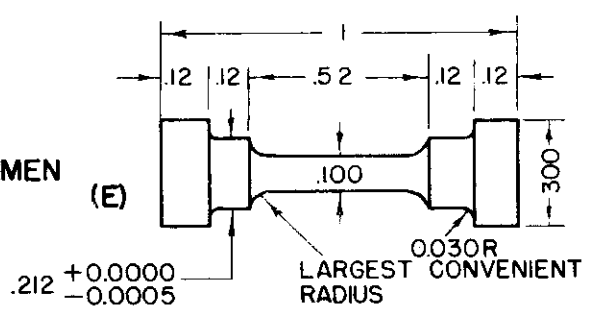
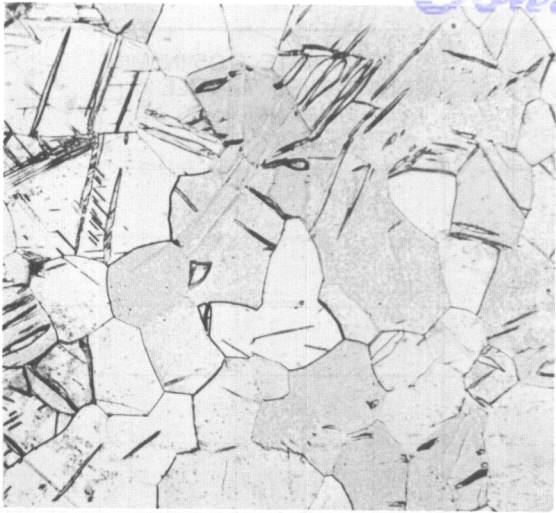
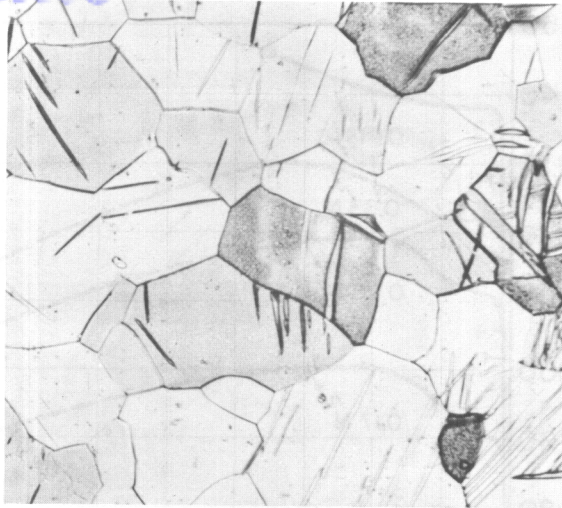


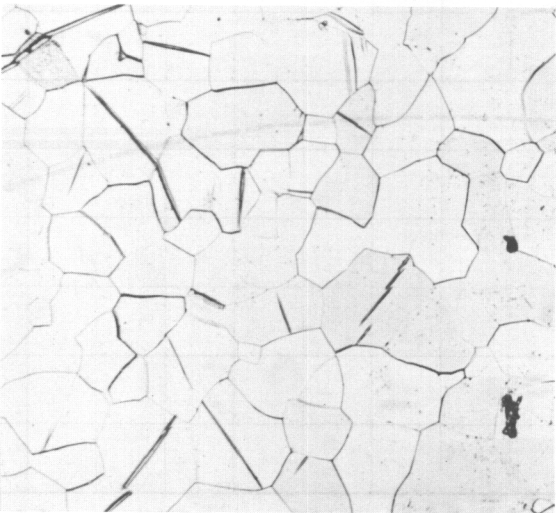
FIG. 1 TEST SPECIMENS.



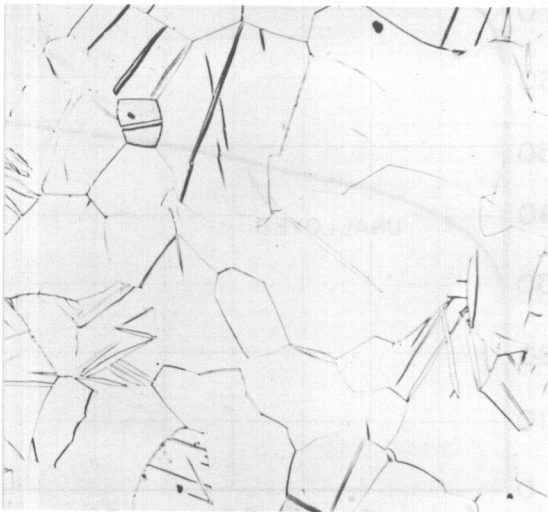
A) UNALLOYED TITANIUM



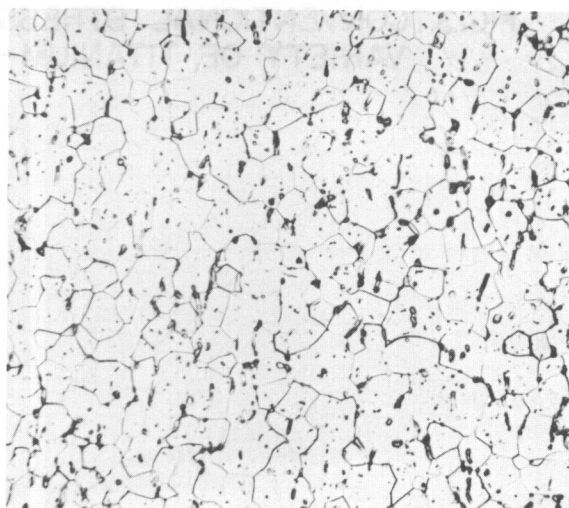
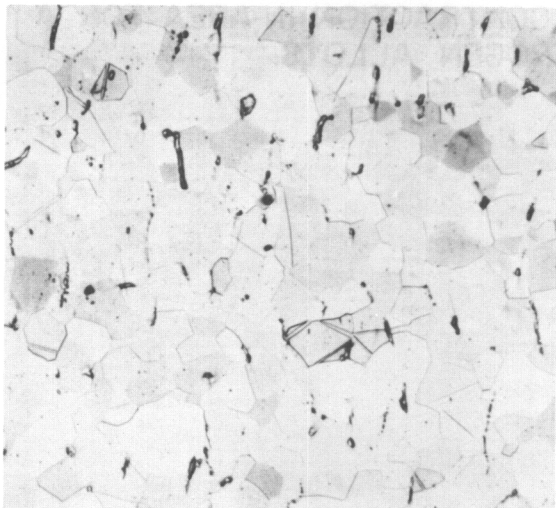
B) .085 N



E) .33 N



F) .41 N



250X

ELECTROLYTIC POLISH. ETCHANT: 1 PART HF - 1 PART HNO₃ - 6 PARTS GLYCERINE.

FIG.2: MICROSTRUCTURE OF VACUUM ANNEALED TITANIUM-NITROGEN ALLOYS (SPECIMEN AND APPLIED STRESS AXIS VERTICAL).

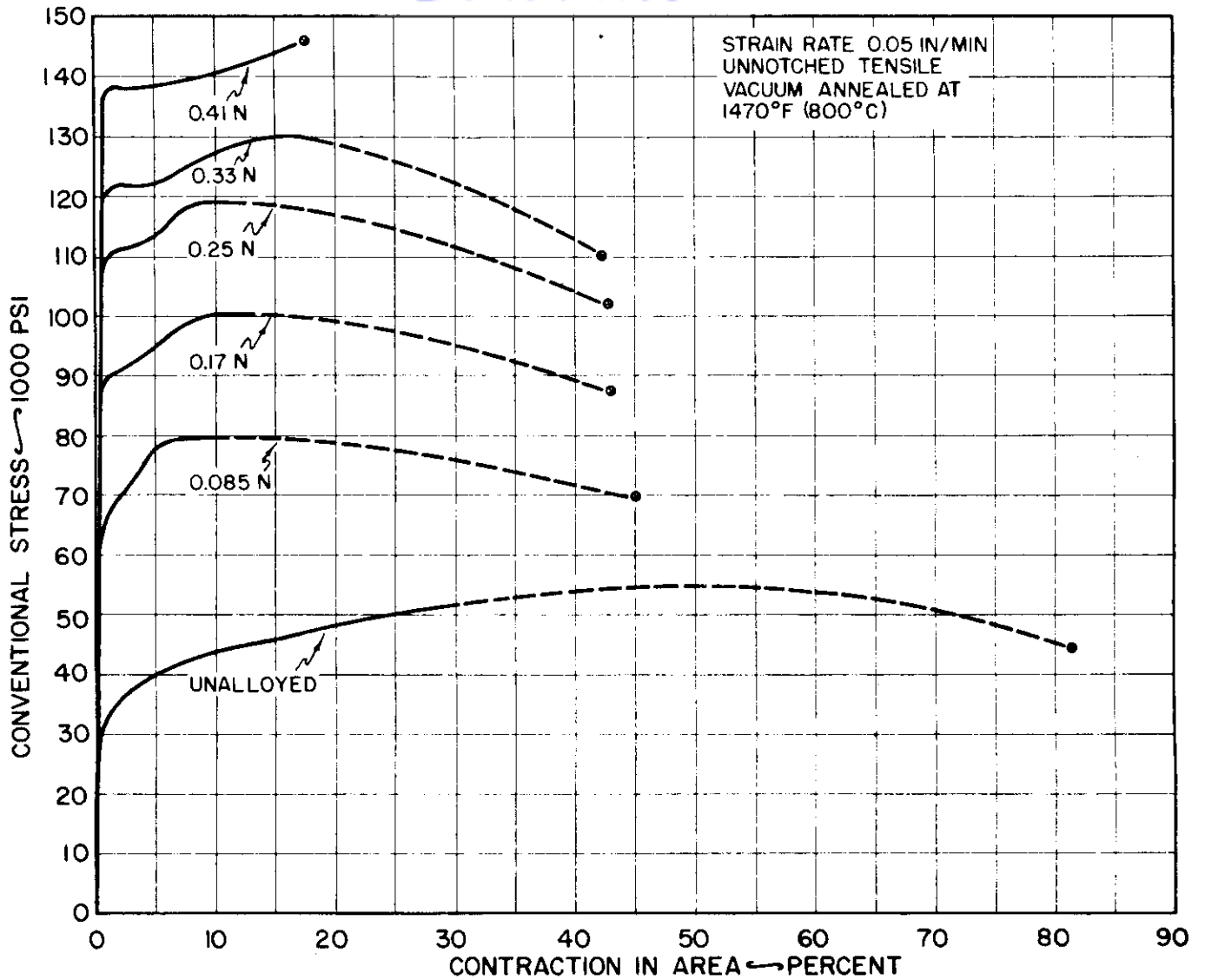


FIG.3 : CONVENTIONAL STRESS vs. CONTRACTION IN AREA FOR A VARIETY OF TITANIUM-NITROGEN ALLOYS.

Contractile

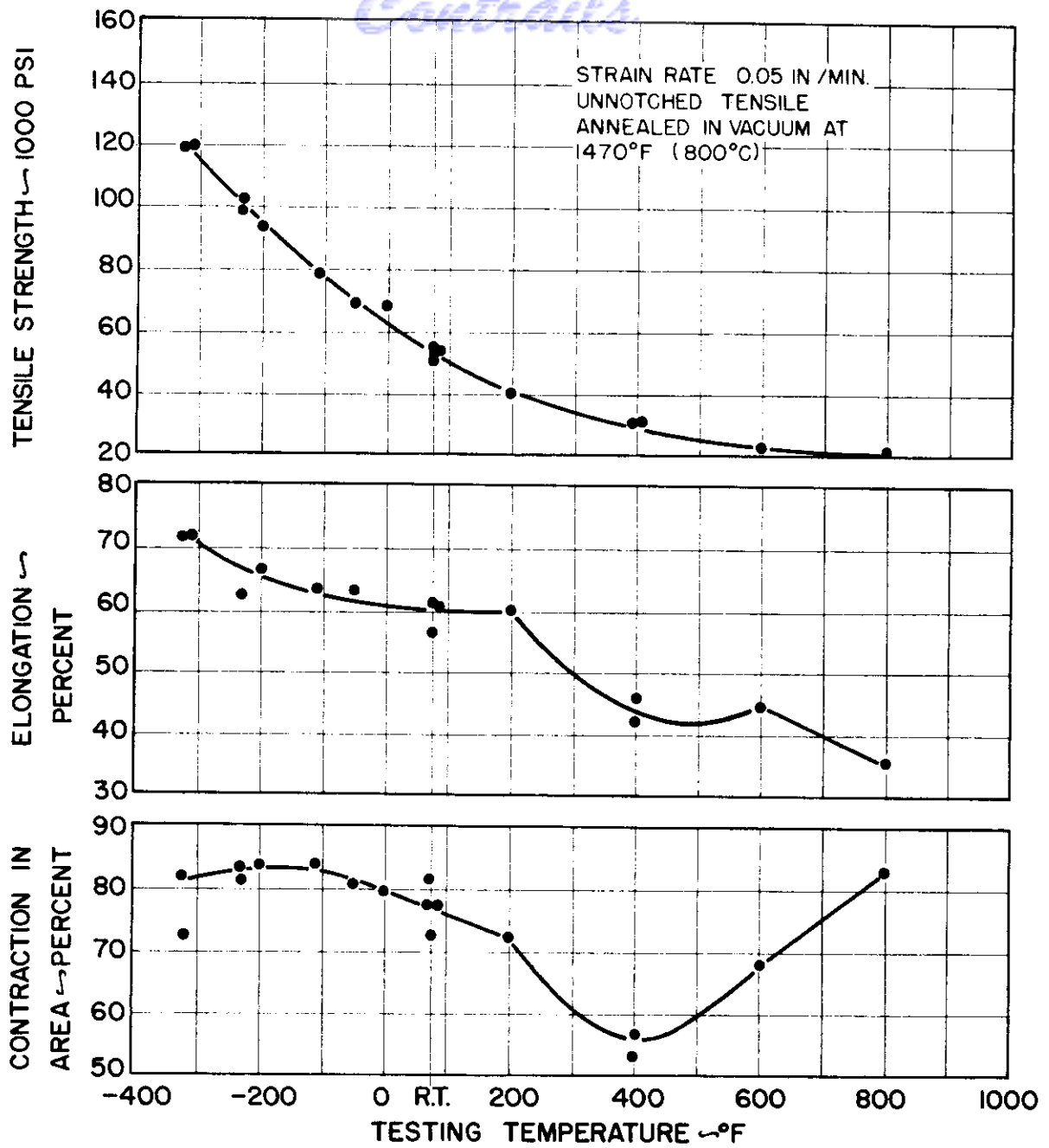


FIG. 4 : UNNOTCHED TENSILE PROPERTIES vs. TESTING TEMPERATURE FOR UNALLOYED TITANIUM.

Contrails

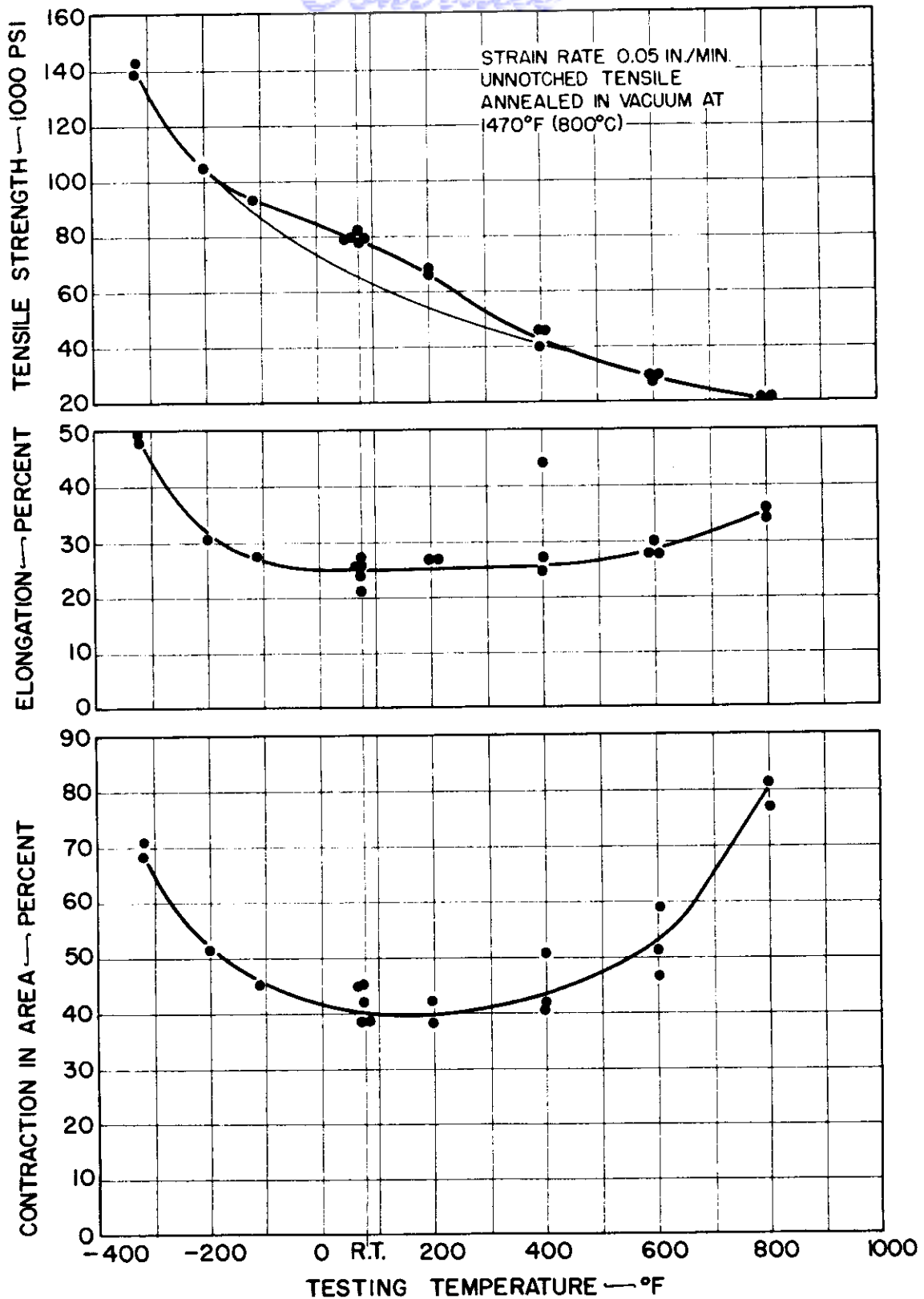


FIG.5 : UNNOTCHED TENSILE PROPERTIES vs. TESTING TEMPERATURE FOR THE TITANIUM-0.085 PERCENT NITROGEN ALLOY.

Controls

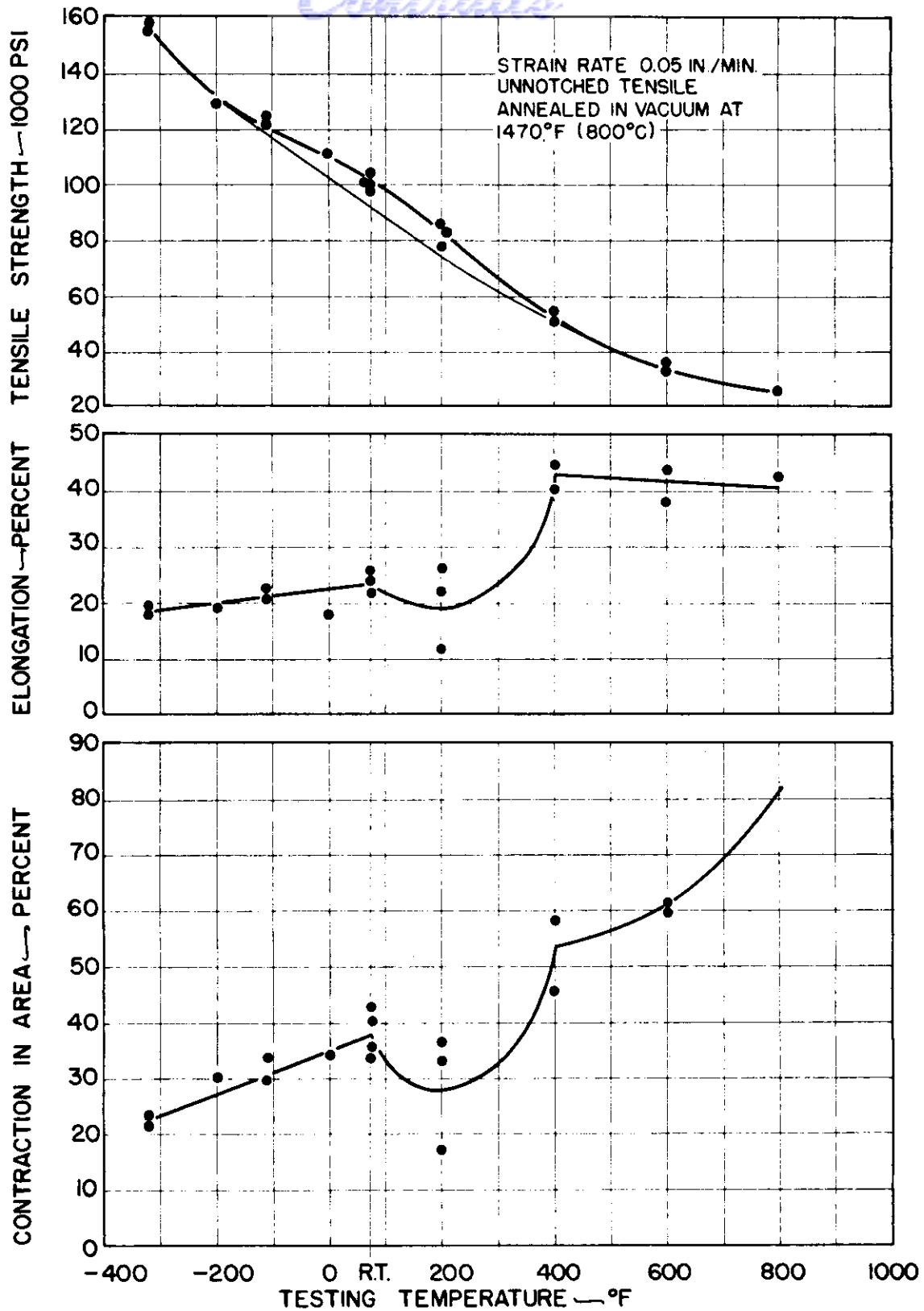


FIG.6: UNNOTCHED TENSILE PROPERTIES vs. TESTING TEMPERATURE FOR THE TITANIUM-0.17 PERCENT NITROGEN ALLOY.

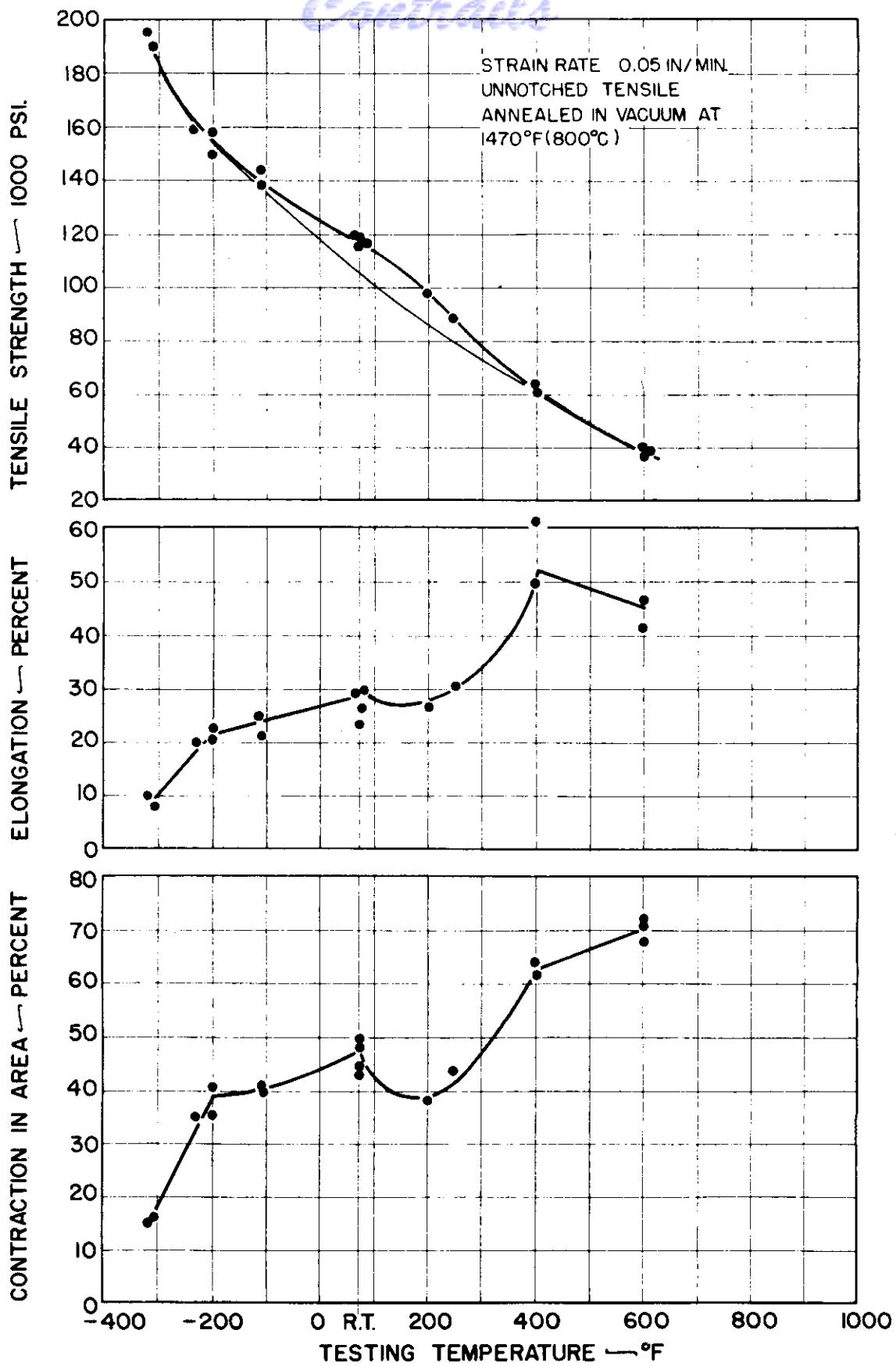


FIG.7: UNNOTCHED TENSILE PROPERTIES vs. TESTING TEMPERATURE FOR THE TITANIUM-0.25 PERCENT NITROGEN ALLOY.

WADC TR 55-5

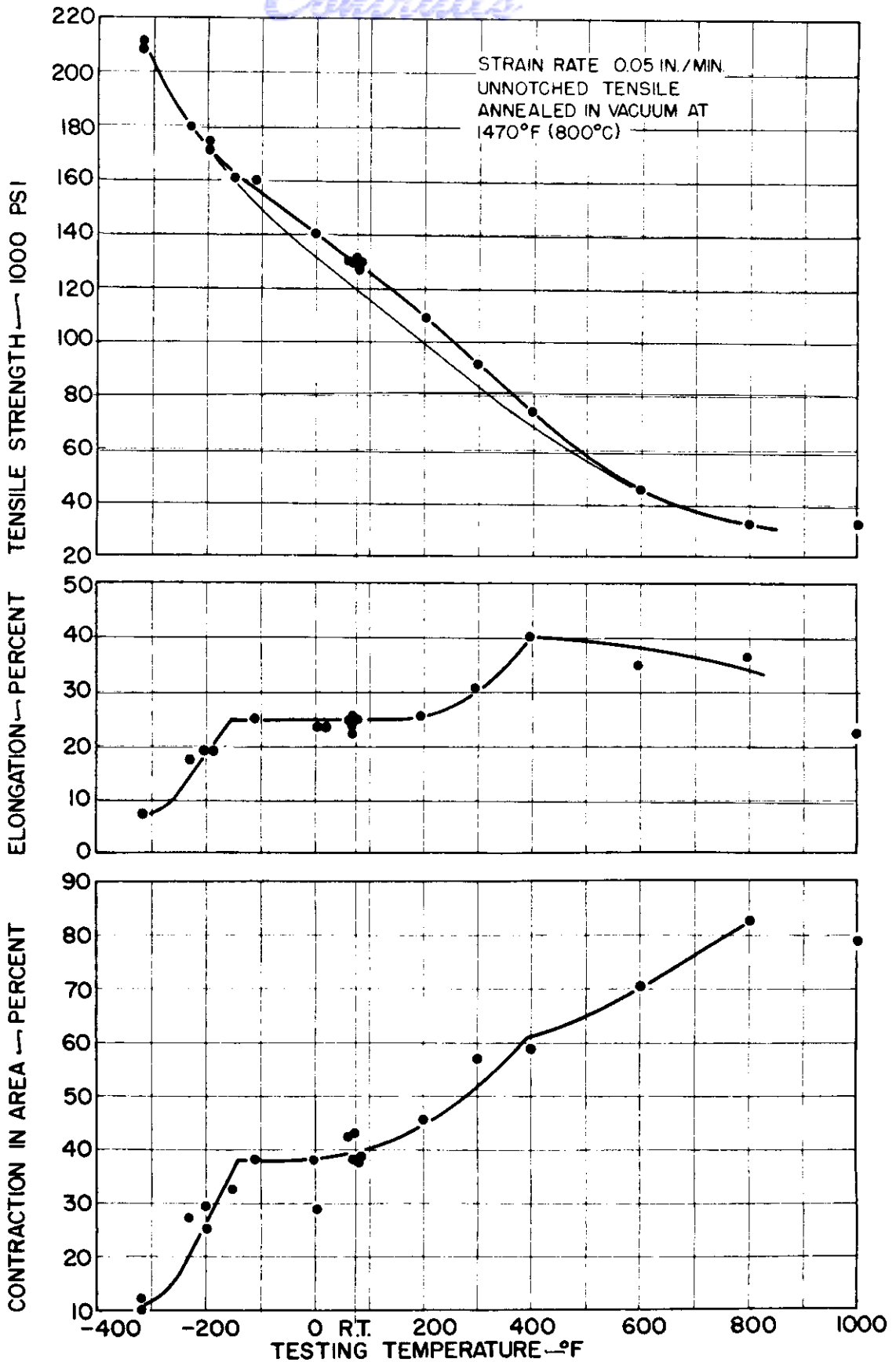


FIG.8 : UNNOTCHED TENSILE PROPERTIES vs. TESTING TEMPERATURE FOR THE TITANIUM - 0.33 PERCENT NITROGEN ALLOY.

Continuity

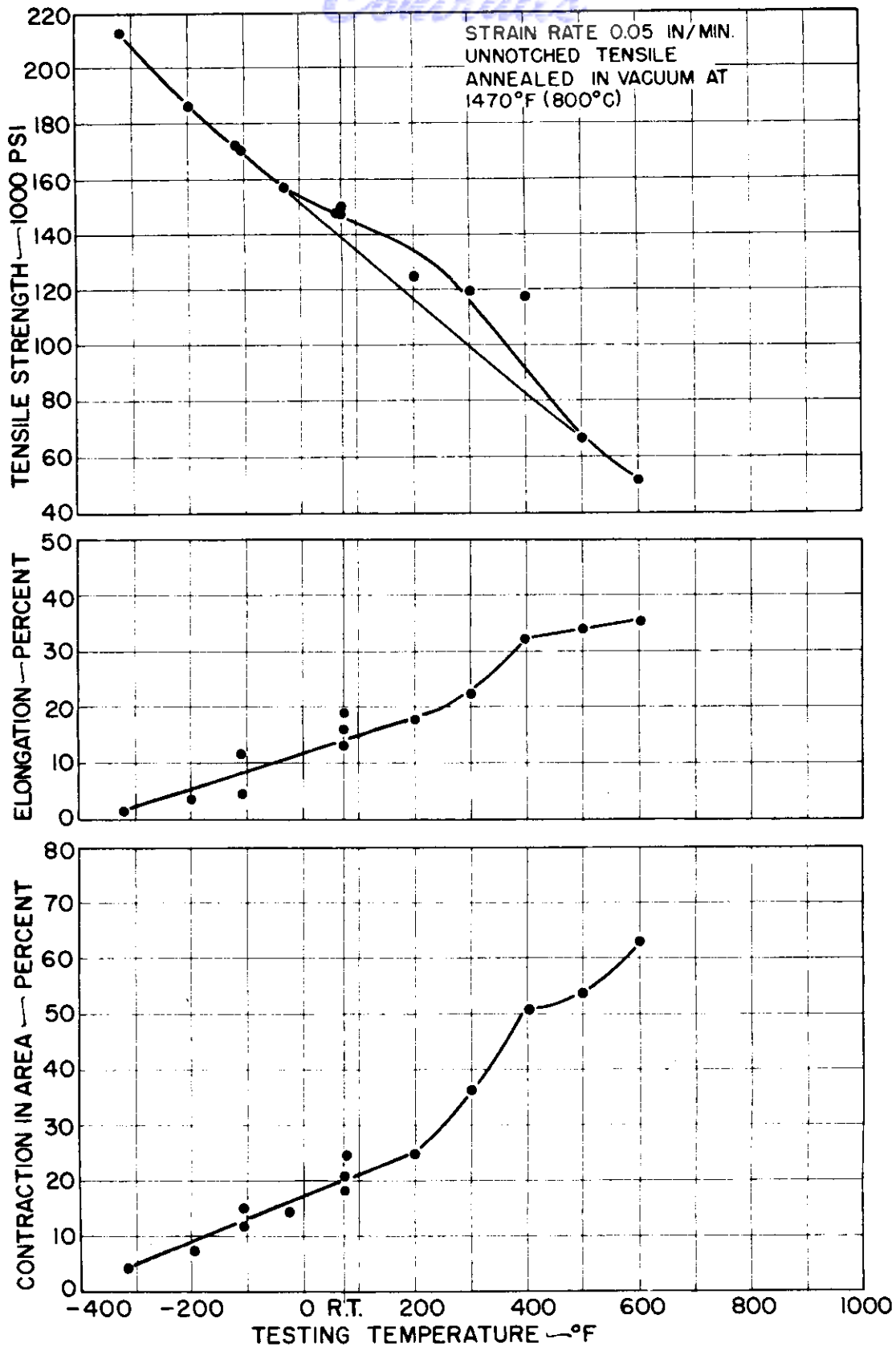


FIG. 9 : UNNOTCHED TENSILE PROPERTIES vs. TESTING TEMPERATURE FOR THE TITANIUM-0.41 PERCENT NITROGEN ALLOY.

Contours

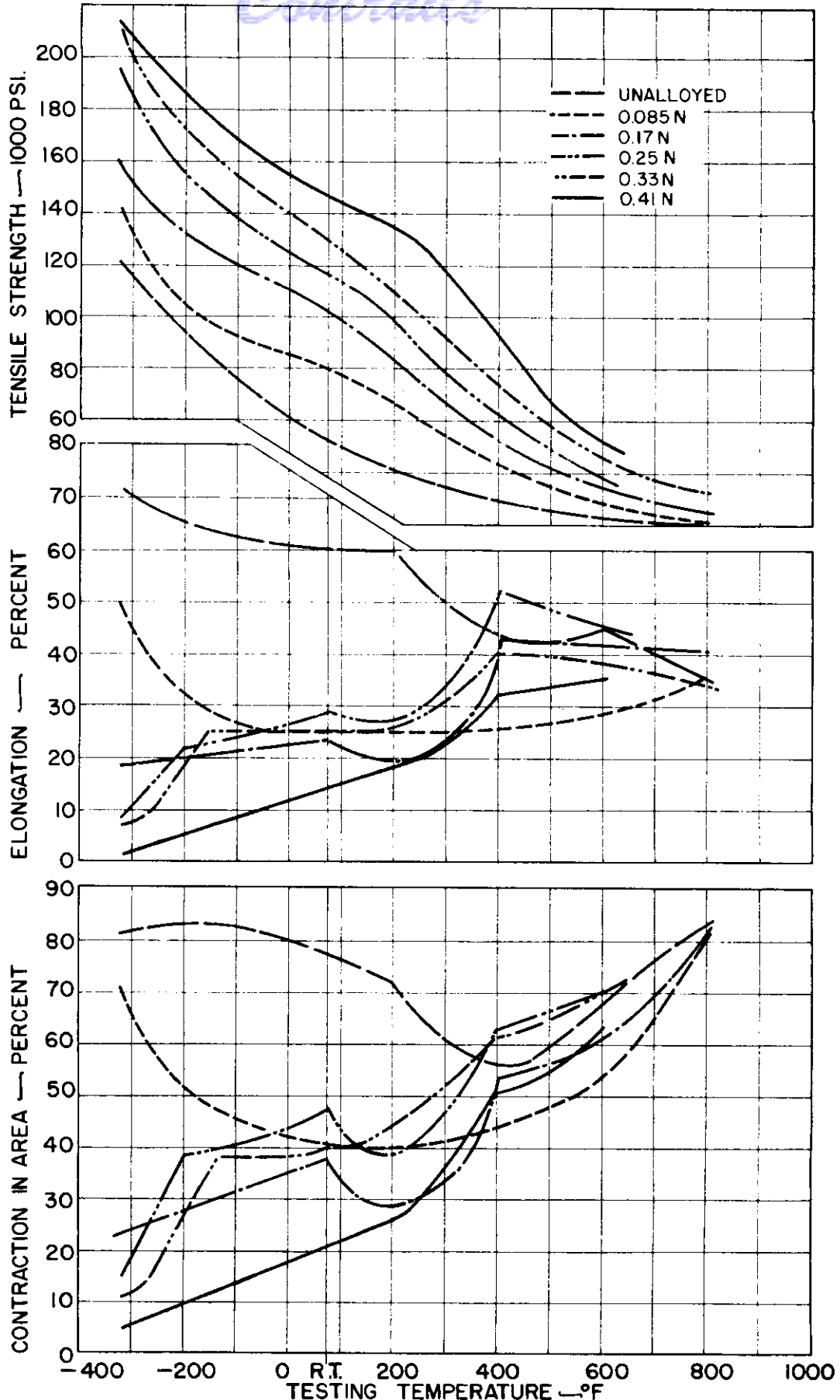


FIG.10: SUMMARY OF UNNOTCHED TENSILE PROPERTIES vs. TESTING TEMP.
WADC TR 55-5

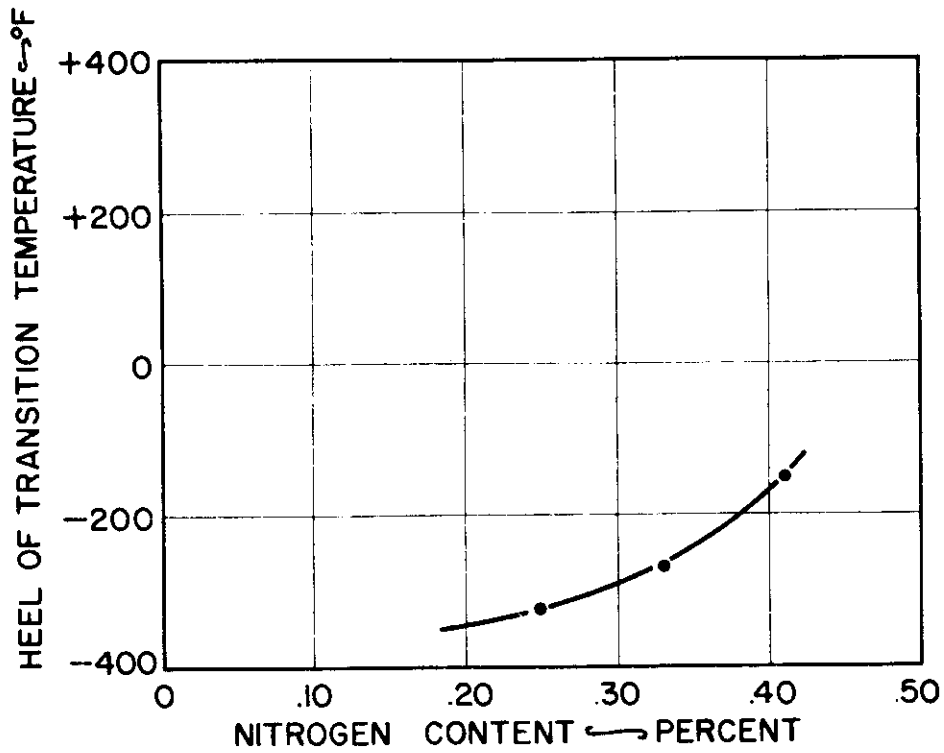
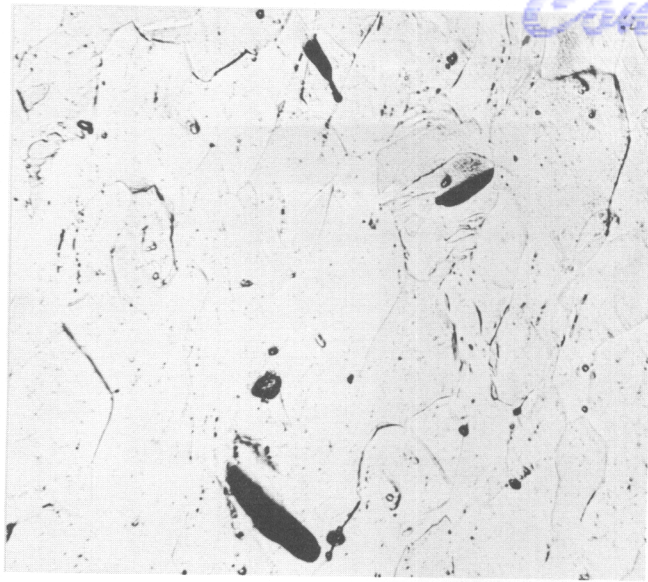
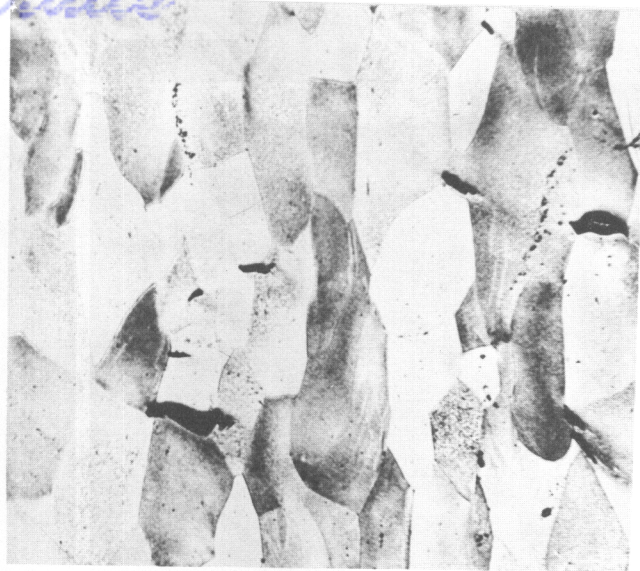


FIG.11: EFFECT OF NITROGEN CONTENT ON THE TRANSITION TEMPERATURE.



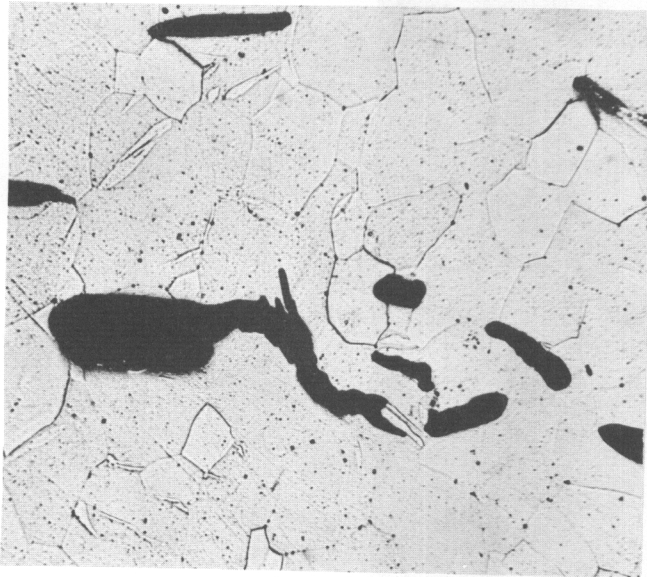
0.17 N



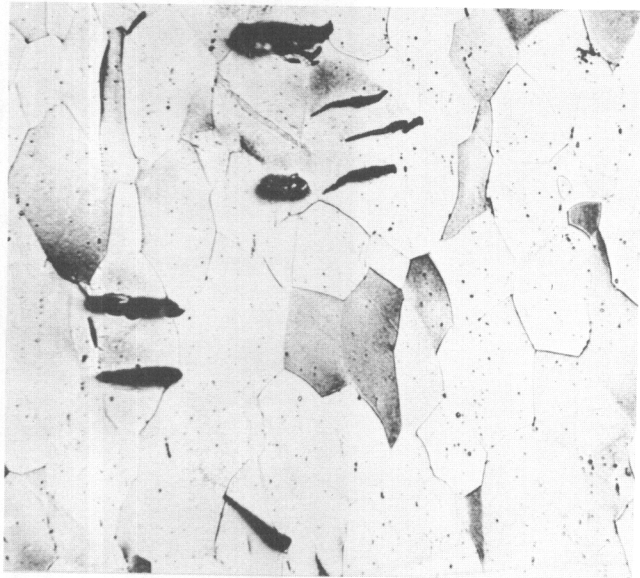
0.25 N

250 X

TESTED AT ROOM TEMPERATURE



0.17 N



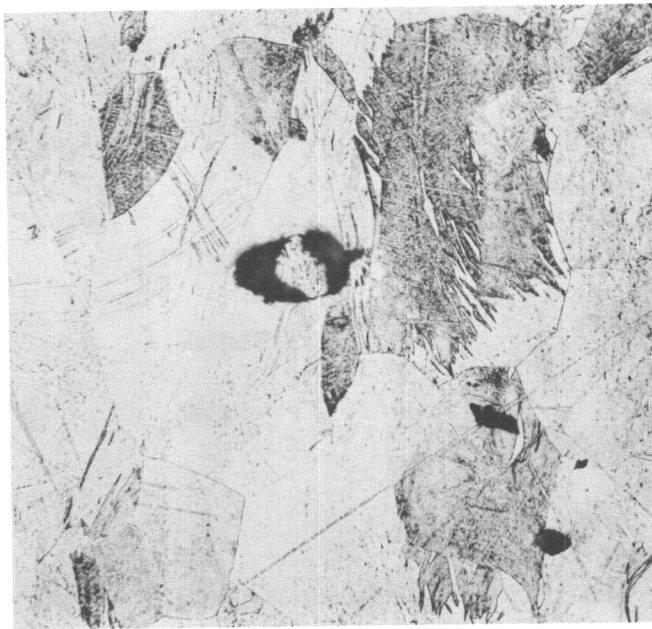
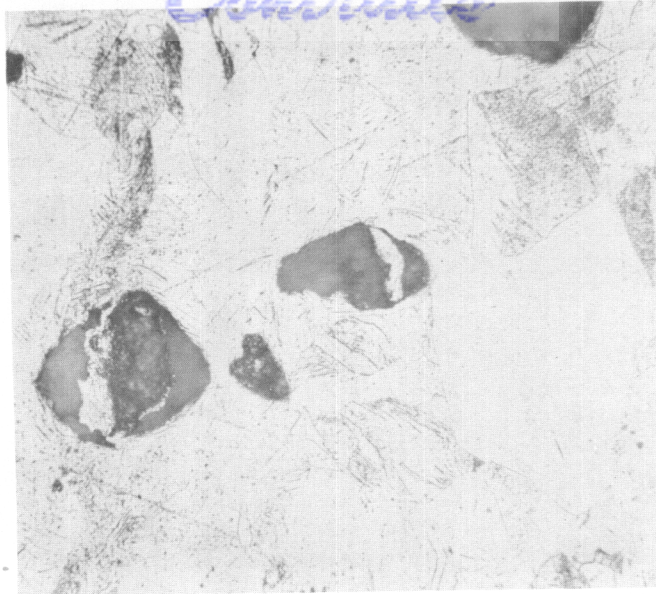
0.25 N

250 X

TESTED AT +200°F

MECHANICAL POLISH. ETCHANT: 1 PART HF, 1 PART HNO₃, 6 PARTS GLYCERINE.

FIG.12 :CRACKS FORMED IN THE VICINITY OF FRACTURE ON TESTING AT ROOM TEMPERATURE AND + 200°F (SPECIMEN AND APPLIED STRESS AXIS VERTICAL).



250 X

MECHANICAL POLISH. ETCHANT: 1 PART HF, 1 PART HNO_3 , 6 PARTS GLYCERINE.

FIG.13: CRACKS FORMED IN VICINITY OF FRACTURE ON TESTING AT TEMPERATURES OF +400°F AND ABOVE (SPECIMEN AND APPLIED STRESS AXIS VERTICAL).

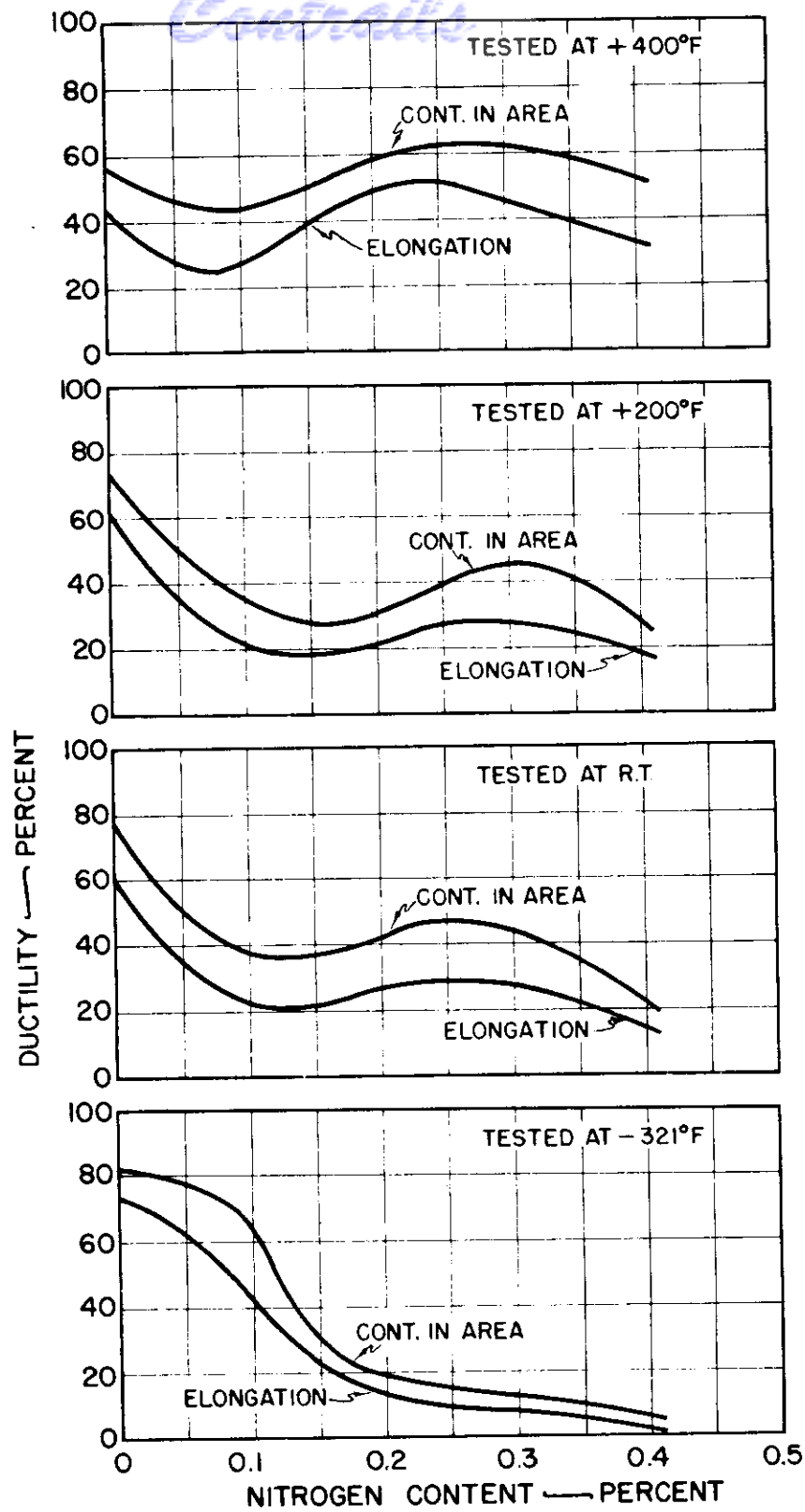


FIG.14: DUCTILITY vs. NITROGEN CONTENT AT A VARIETY OF TESTING TEMPERATURES.

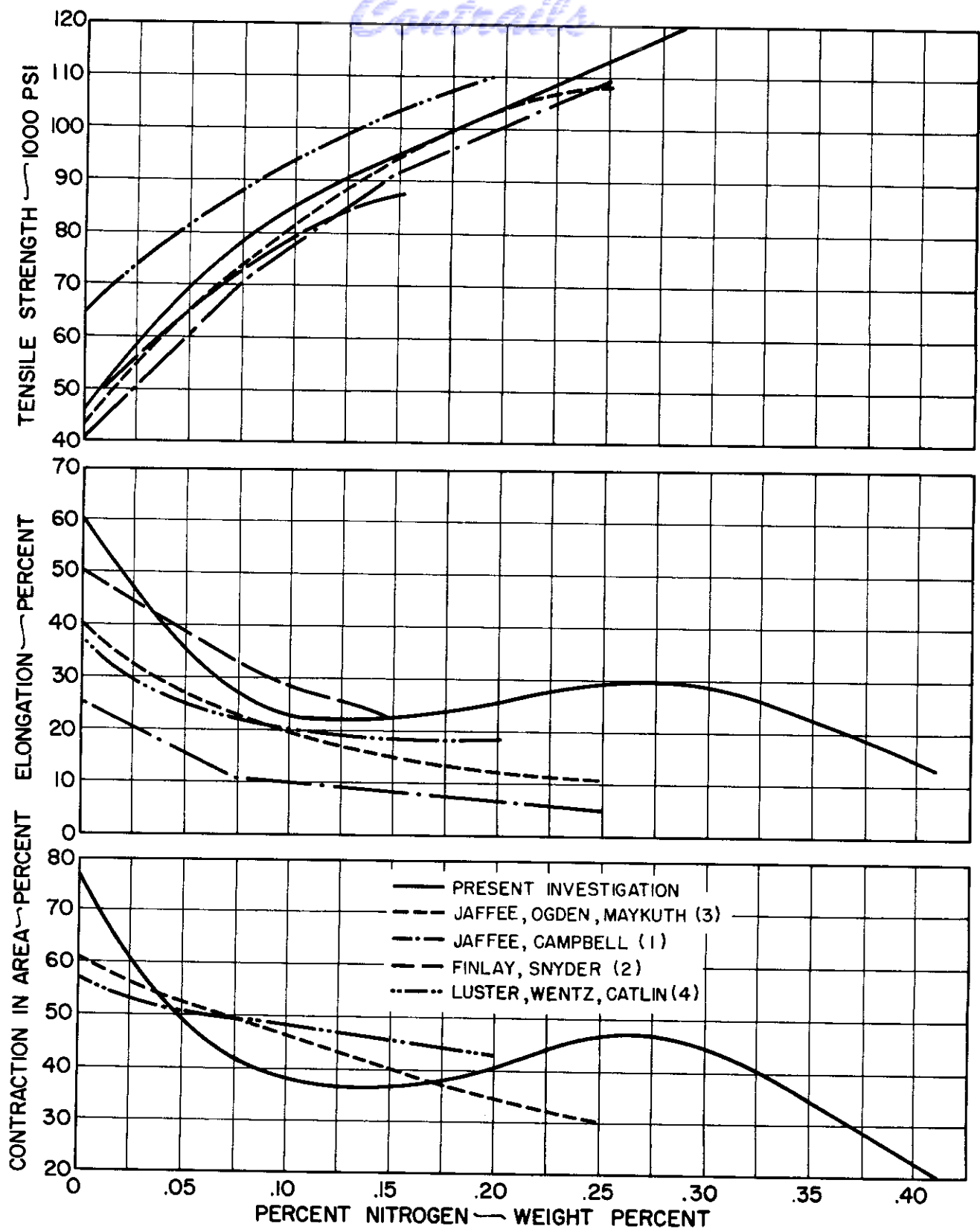


FIG.15: COMPARISON OF PREVIOUSLY REPORTED ROOM TEMPERATURE TENSILE PROPERTIES OF TITANIUM-NITROGEN ALLOYS WITH THOSE OBTAINED IN THE PRESENT INVESTIGATION.

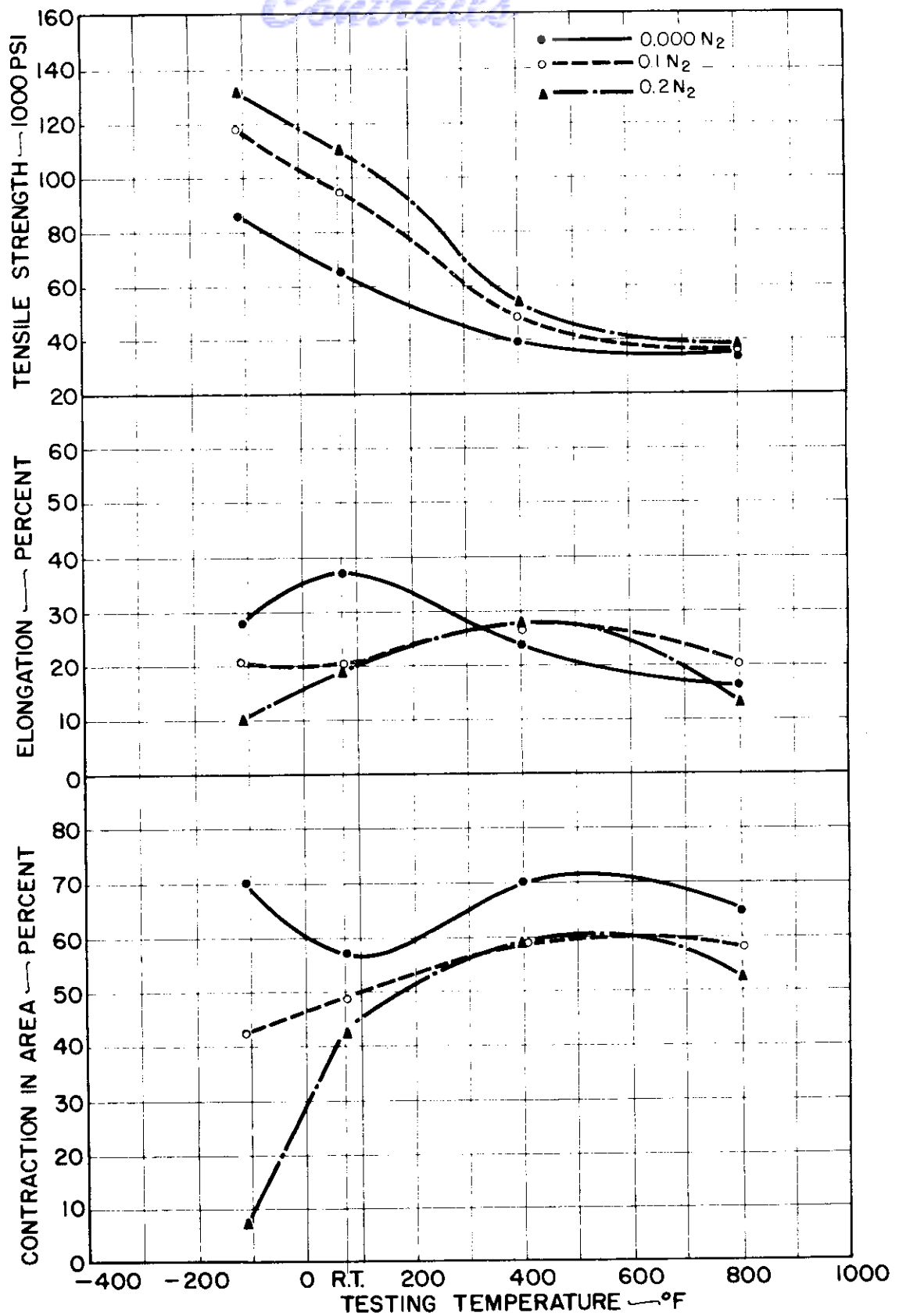


FIG.16: UNNOTCHED TENSILE PROPERTIES vs. TESTING TEMPERATURE CURVES AS REPORTED BY LUSTER, WENTZ, AND CATLIN (4).

Centrals

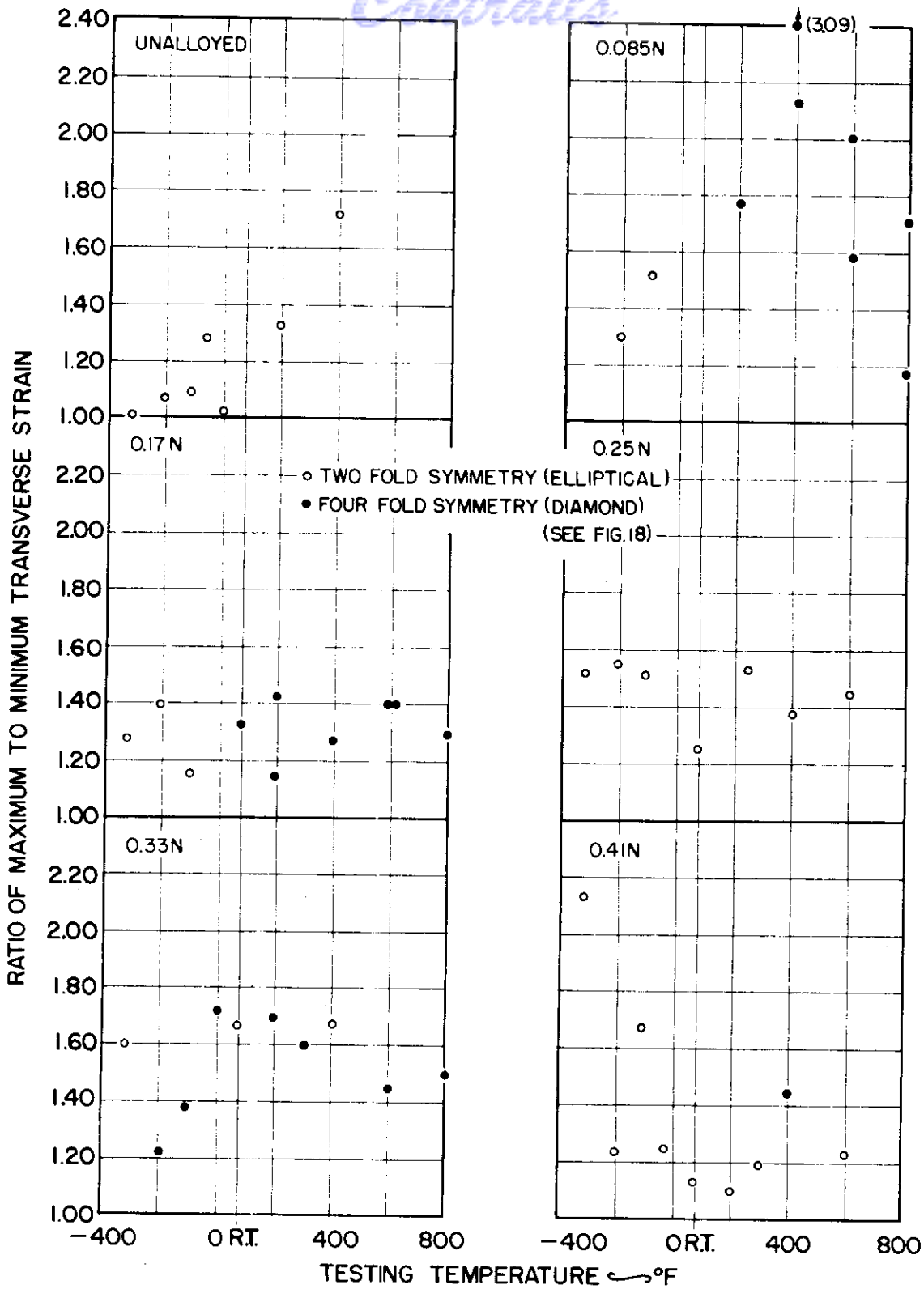


FIG. 17: ANISOTROPY (RATIO OF MAXIMUM TO MINIMUM TRANSVERSE STRAINS) OF FRACTURED SPECIMENS vs. TESTING TEMPERATURE.

Centrails

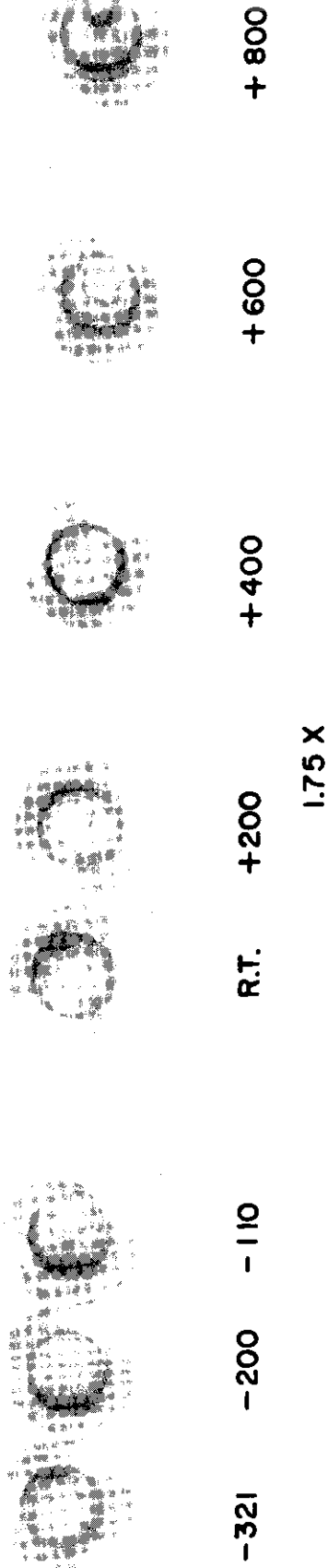


FIG.18: APPEARANCE OF BROKEN TEST BAR OF THE TITANIUM - 0.17 PERCENT NITROGEN ALLOY.

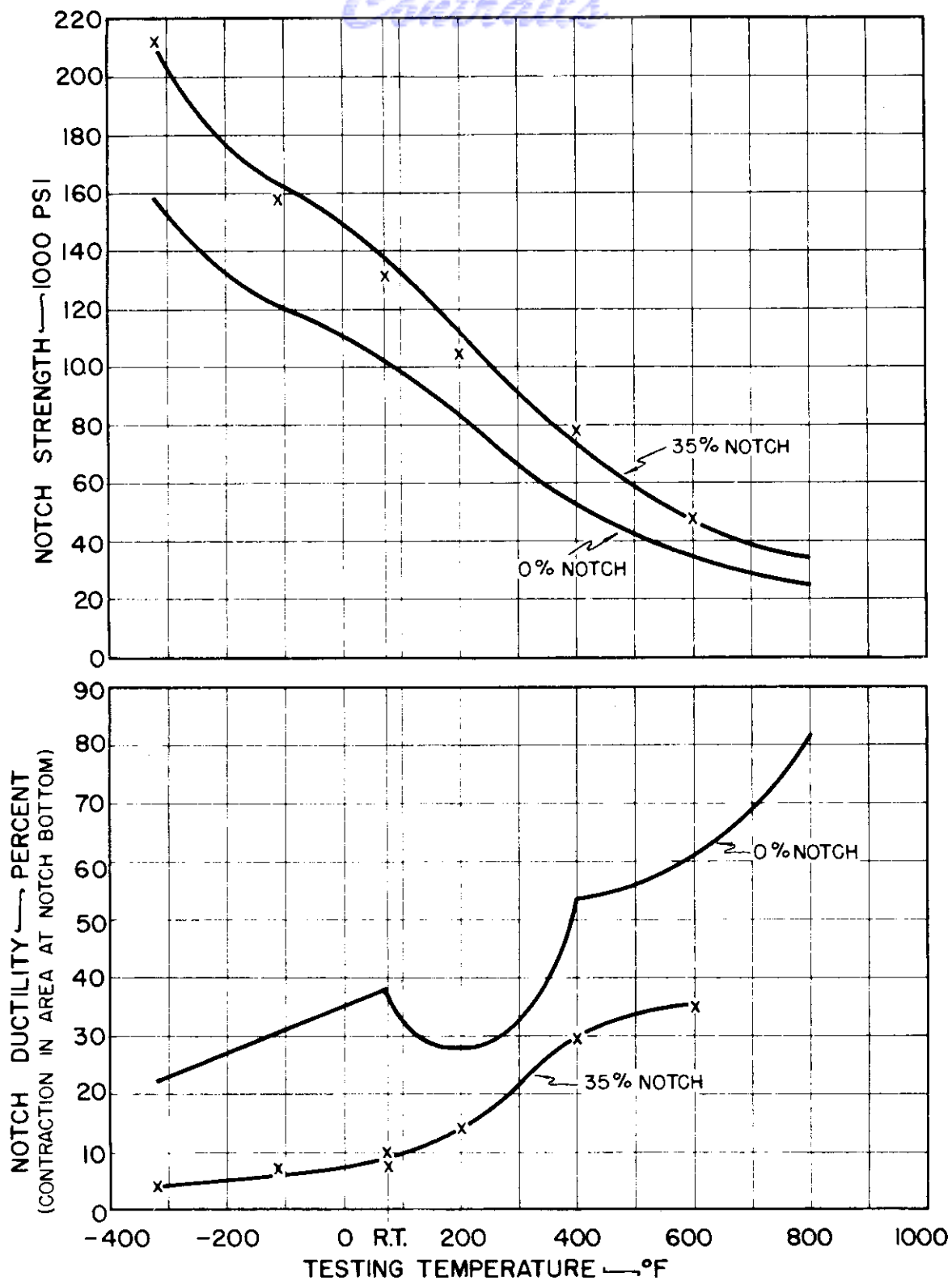


FIG.19:NOTCHED TENSILE PROPERTIES vs. TESTING TEMPERATURE FOR THE TITANIUM-0.17 PERCENT NITROGEN ALLOY.

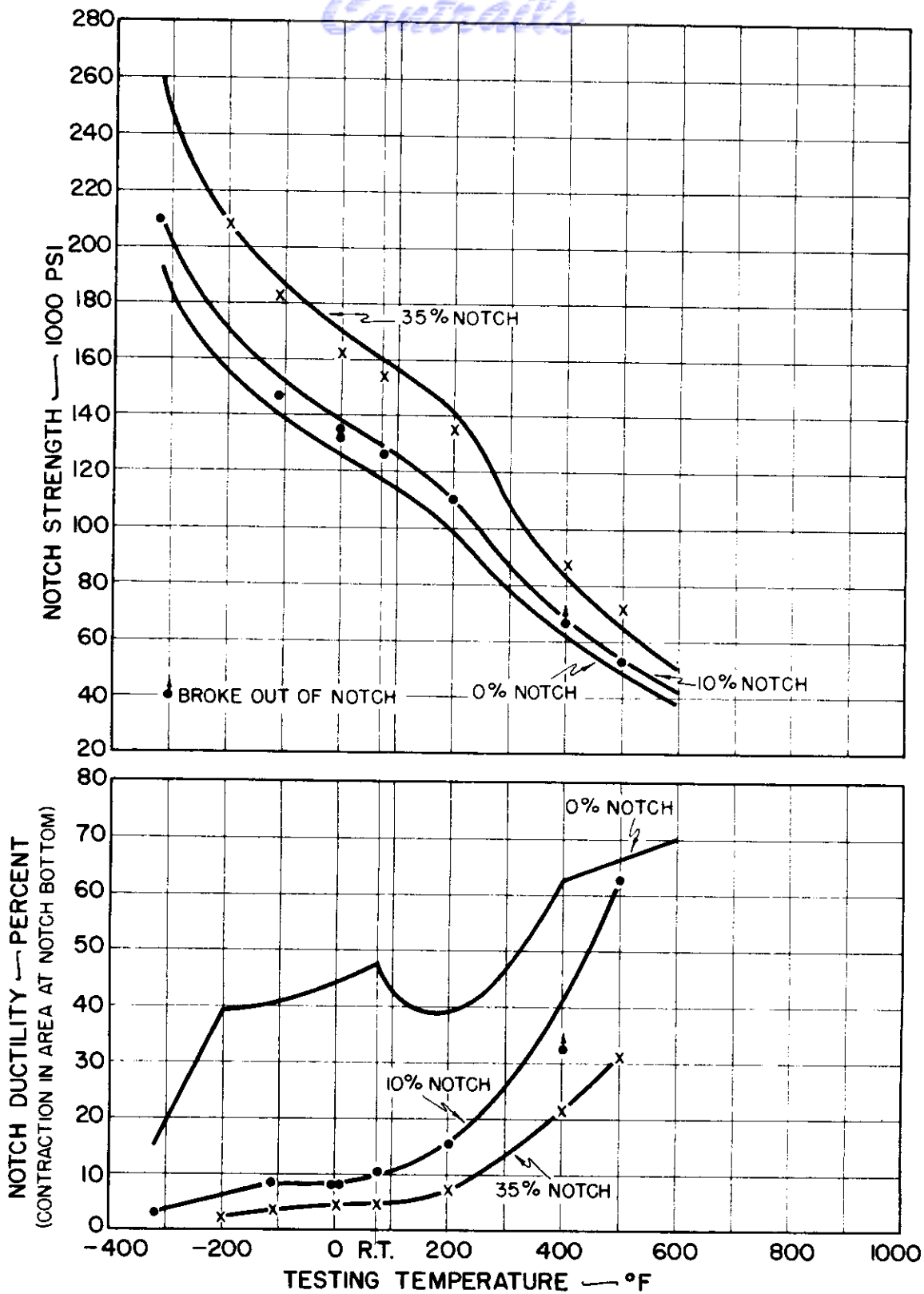


FIG.20:NOTCHED TENSILE PROPERTIES vs. TESTING TEMPERATURE FOR THE TITANIUM-0.25 PERCENT NITROGEN ALLOY.

Contrails

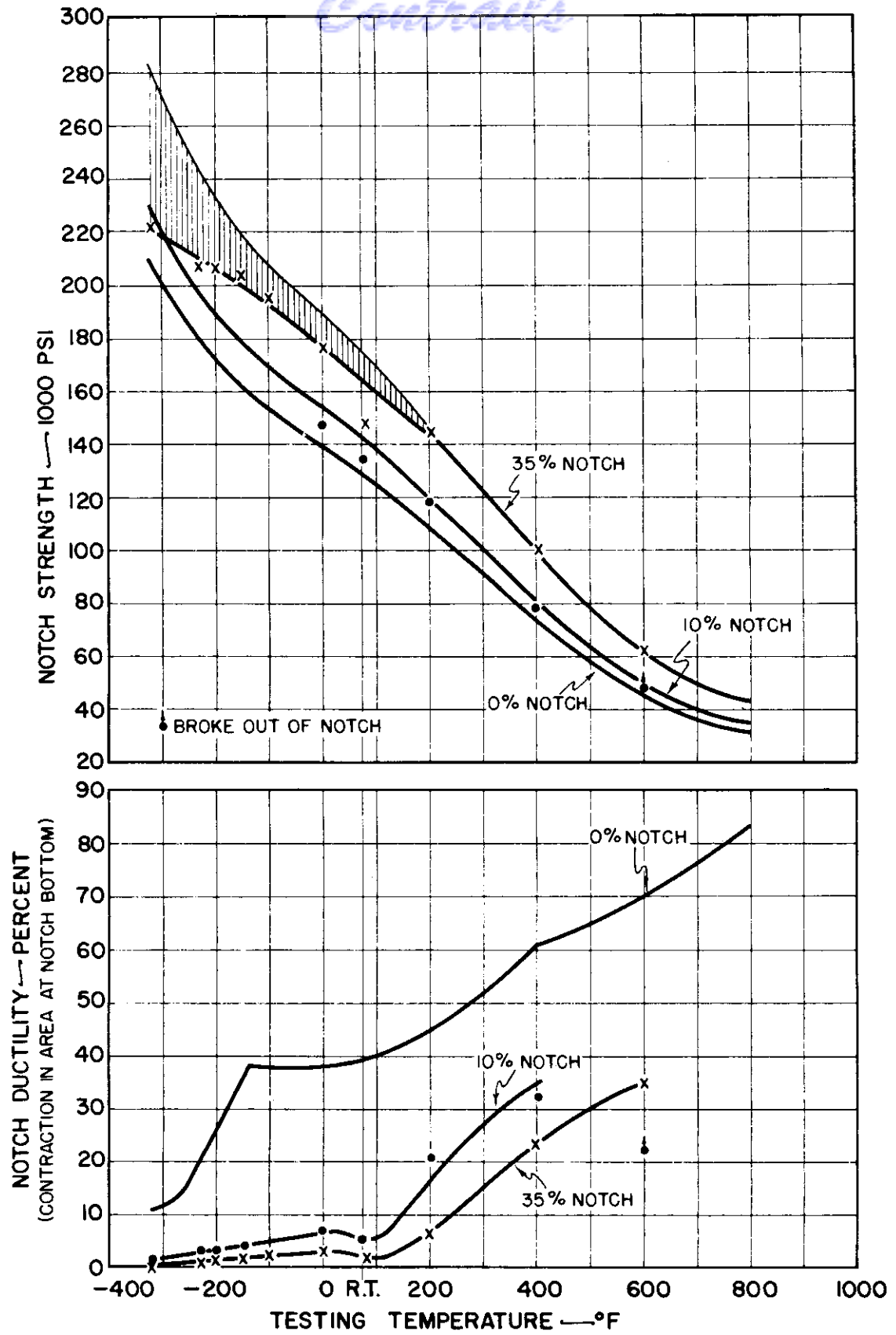


FIG. 21 : NOTCHED TENSILE PROPERTIES vs. TESTING TEMPERATURE FOR THE TITANIUM - 0.33 PERCENT NITROGEN ALLOY.

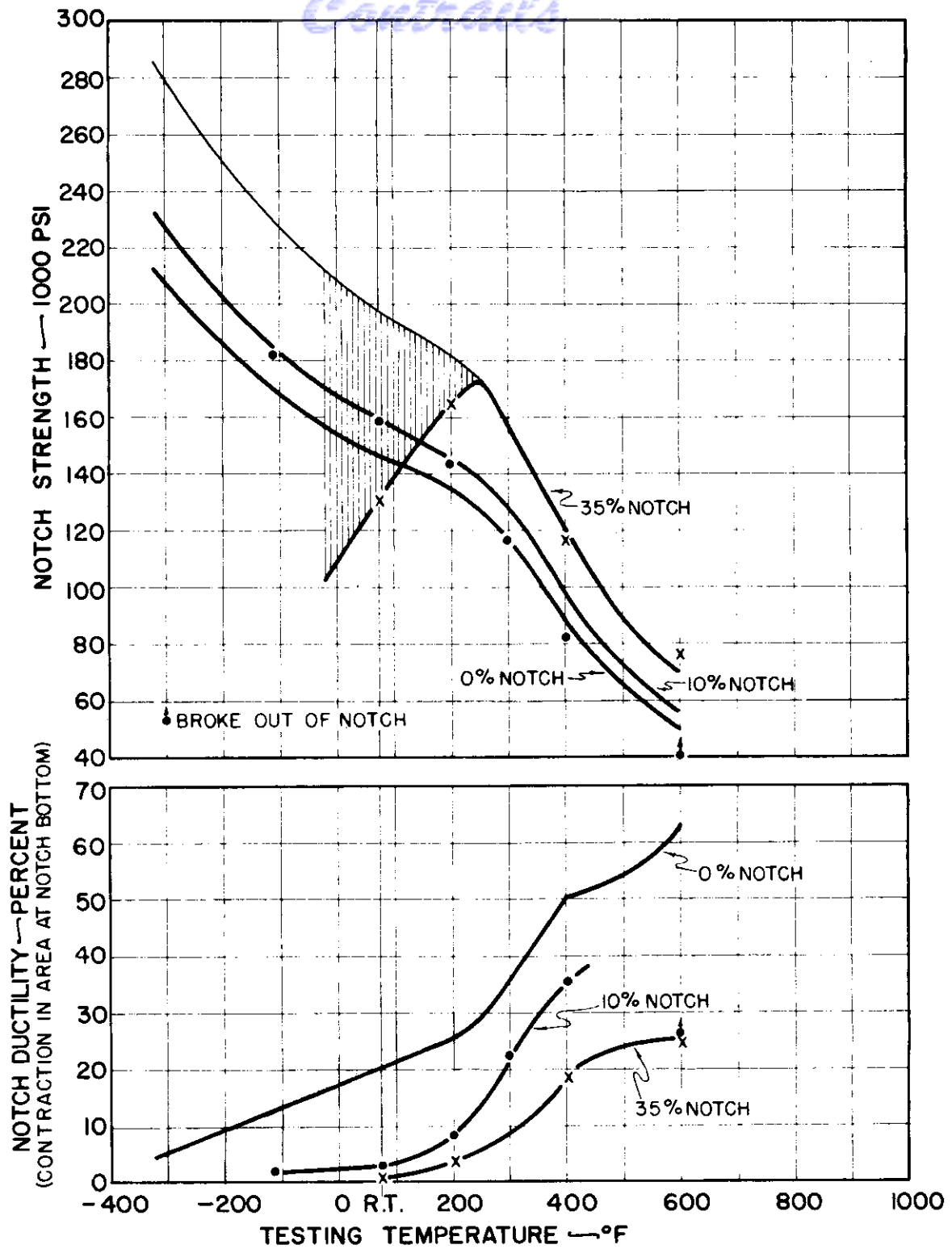


FIG.22 :NOTCHED TENSILE PROPERTIES vs. TESTING TEMPERATURE FOR THE TITANIUM-0.41 PERCENT NITROGEN ALLOY.

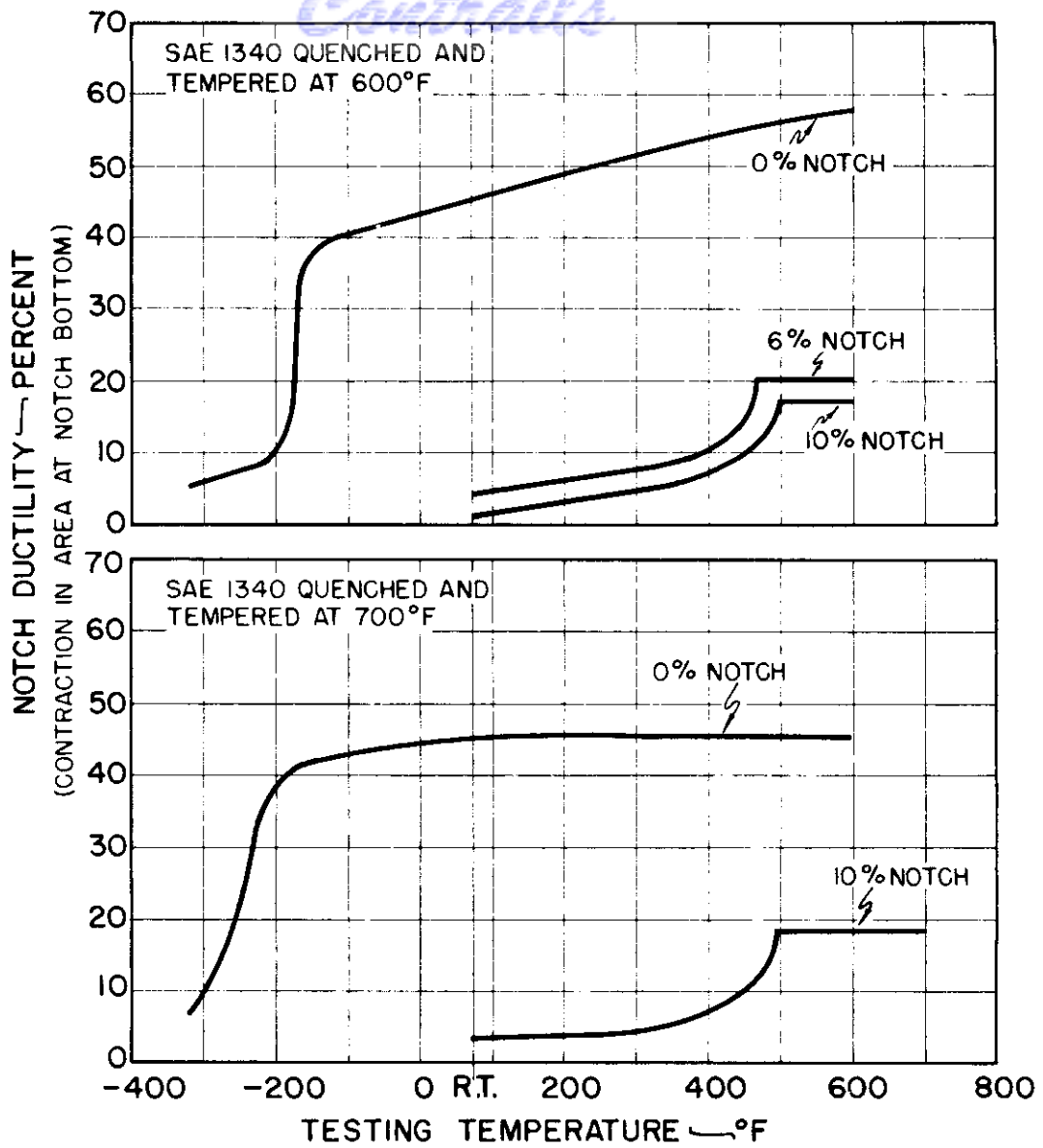


FIG.23: UNNOTCHED AND NOTCHED TENSILE PROPERTIES vs. TESTING TEMPERATURE FOR QUENCHED AND TEMPERED SAE 1340 STEEL (20).

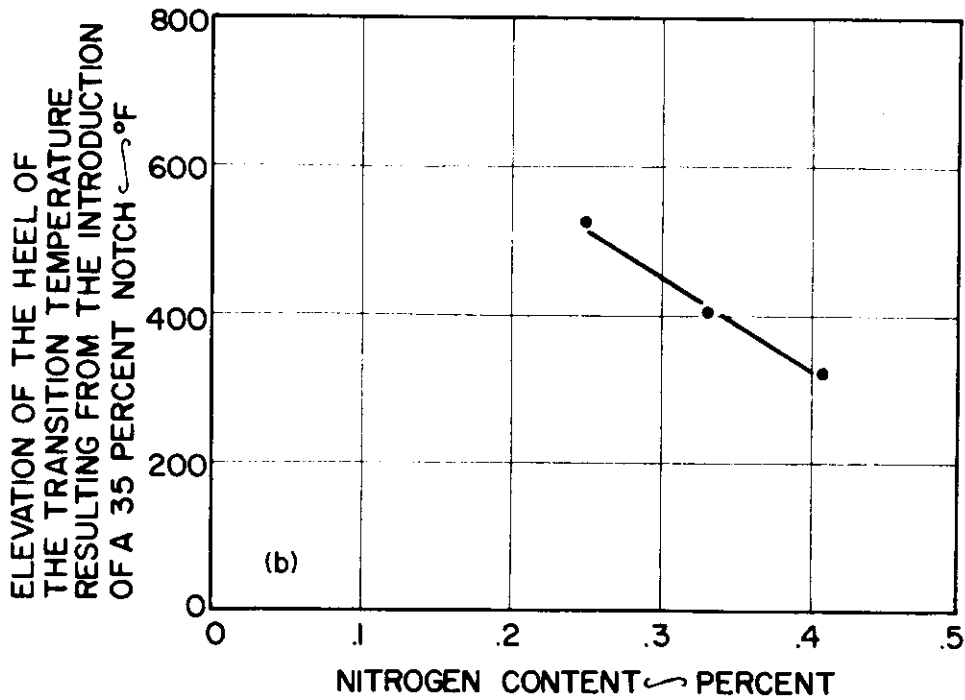
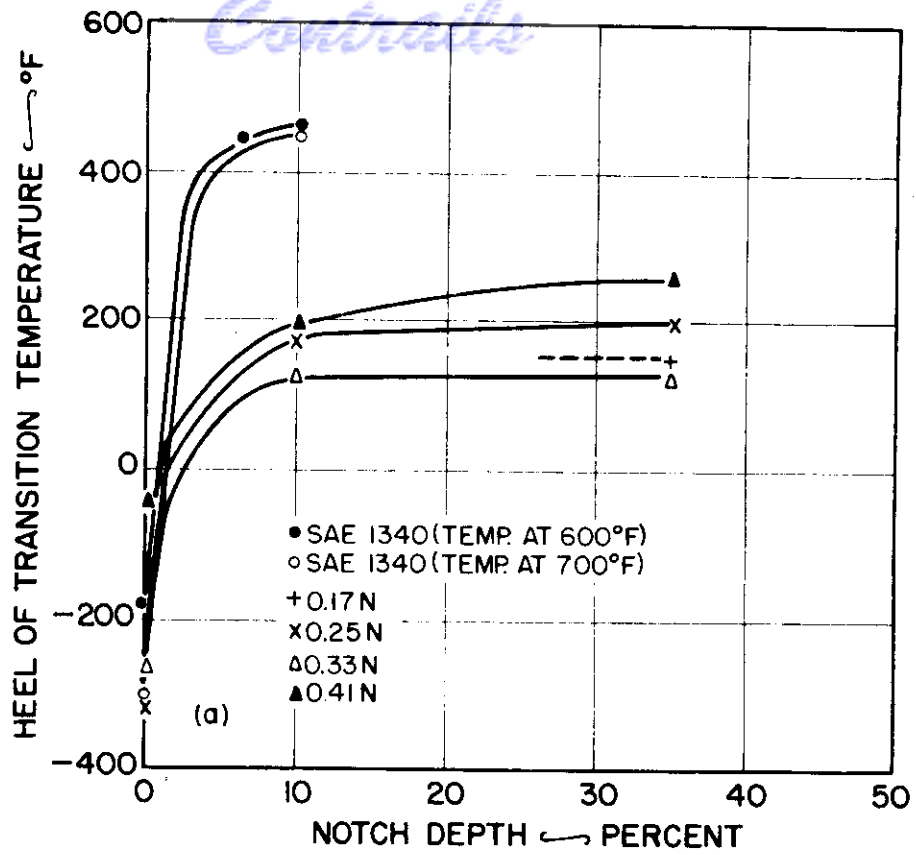


FIG.24 DEPENDENCE OF HEEL OF TRANSITION ON NOTCH DEPTH AND NITROGEN CONTENT.

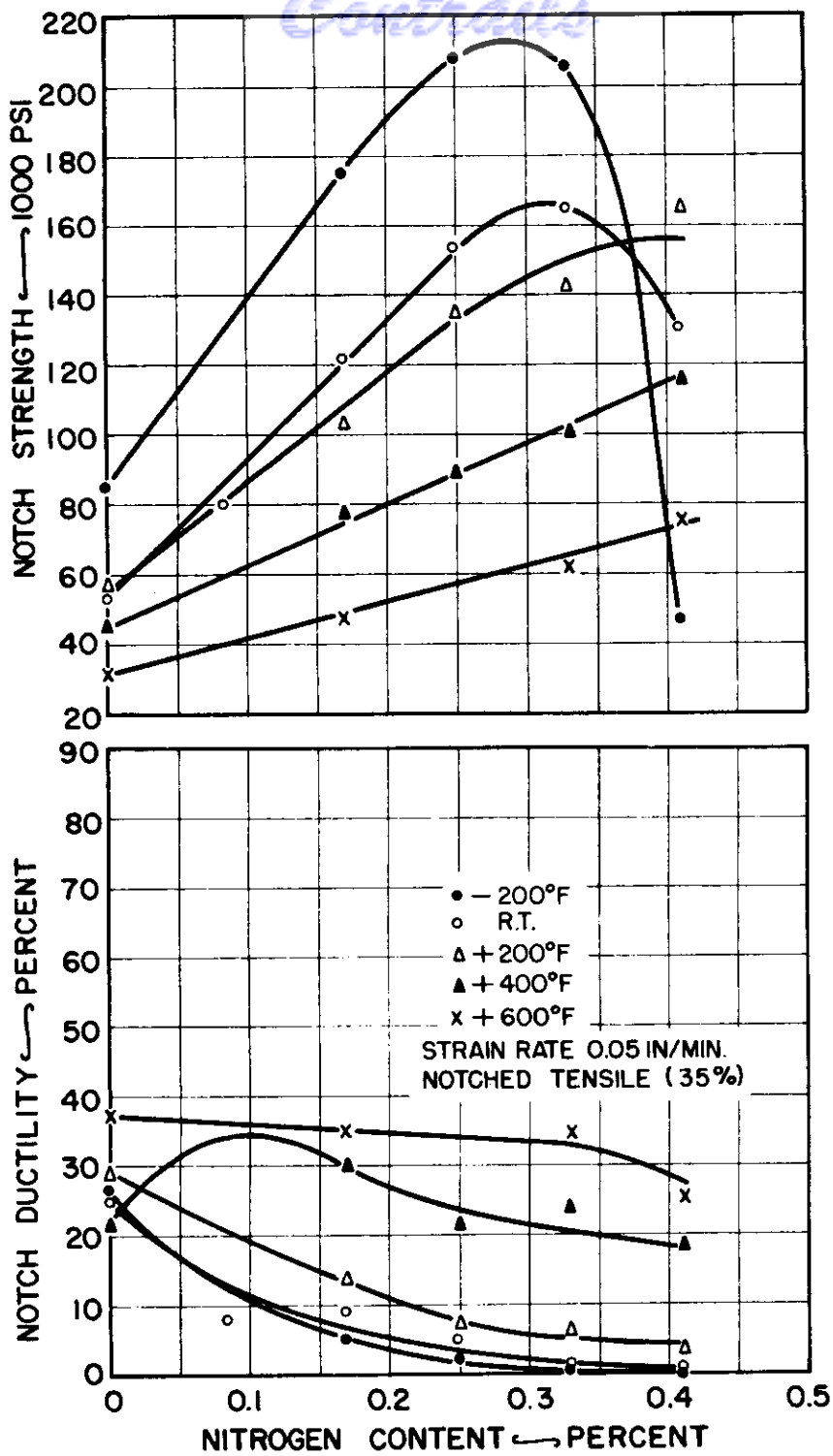


FIG.25: NOTCH DUCTILITY AND NOTCH STRENGTH vs. NITROGEN CONTENT AT A VARIETY OF TEMPERATURES.

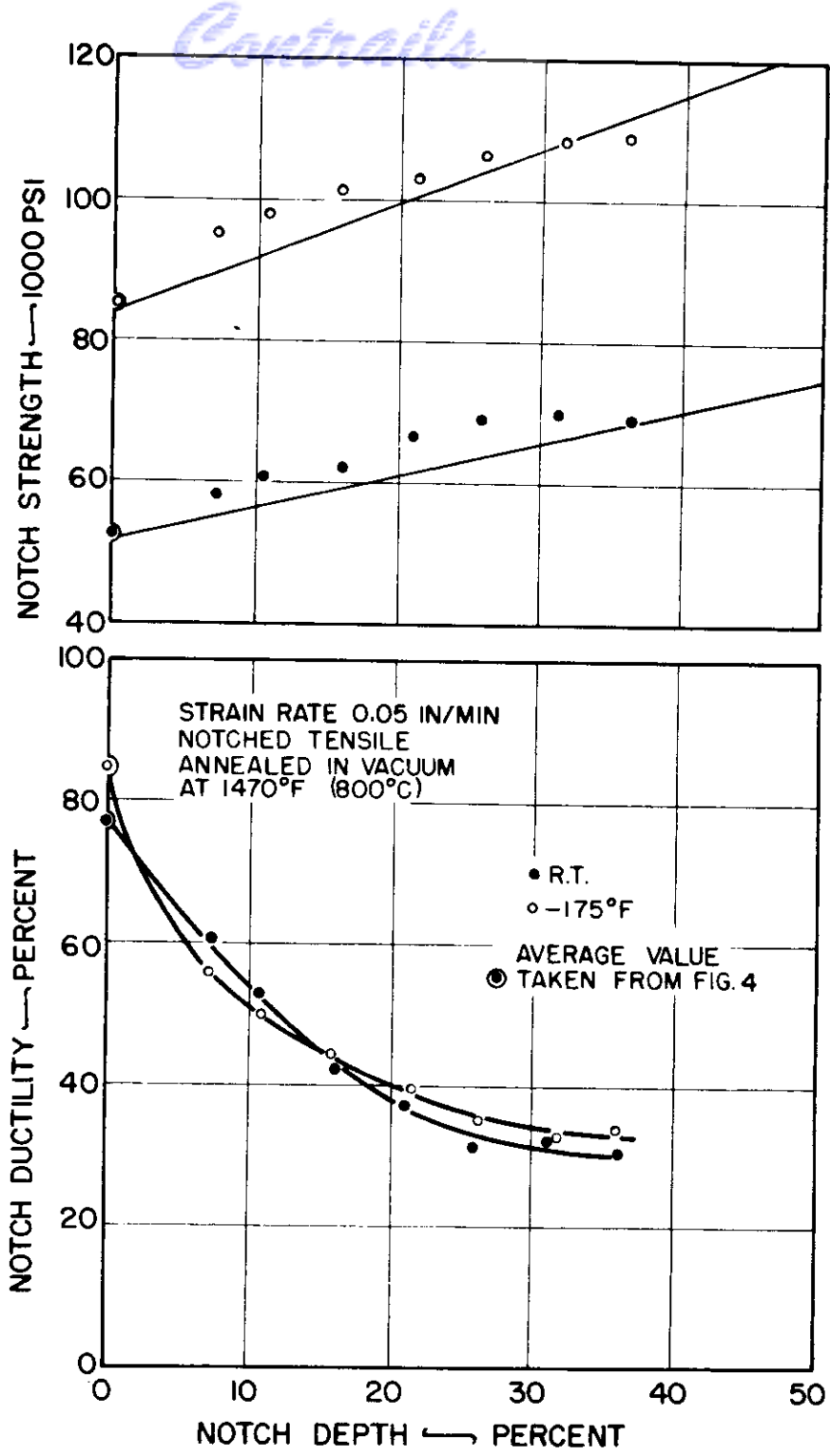


FIG.26: NOTCH STRENGTH AND NOTCH DUCTILITY vs. NOTCH DEPTH AT ROOM TEMPERATURE AND -175°F FOR THE UNALLOYED TITANIUM.

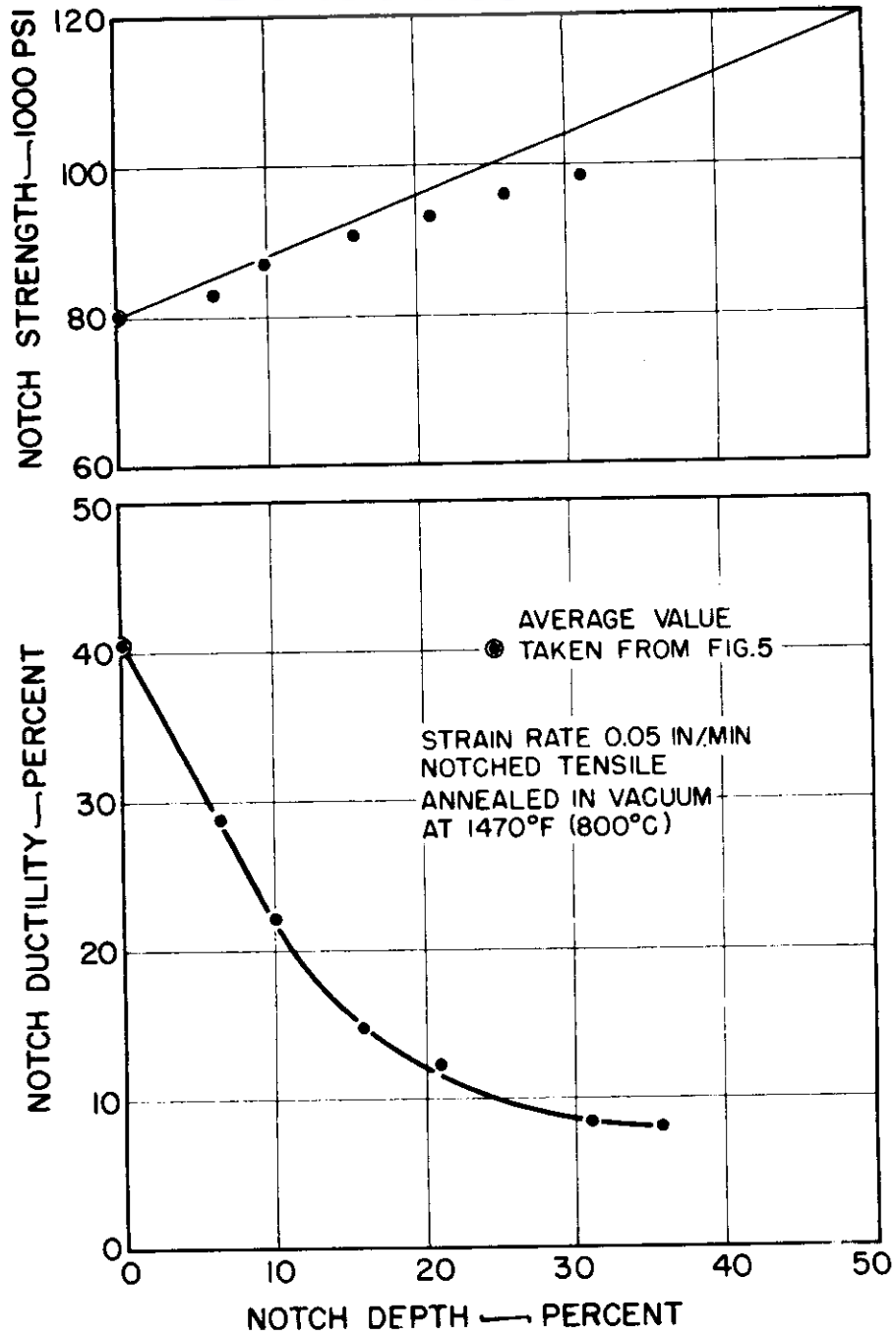


FIG.27: NOTCH STRENGTH AND NOTCH DUCTILITY vs. NOTCH DEPTH AT ROOM TEMPERATURE FOR THE TITANIUM-0.085 PERCENT NITROGEN ALLOY.

Contrails

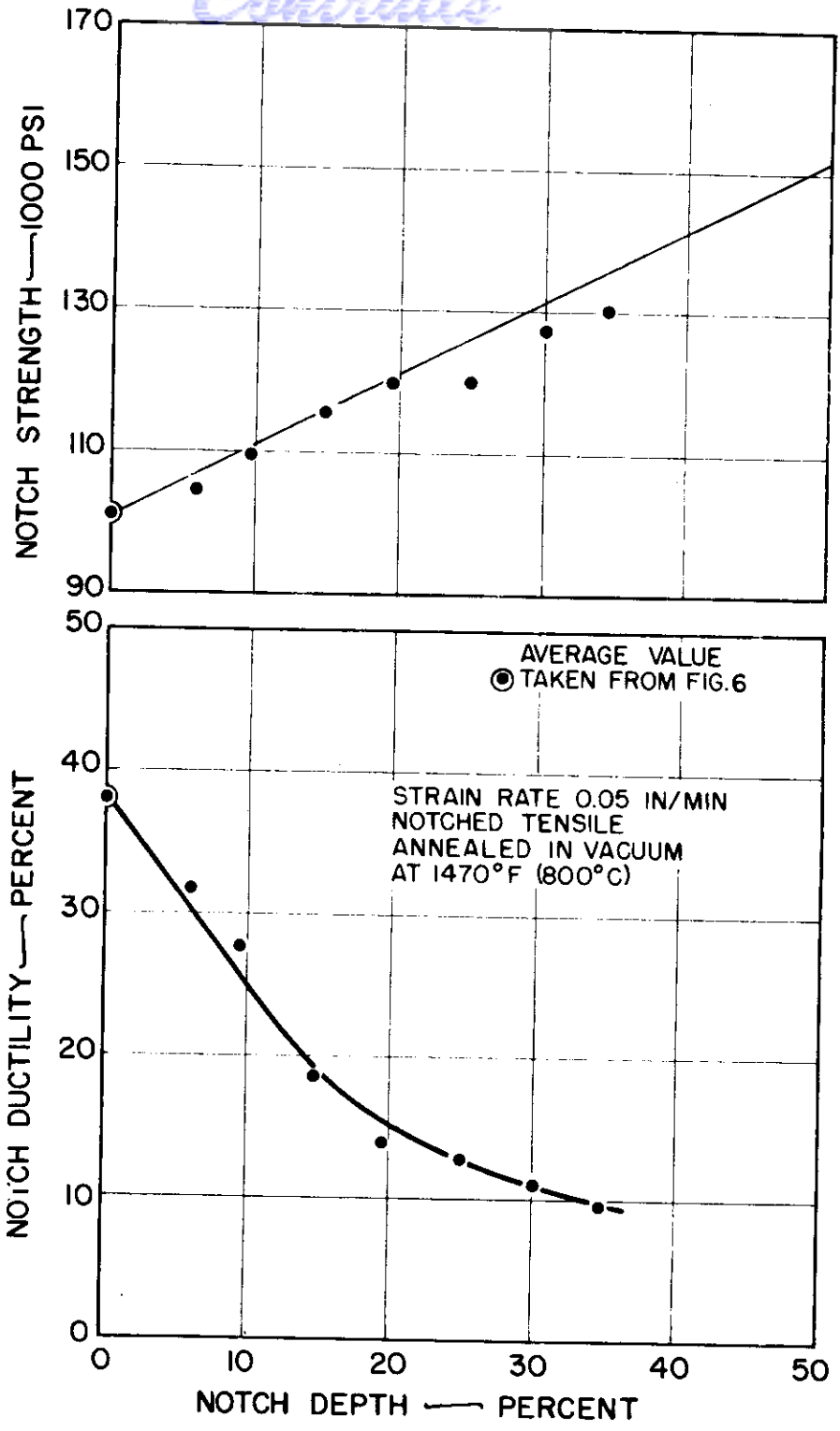


FIG.28:NOTCH STRENGTH AND NOTCH DUCTILITY vs. NOTCH DEPTH AT ROOM TEMPERATURE FOR THE TITANIUM-0.17 PERCENT NITROGEN ALLOY.

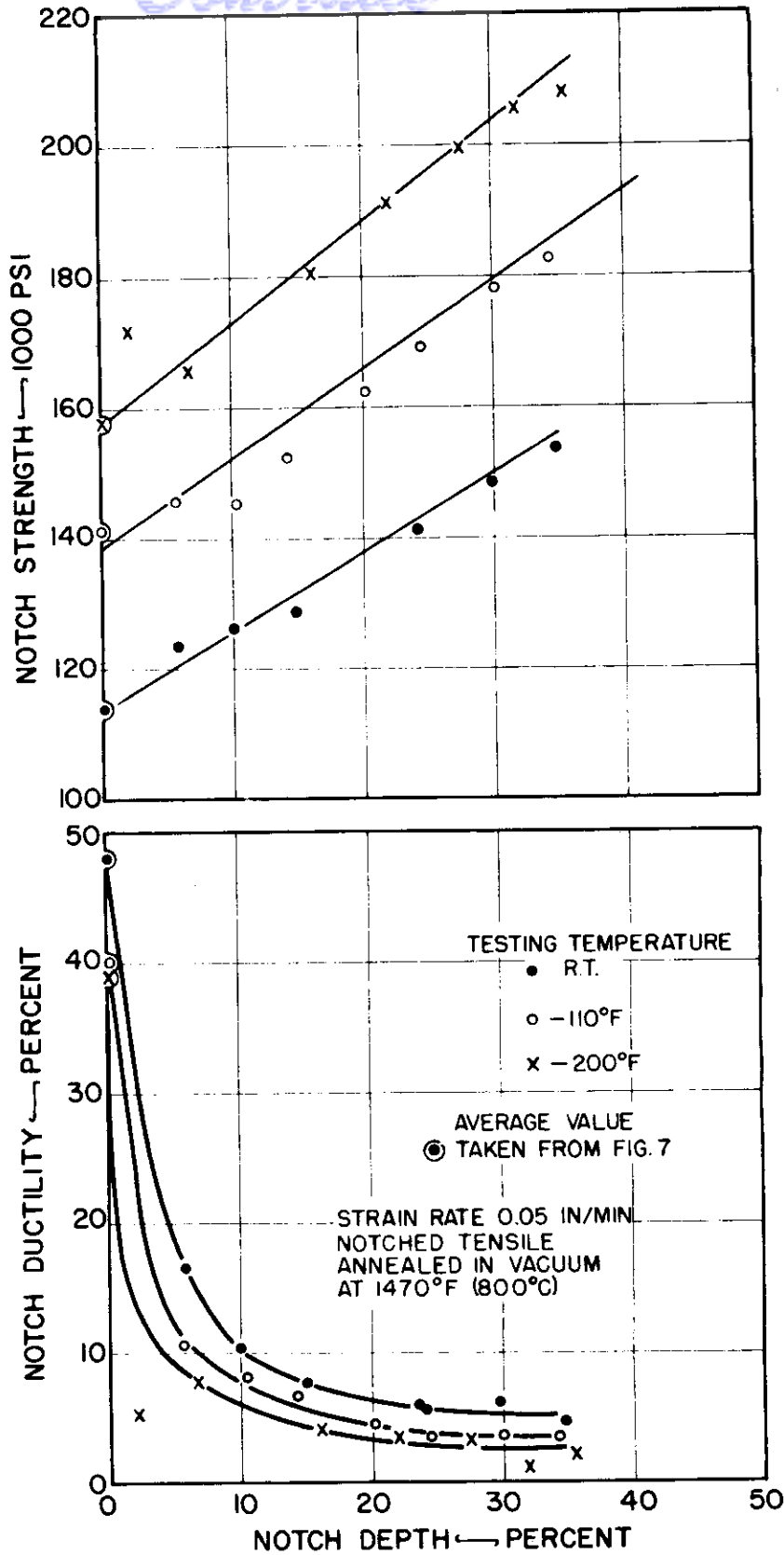


FIG.29:NOTCH STRENGTH AND NOTCH DUCTILITY vs. NOTCH DEPTH AT ROOM TEMPERATURE, -110°F AND -200°F FOR THE TITANIUM -0.25 PERCENT NITROGEN ALLOY.

Controls

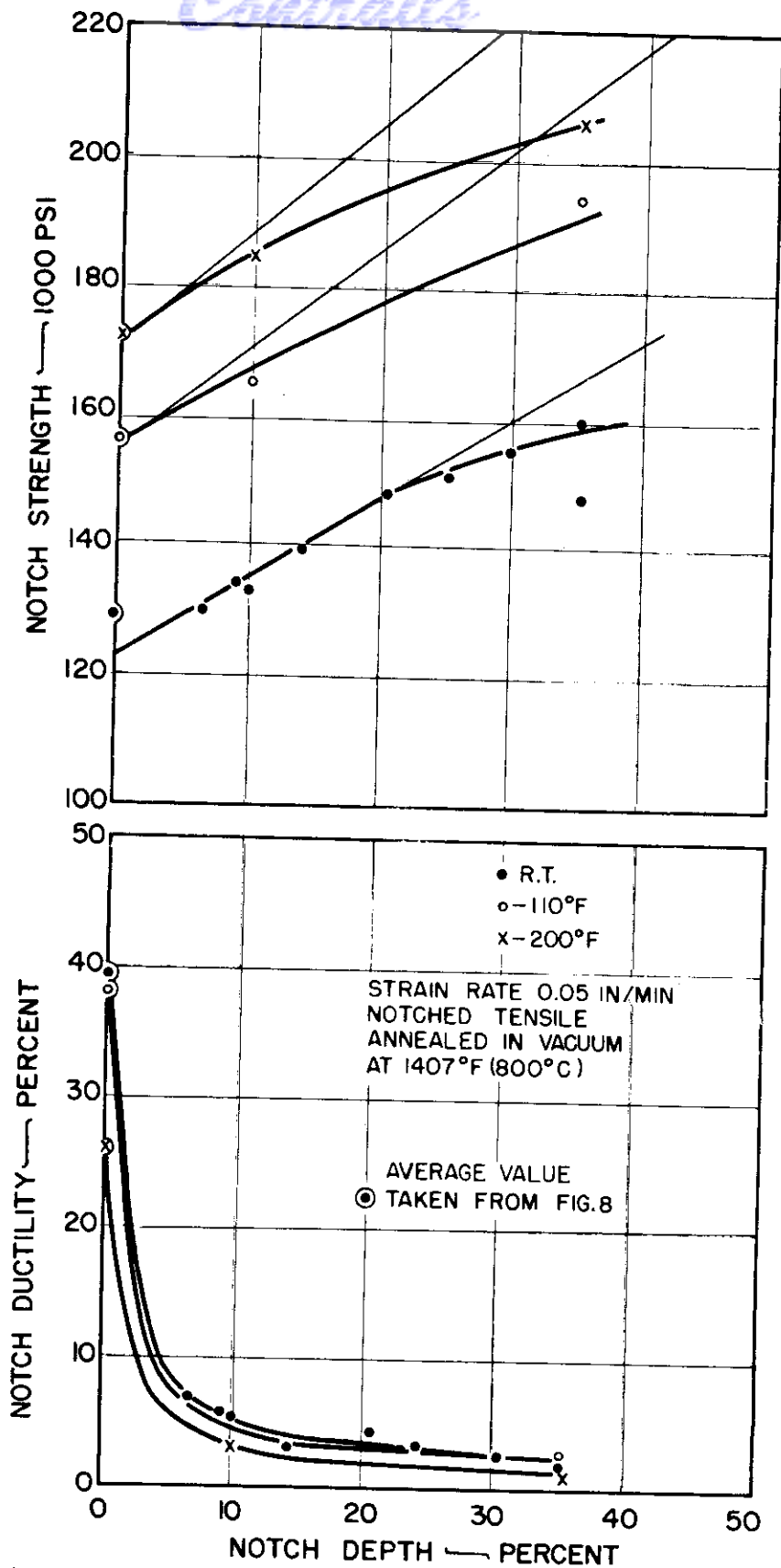


FIG.30: NOTCH STRENGTH AND NOTCH DUCTILITY vs. NOTCH DEPTH AT ROOM TEMPERATURE, -110°F AND -200°F FOR THE TITANIUM-0.33 PERCENT NITROGEN ALLOY.

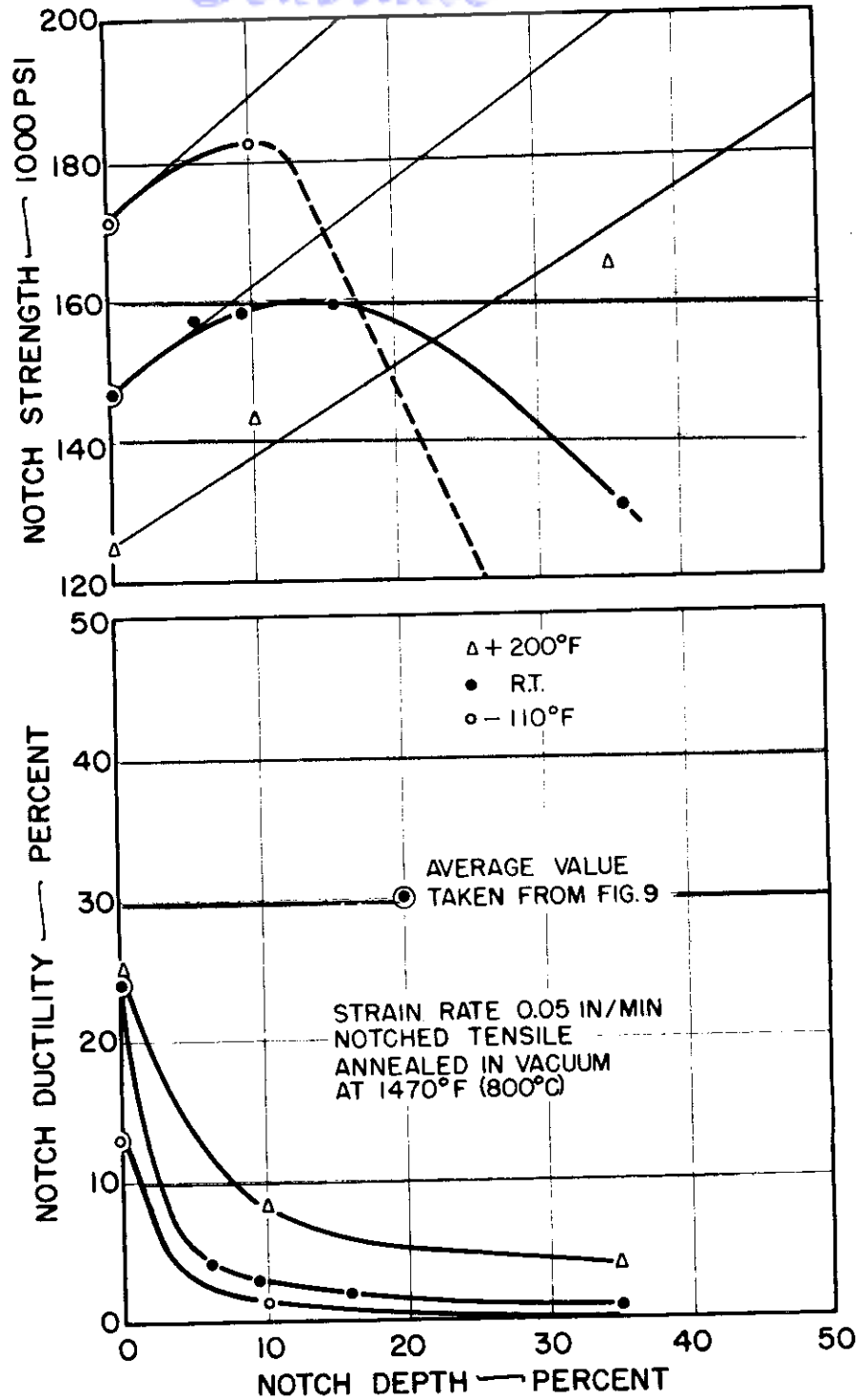


FIG.31:NOTCH STRENGTH AND NOTCH DUCTILITY vs.NOTCH DEPTH AT +200, ROOM TEMPERATURE AND -110°F FOR THE TITANIUM-0.41 PERCENT NITROGEN ALLOY.

Contrails

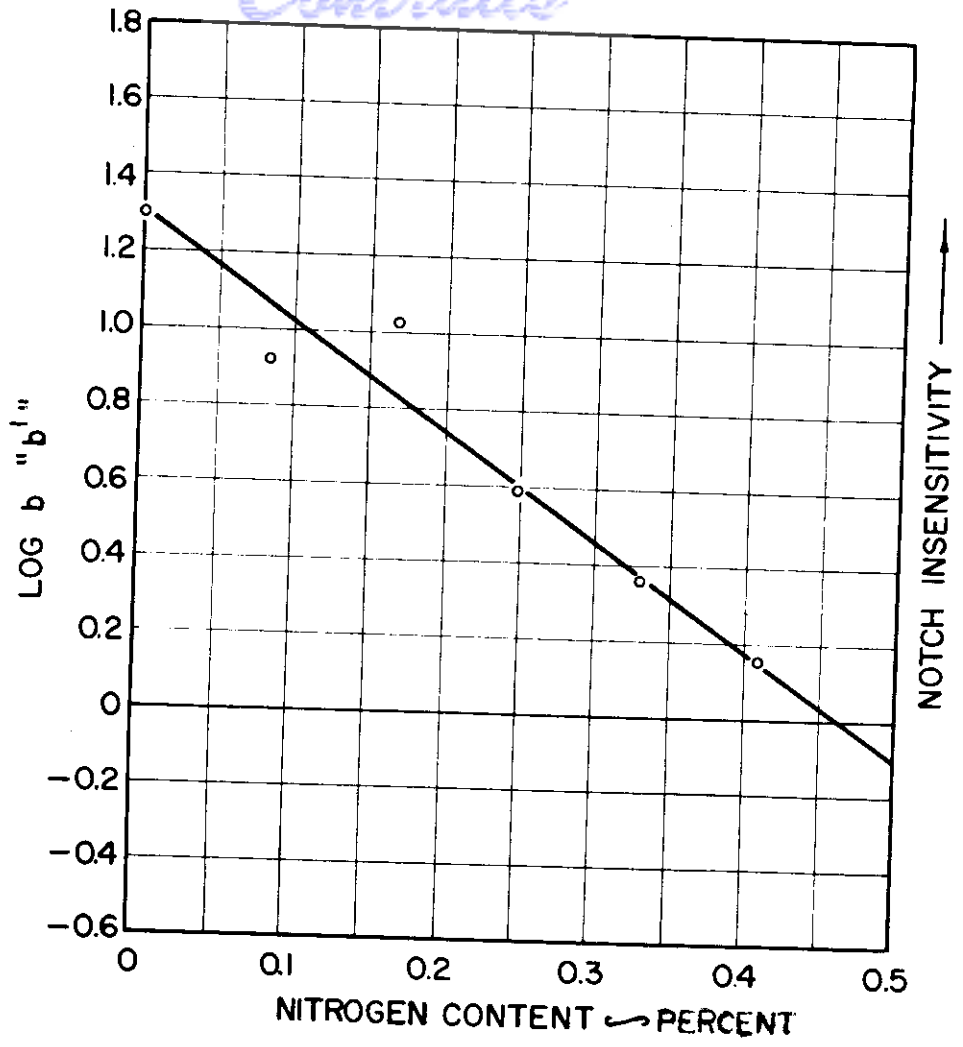


FIG.32:ROOM TEMPERATURE NOTCH SENSITIVITY vs. NITROGEN CONTENT.

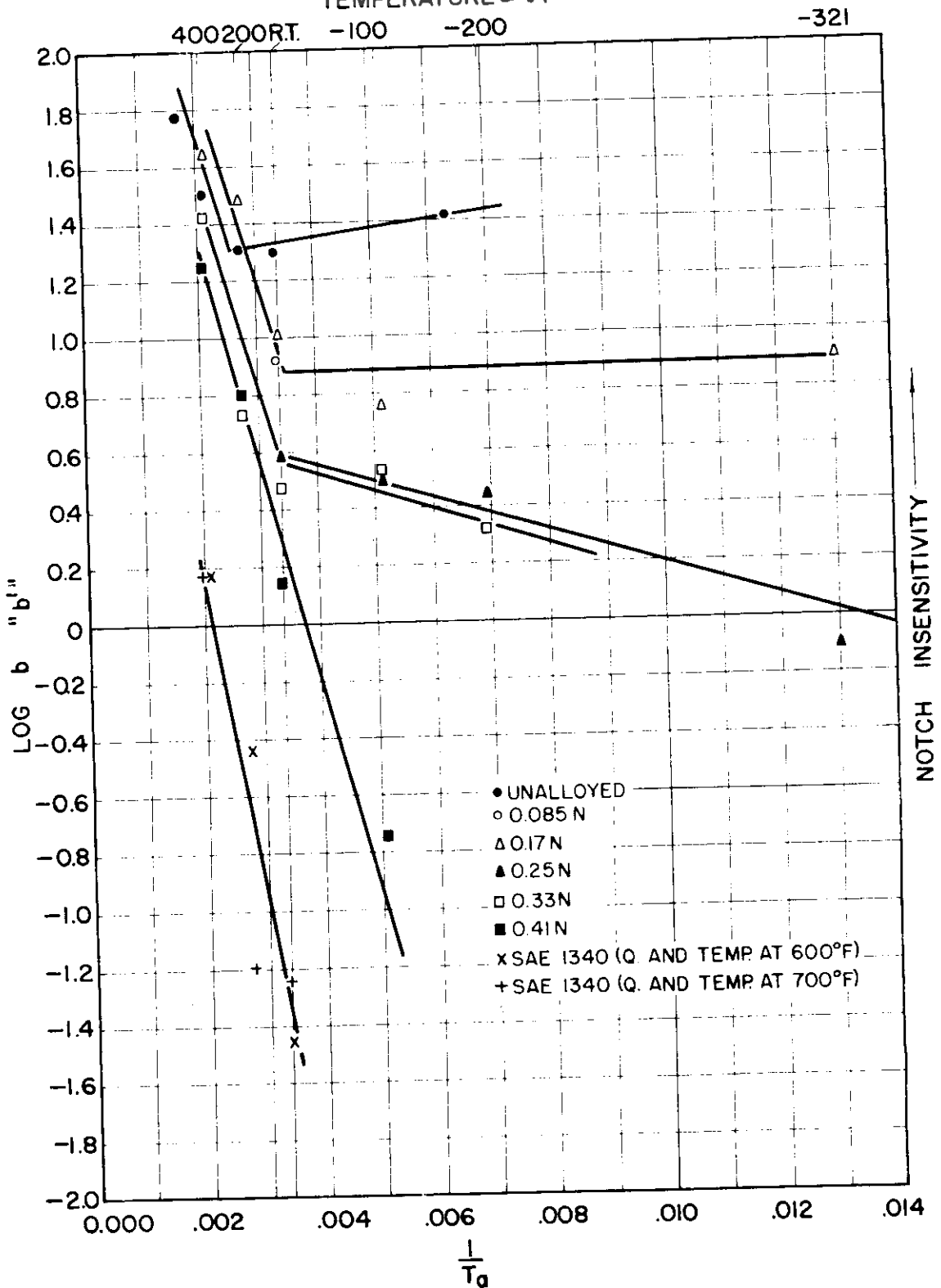


FIG.33:ARRHENIUS TYPE PLOT OF LOG b (b') vs $\frac{1}{T_a}$

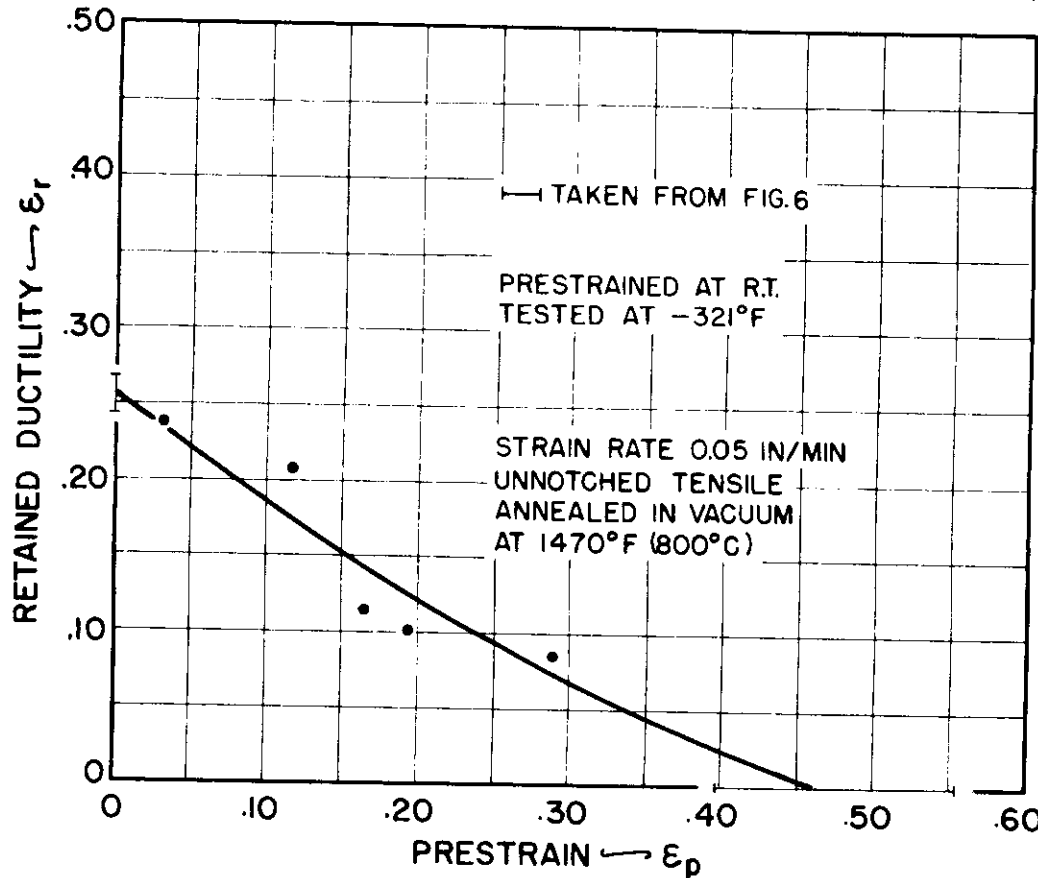
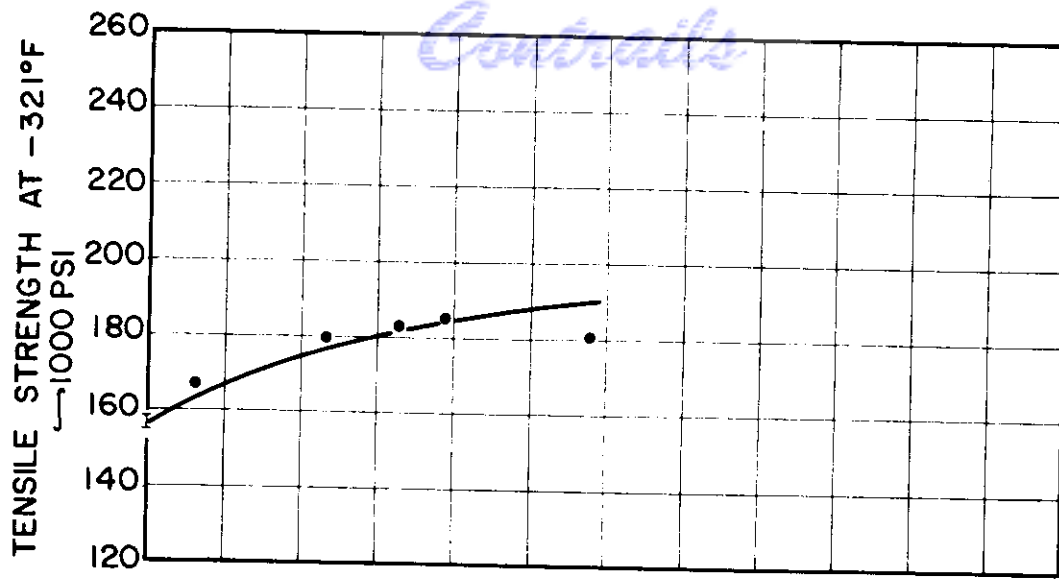


FIG.34: RHEOTROPIC BEHAVIOR OF THE TITANIUM - 0.17 PERCENT NITROGEN ALLOY.

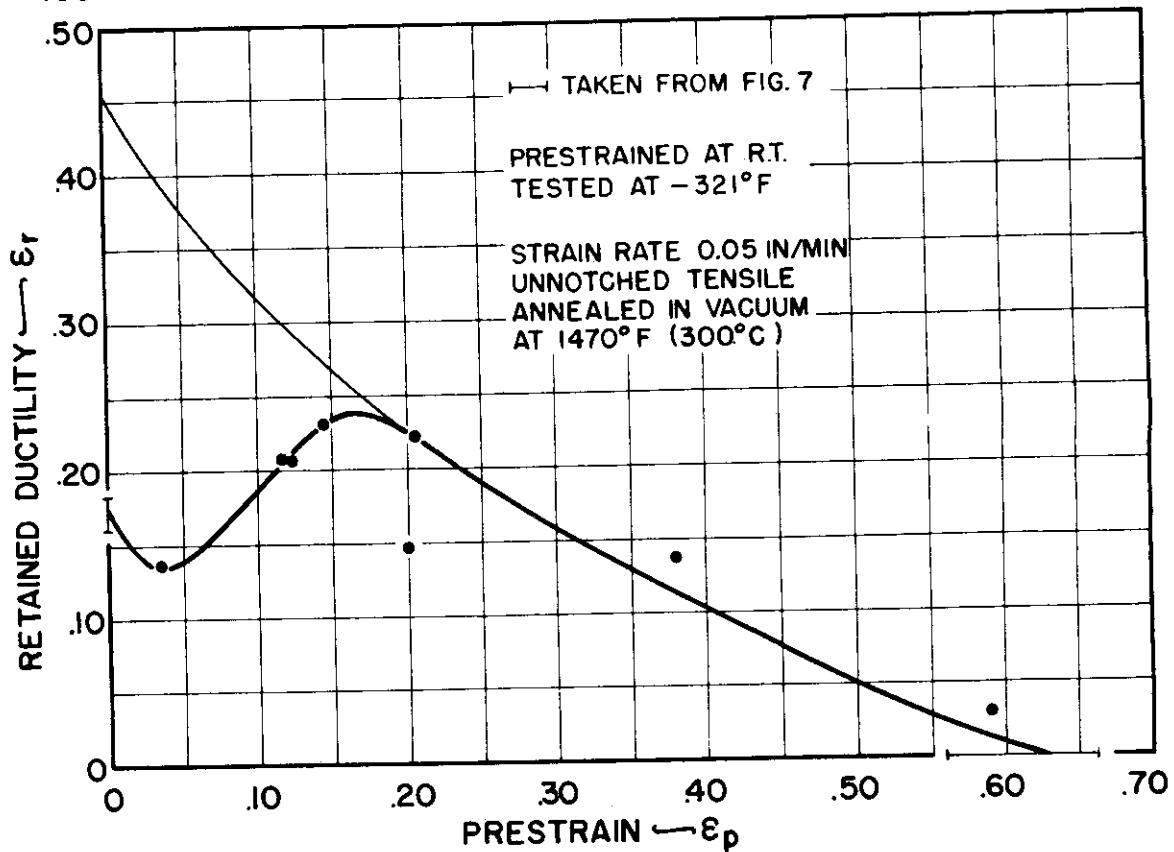
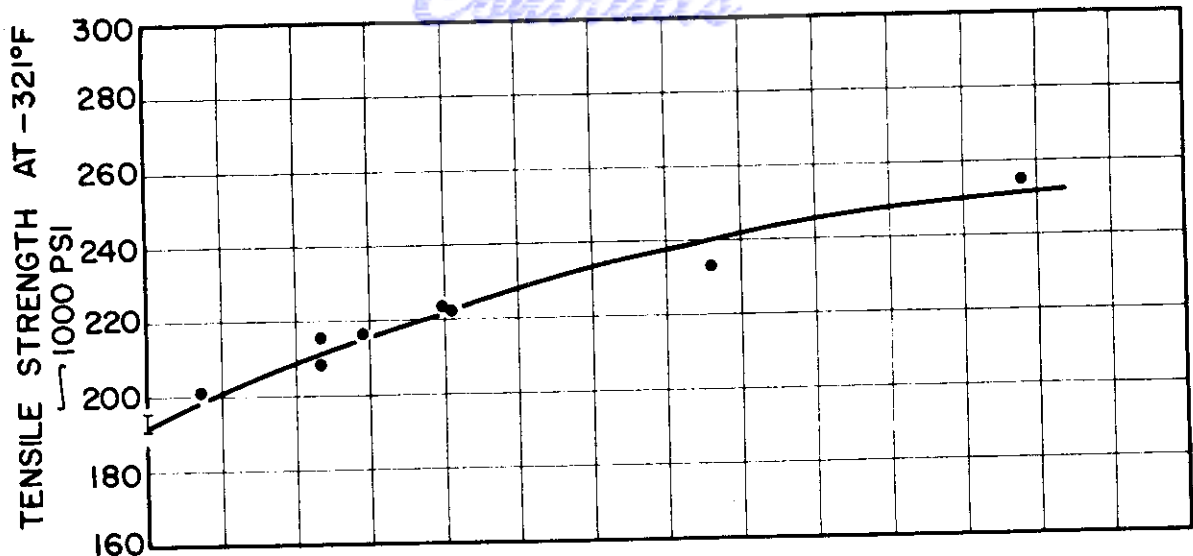


FIG.35. RHEOTROPIC BEHAVIOR OF THE TITANIUM-0.25 PERCENT NITROGEN ALLOY.

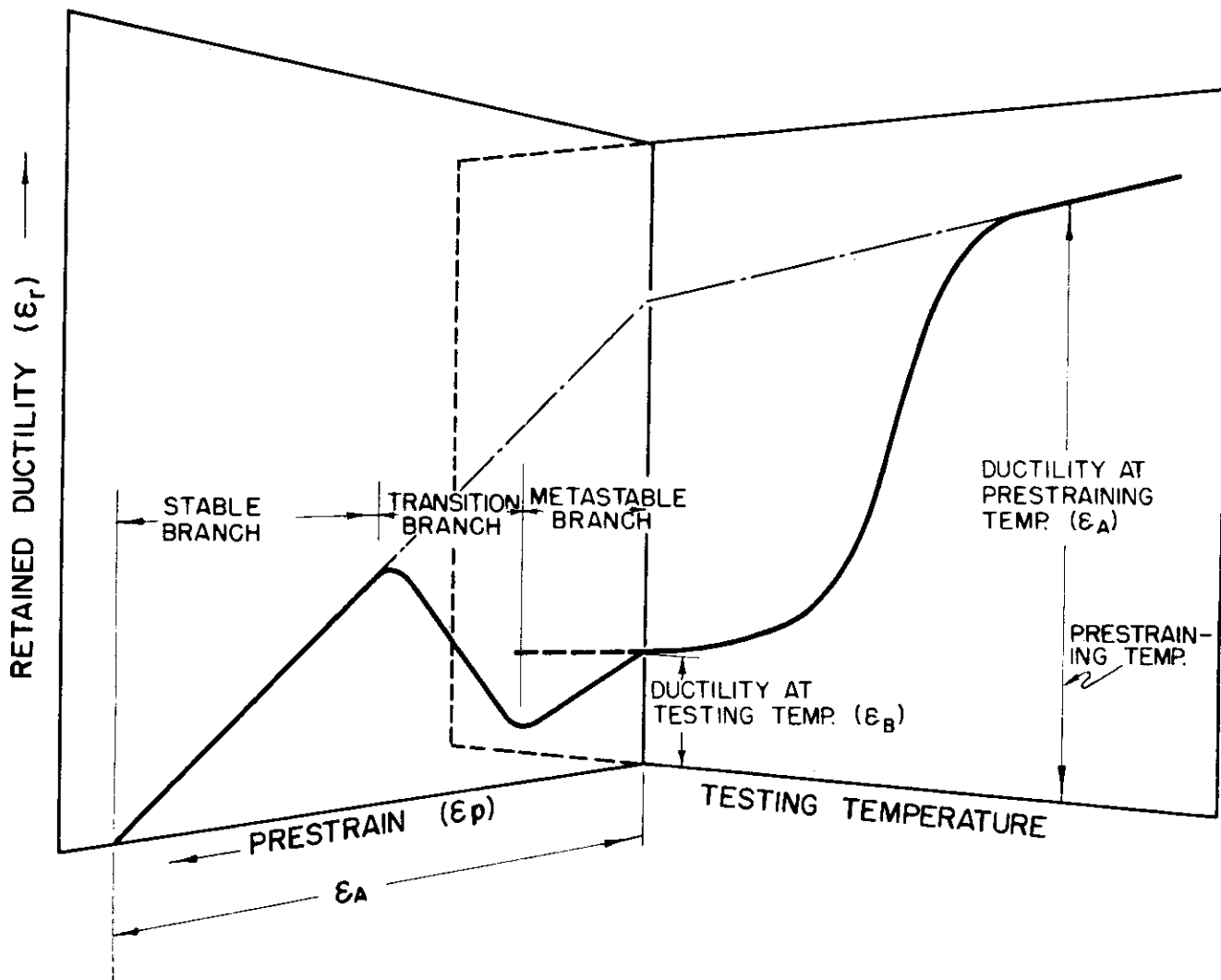


FIG.36: SCHEMATIC REPRESENTATION SHOWING THE CHARACTERISTICS AND NOMENCLATURES APPLIED TO RHEOTROPIC BRITTLENESS.

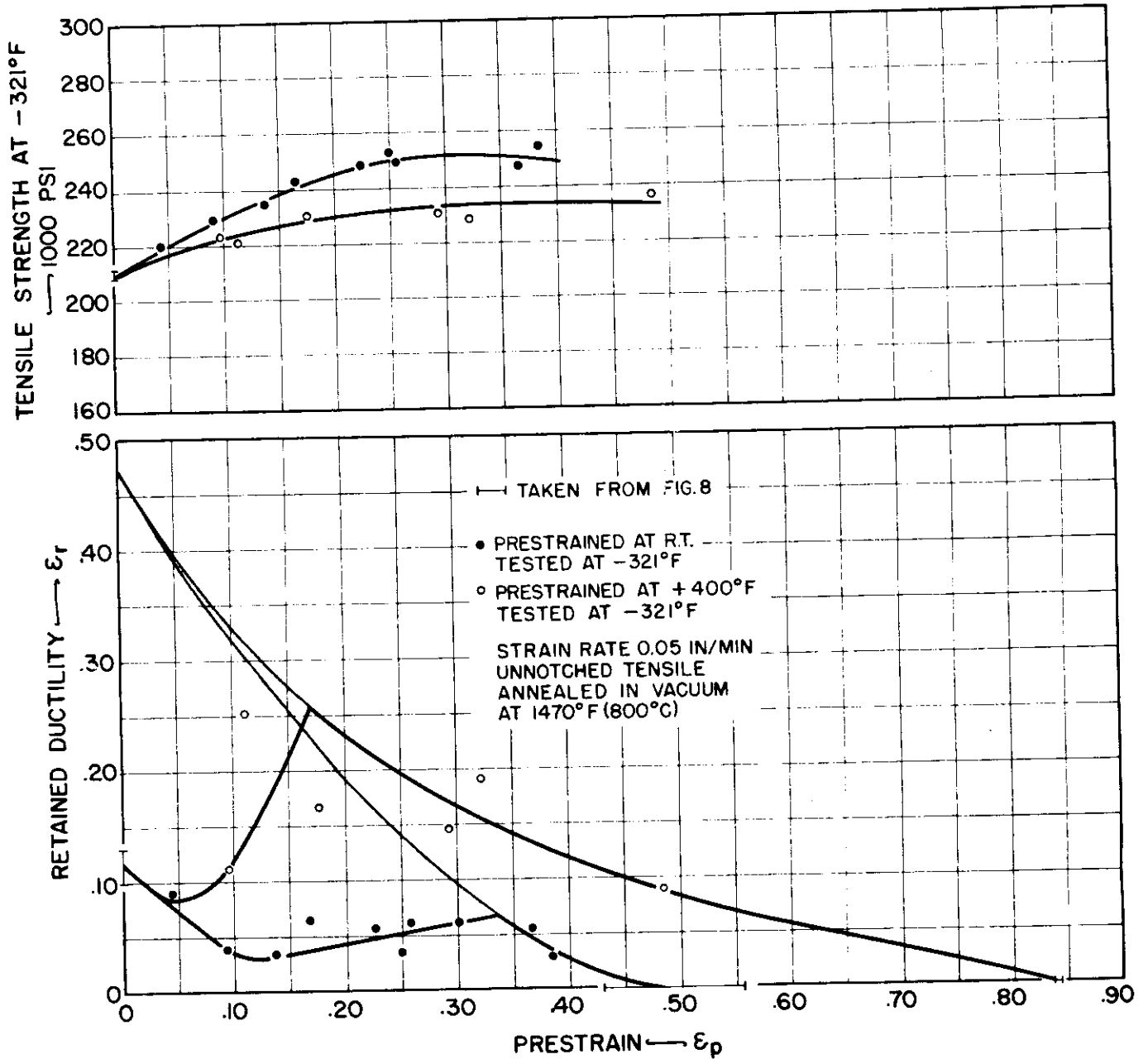


FIG.37 RHEOTROPIC BEHAVIOR OF THE TITANIUM-0.33 PERCENT NITROGEN ALLOY.

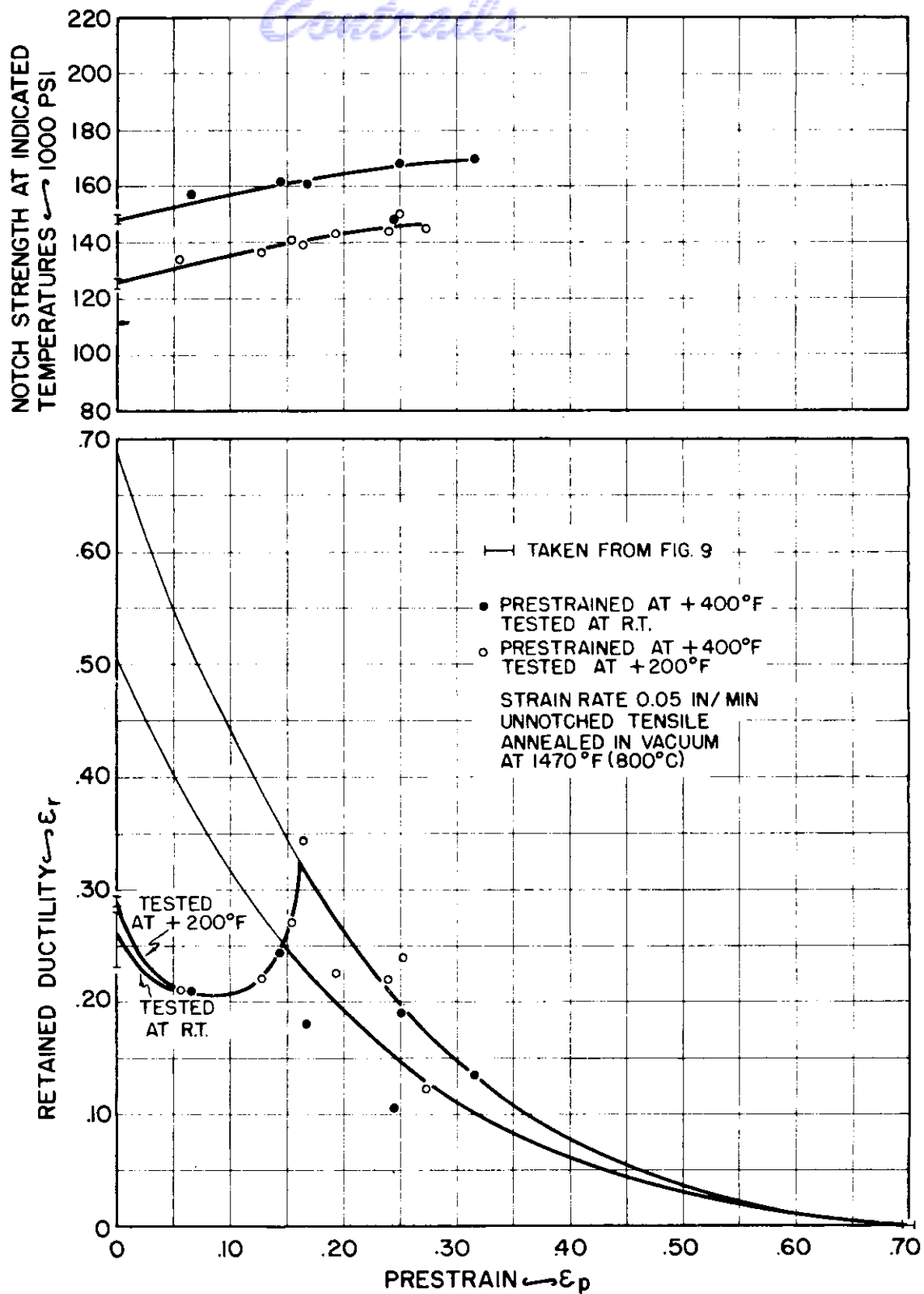


FIG.38: RHEOTROPIC BEHAVIOR OF THE TITANIUM-0.41 PERCENT NITROGEN ALLOY.

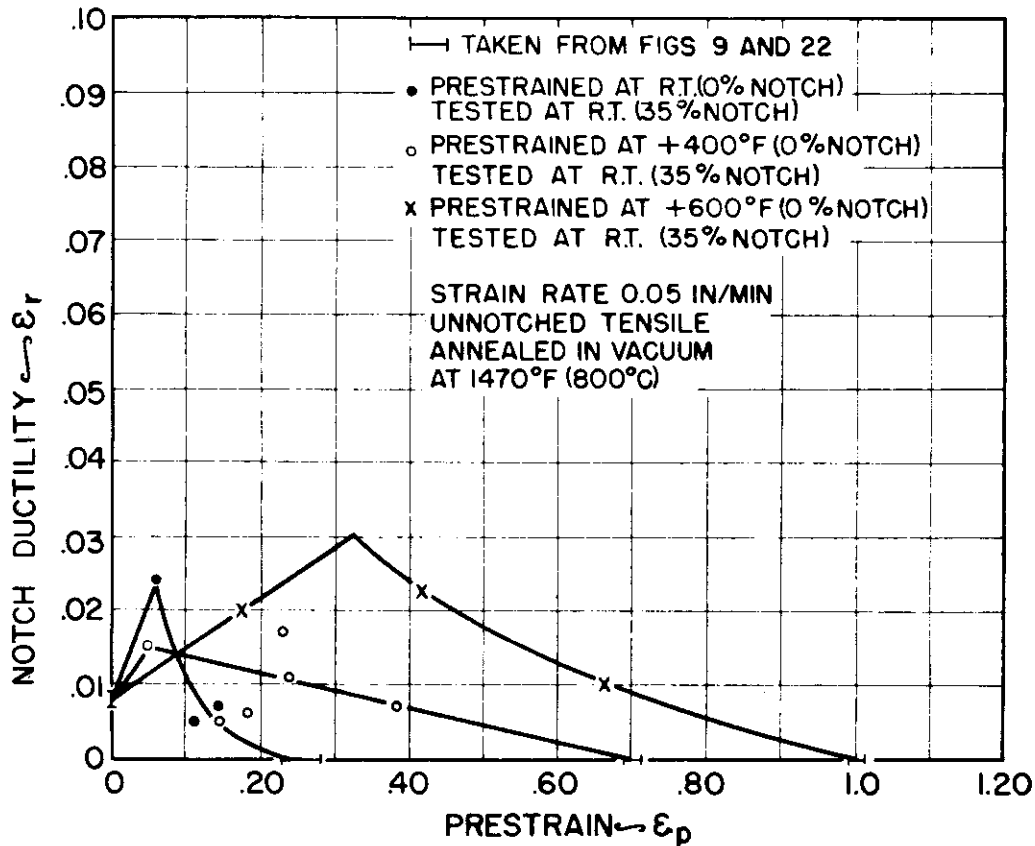
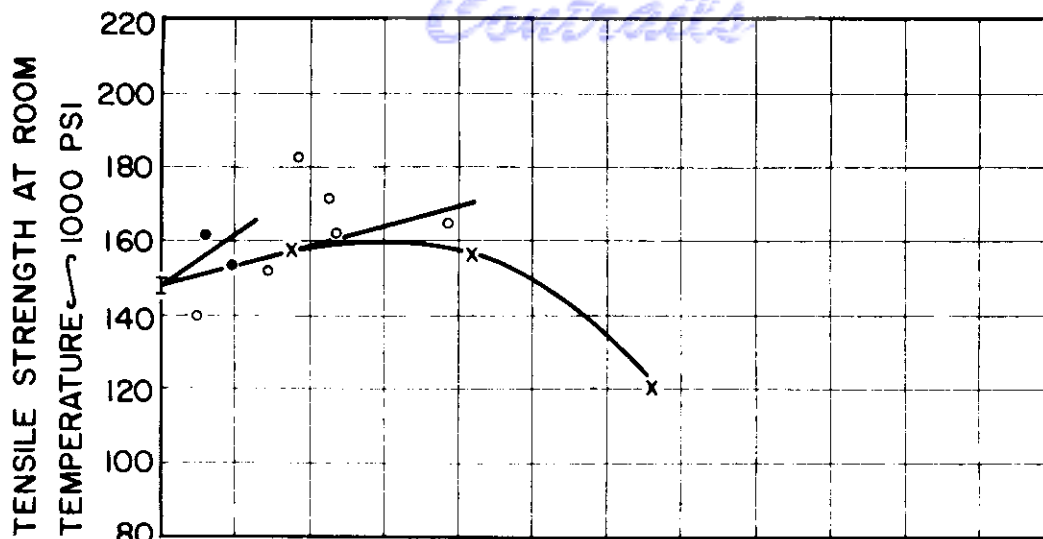


FIG.39: RHEOTROPIC BEHAVIOR OF THE TITANIUM-0.41 PERCENT NITROGEN ALLOY, PRESTRAINED IN THE UNNOTCHED CONDITION AND TESTED IN THE NOTCHED (35%) CONDITION.

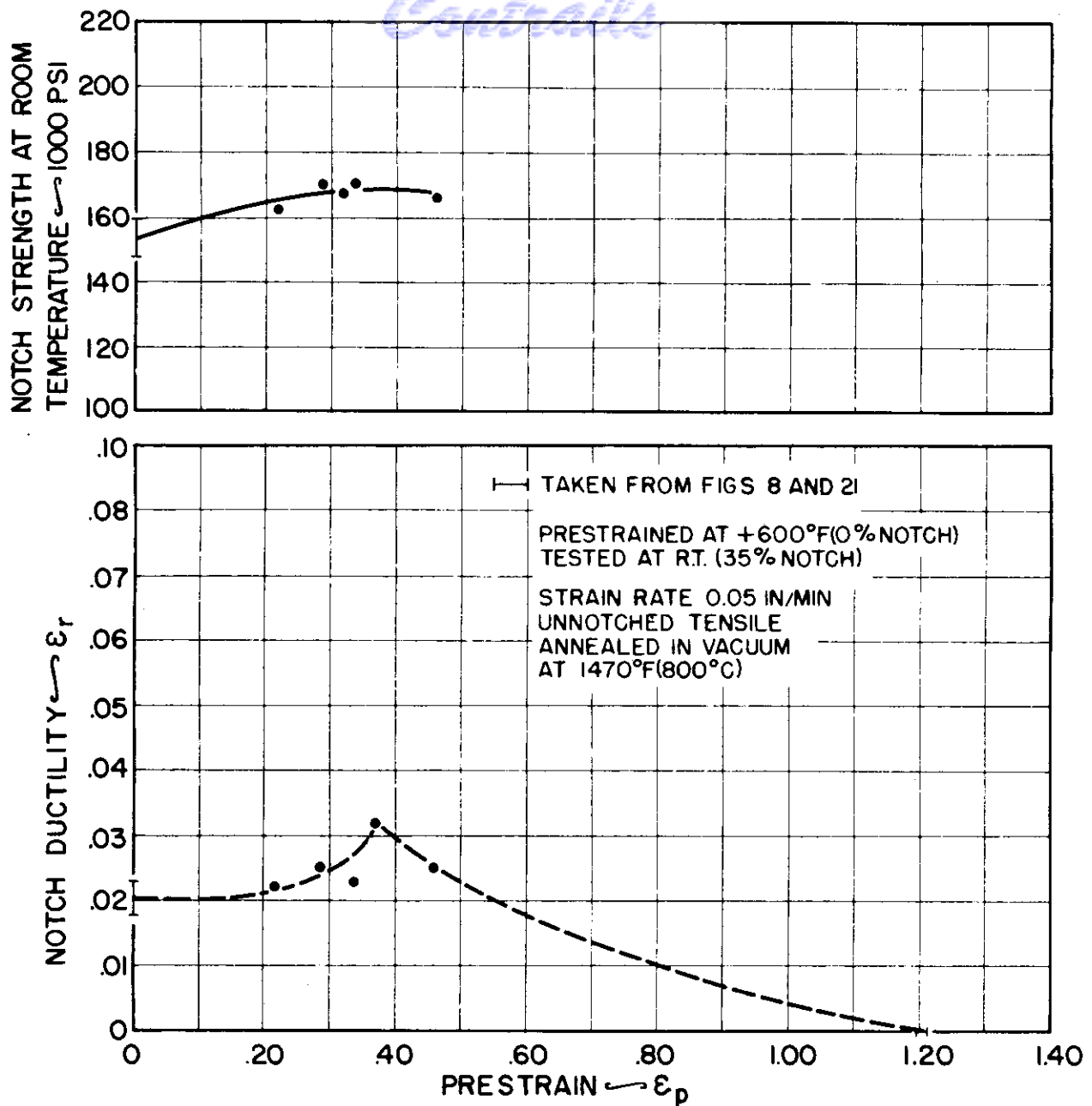


FIG.40: RHEOTROPIC BEHAVIOR OF THE TITANIUM-0.33 PERCENT NITROGEN ALLOY, PRESTRAINED IN THE UNNOTCHED CONDITION AND TESTED IN THE NOTCHED (35%) CONDITION.

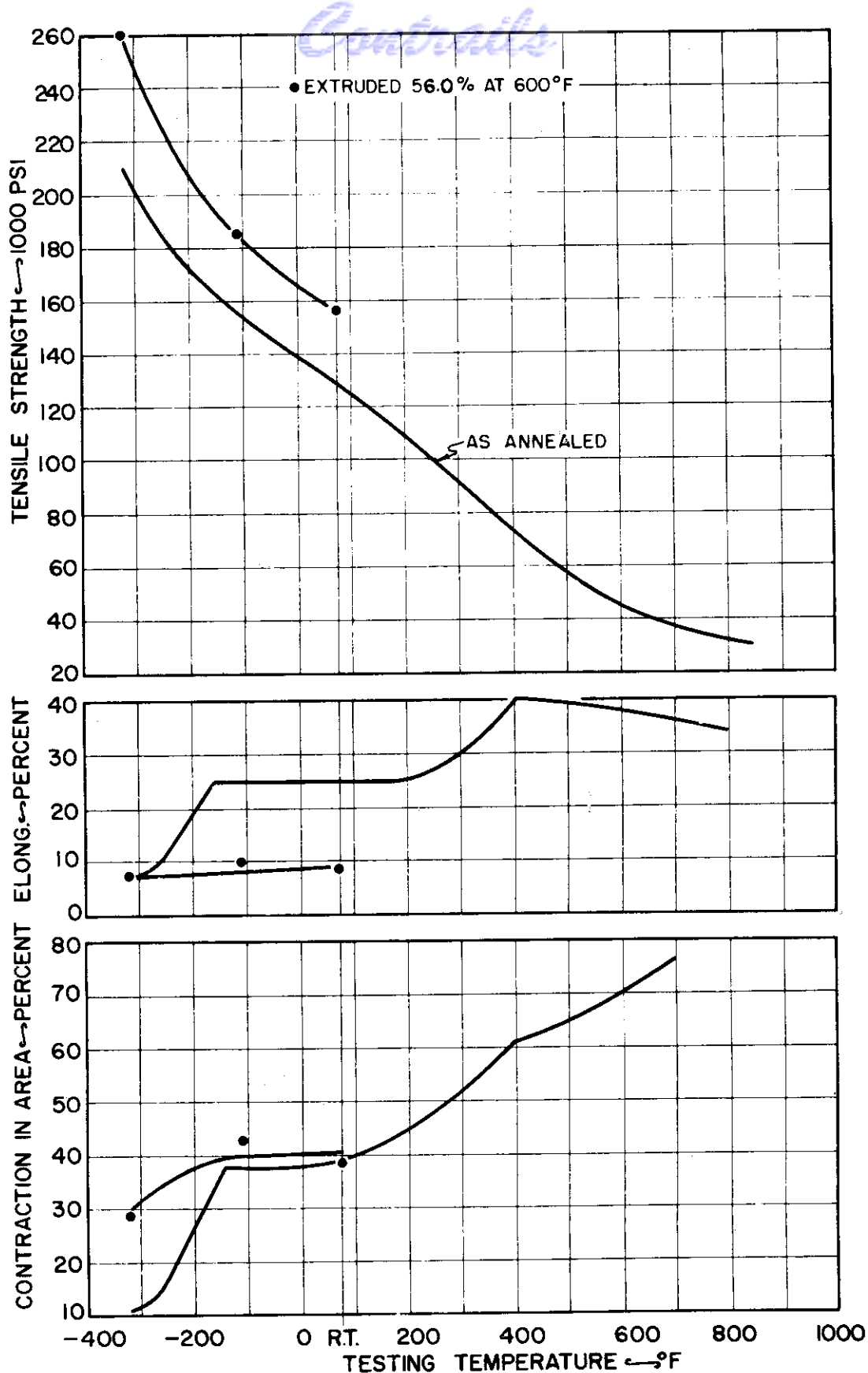


FIG. 41 : RHEOTROPIC RECOVERY PRODUCED IN THE TITANIUM-0.33 PERCENT NITROGEN ALLOY BY EXTRUDING.

Contrails

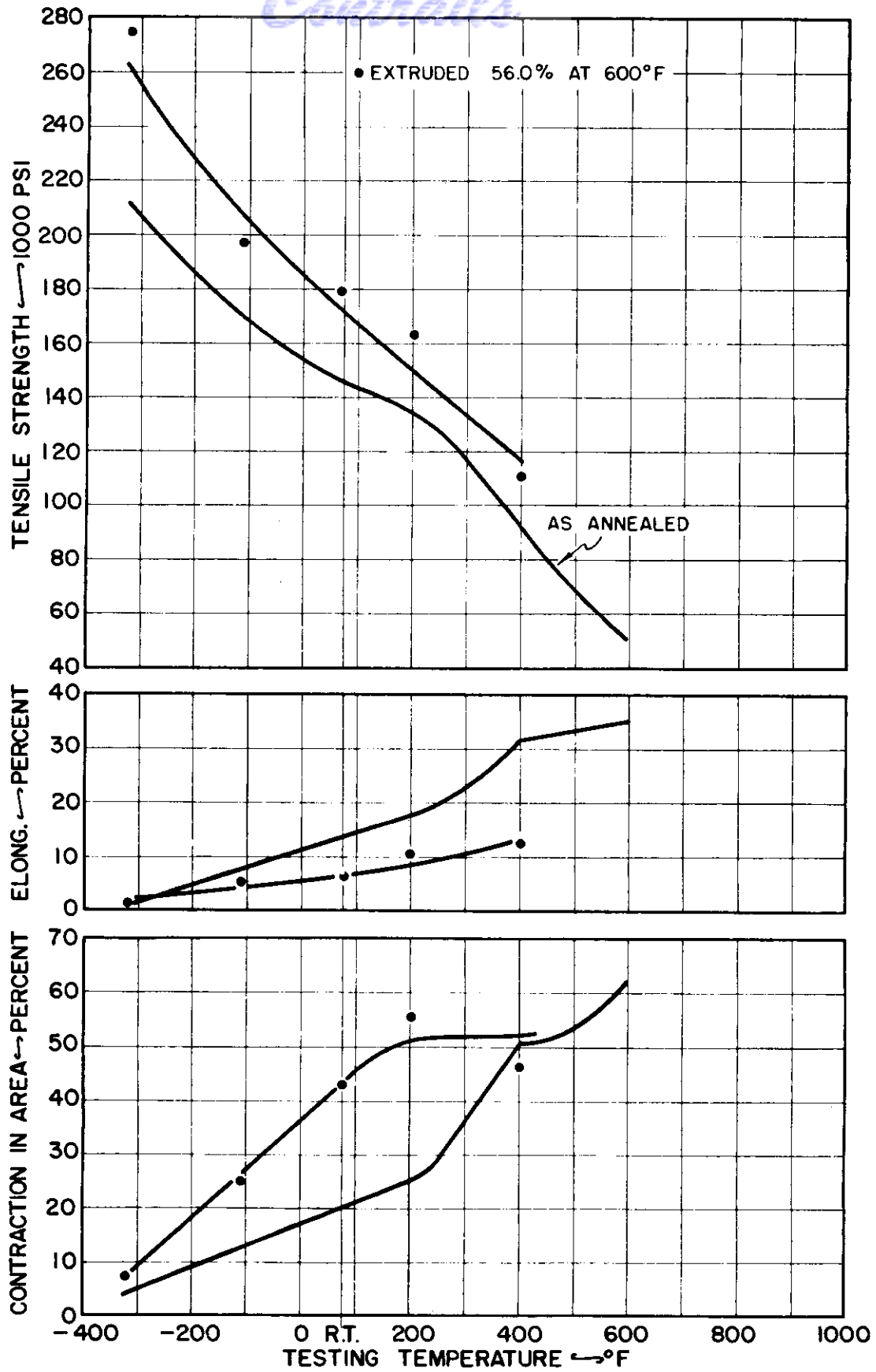


FIG.42: RHEOTROPIC RECOVERY PRODUCED IN THE TITANIUM-0.41 PERCENT NITROGEN ALLOY BY EXTRUDING.

TENSILE AND RHEOTROPIC BEHAVIOR
OF TITANIUM-MANGANESE ALLOYSINTRODUCTION

Hardening and a concurrent reduction of ductility in titanium alloys is produced not only by interstitial contaminants such as nitrogen, but also by alloying elements of a substitutional type as well. This latter class of alloying elements, however, is thought to produce the strengthening with only minor losses in ductility and toughness as compared with the ductility damage done by interstitial alloying elements.

In order to determine whether or not the addition of a substitutional alloying element produces a transition effect, or shifts an already existent transition temperature, the tensile and rheotropic behavior of a number of titanium-manganese alloys were also investigated. The investigation of these alloys was restricted to a study of whether or not the alloying element additions developed a transition temperature in the titanium base alloy and if so, whether or not the sub-transition temperature ductility deficiency is amenable to a rheotropic recovery.

Manganese was chosen as the alloying element in this test series because it is a beta stabilizer and hence made possible the study of alpha-beta alloys. Further, a large amount of data are

Contrails
already available on this alloy system.

Because manganese is a beta stabilizer, the investigation was complicated by the vast number of microstructures that could be developed in these alloys. For this reason, the alloys were used in the annealed condition, and the annealing temperature was selected for each of the alloys so as to form approximately the same relative amounts of alpha and beta on heat treating. The greatest difference in the alloys was presumed to be the composition of the beta.

MATERIAL AND PROCEDURE

Six binary titanium-manganese alloys were made for this investigation by the Battelle Memorial Institute using the same base sponge as that used in making the titanium-nitrogen alloys. The manganese was added as a 50-50 master alloy. The alloys were melted and further processed in the same fashion as that described in Part I for the titanium-nitrogen alloys. The composition of the alloys used in this investigation along with their annealing temperatures are shown in Table II.

TABLE II

MANGANESE CONTENT AND
ANNEALING TEMPERATURES OF ALLOYS

Manganese Content	Annealing Temperature
Unalloyed	1470°F (800°C)
1.69 percent	1470 (800)
4.68	1380 (750)
5.40	1380 (750)
5.75	1380 (750)
8.0	1290 (700)

The specimens were rough machined to the shape shown in Fig. 1-a of Part I, after which they were vacuum annealed for two hours at the temperatures shown in Table II, and slowly cooled. The heat treating temperatures in Table I were selected so that the alloys had roughly the same relative beta contents. These annealed specimens were then finish machined to the shapes shown in Fig. 1-a, Part I.

Photomicrographs of the heads of broken test bars are shown in Fig. 43.

The testing procedure used on these alloys is the same as that previously described for the nitrogen alloys.

RESULTS AND DISCUSSION

The tensile properties of the annealed alloys are shown in Figs. 44 to 49 as a function of the testing temperature. A manganese

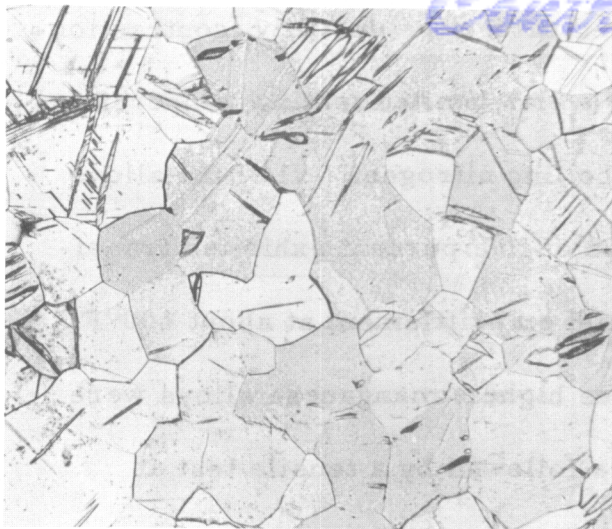
content of 5.4 percent was required before the ductility (contraction in area) exhibited an abrupt drop over a limited testing temperature range, above the temperature of boiling nitrogen. All of the alloys with manganese contents in excess of five percent exhibited transition temperatures as well as a mild embrittlement at about 600°F.

Specimens of each of the three highest manganese alloys were prestretched at room temperature followed by a tensile test at -321°F. As shown in Figs. 50, 51 and 52, the 5.4 and the 5.8 manganese alloys underwent a rheotropic recovery while the 8.0 manganese alloy did not.

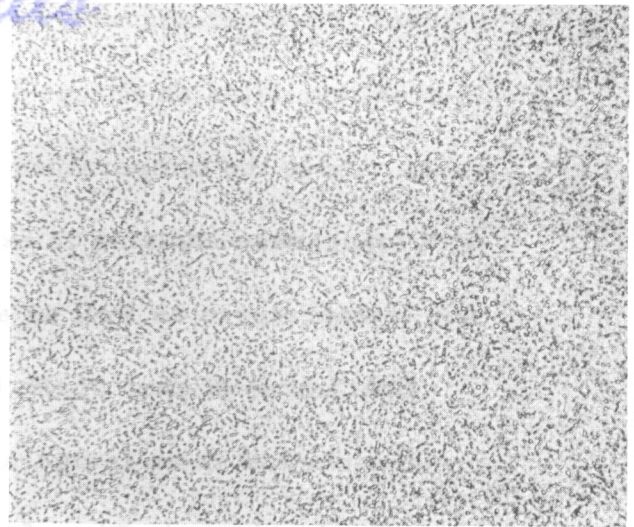
CONCLUSIONS

1. Annealed alpha-beta binary alloys (titanium-manganese) exhibit a transition above the temperature of boiling nitrogen when a sufficiently large amount of alloying element was added.
2. This transition temperature may or may not be amenable to a rheotropic recovery depending on the alloy content.

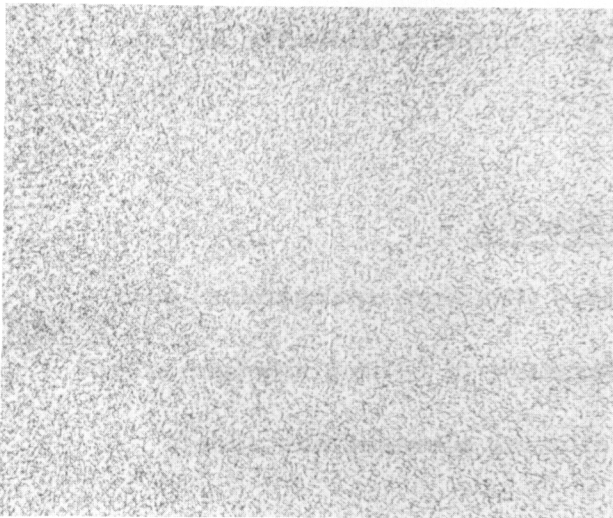
Contrails



UNALLOYED



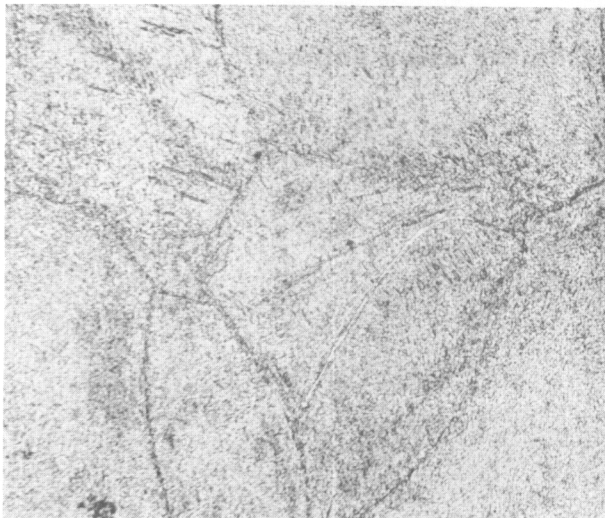
1.69 Mn



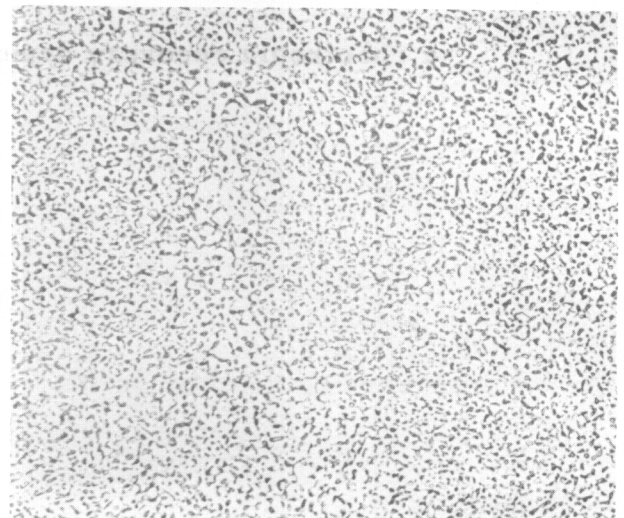
4.65 Mn



5.40 Mn



5.75 Mn



8.0 Mn
250X

ELECTROLYTIC POLISH AND ETCH

FIG.43 MICROSTRUCTURE OF VACUUM ANNEALED TITANIUM-Mn ALLOYS.

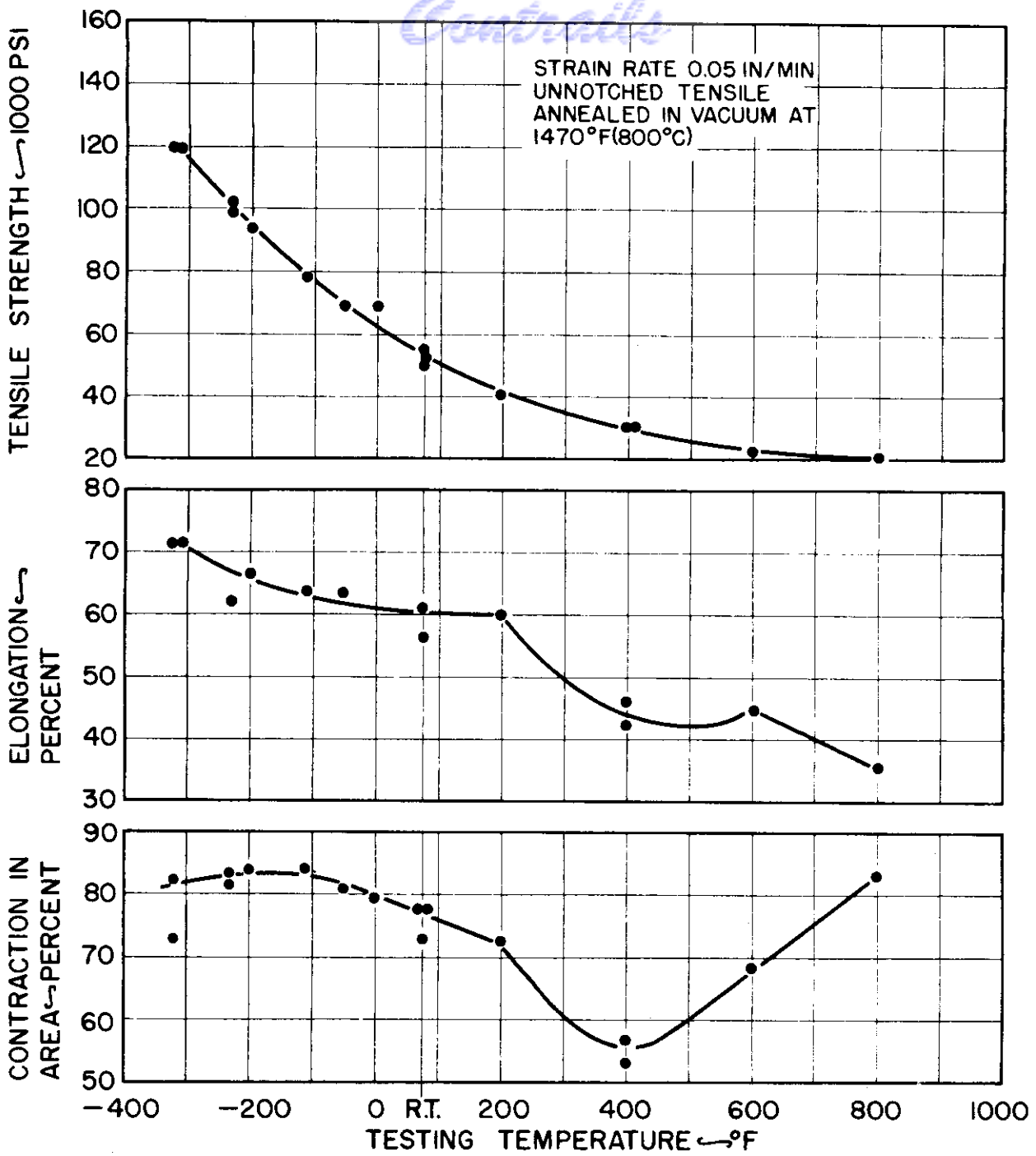


FIG.44:UNNOTCHED TENSILE PROPERTIES vs. TESTING TEMPERATURE FOR UNALLOYED TITANIUM.

Contrails

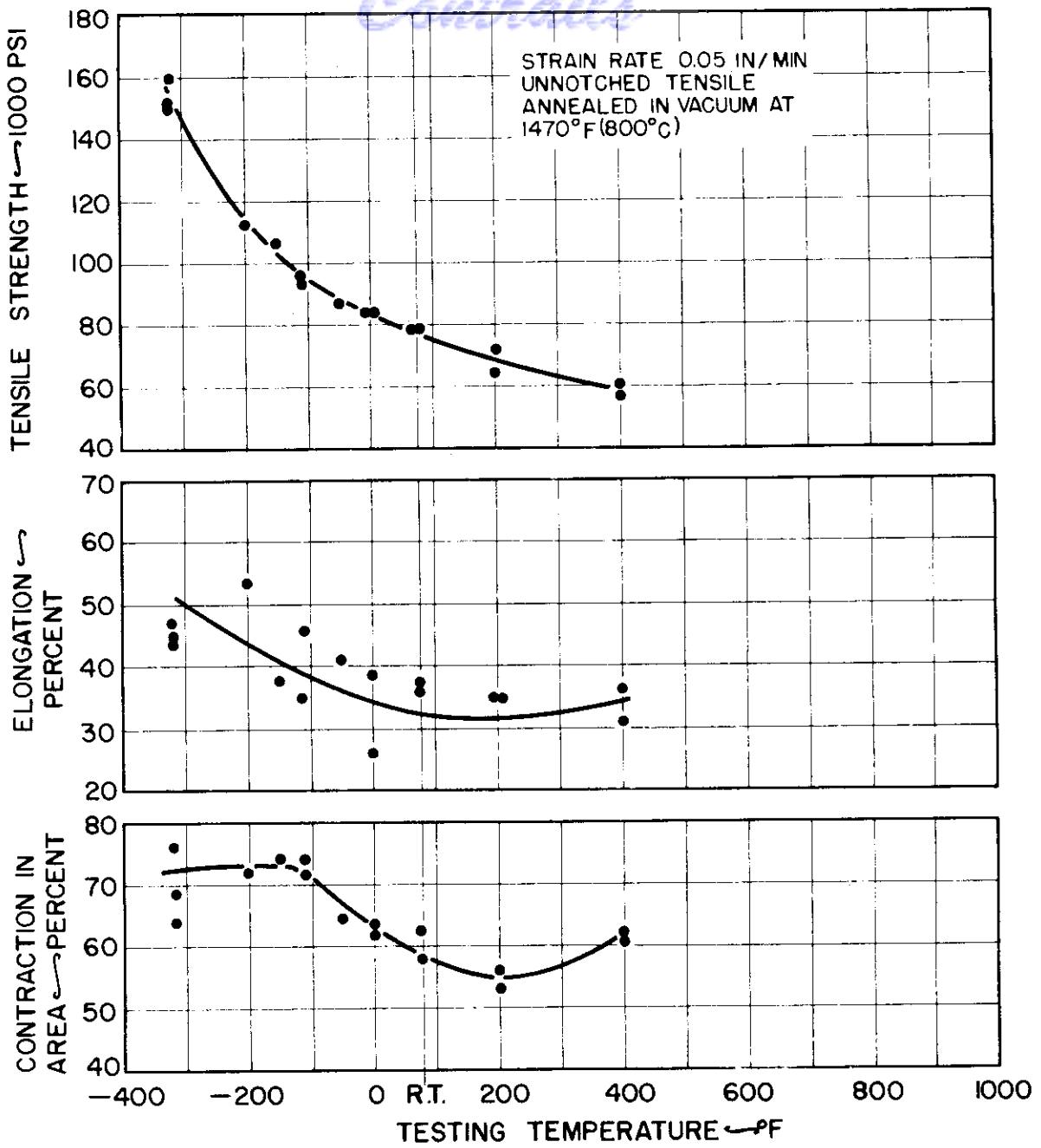


FIG.45 UNNOTCHED TENSILE PROPERTIES vs. TESTING TEMPERATURE FOR THE TITANIUM-1.69 PERCENT MANGANESE ALLOY.

Continuity

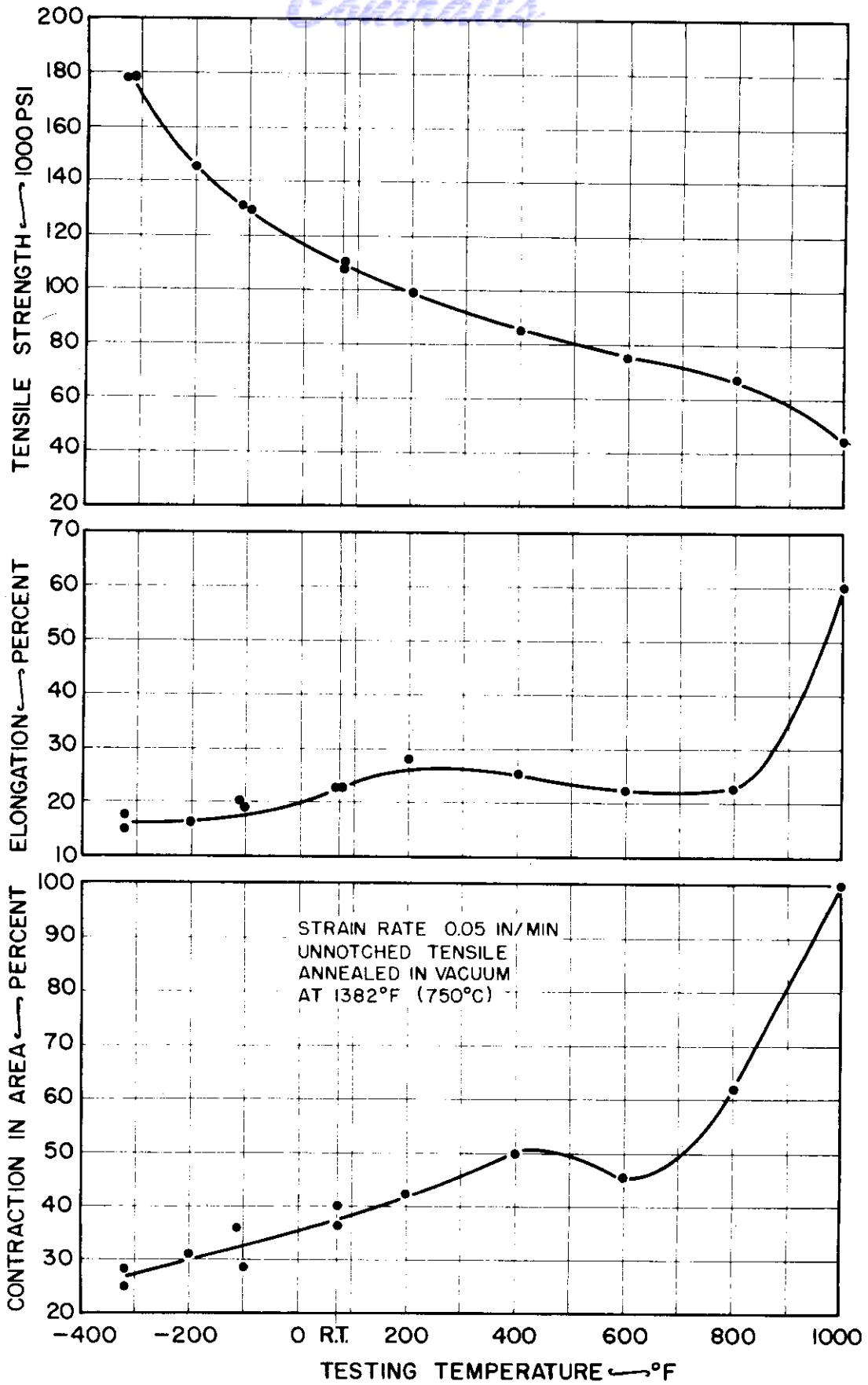


FIG.46: UNNOTCHED TENSILE PROPERTIES vs. TESTING TEMPERATURE FOR THE TITANIUM-4.68 PERCENT MANGANESE ALLOY.

WADC TR 55-5

Controls

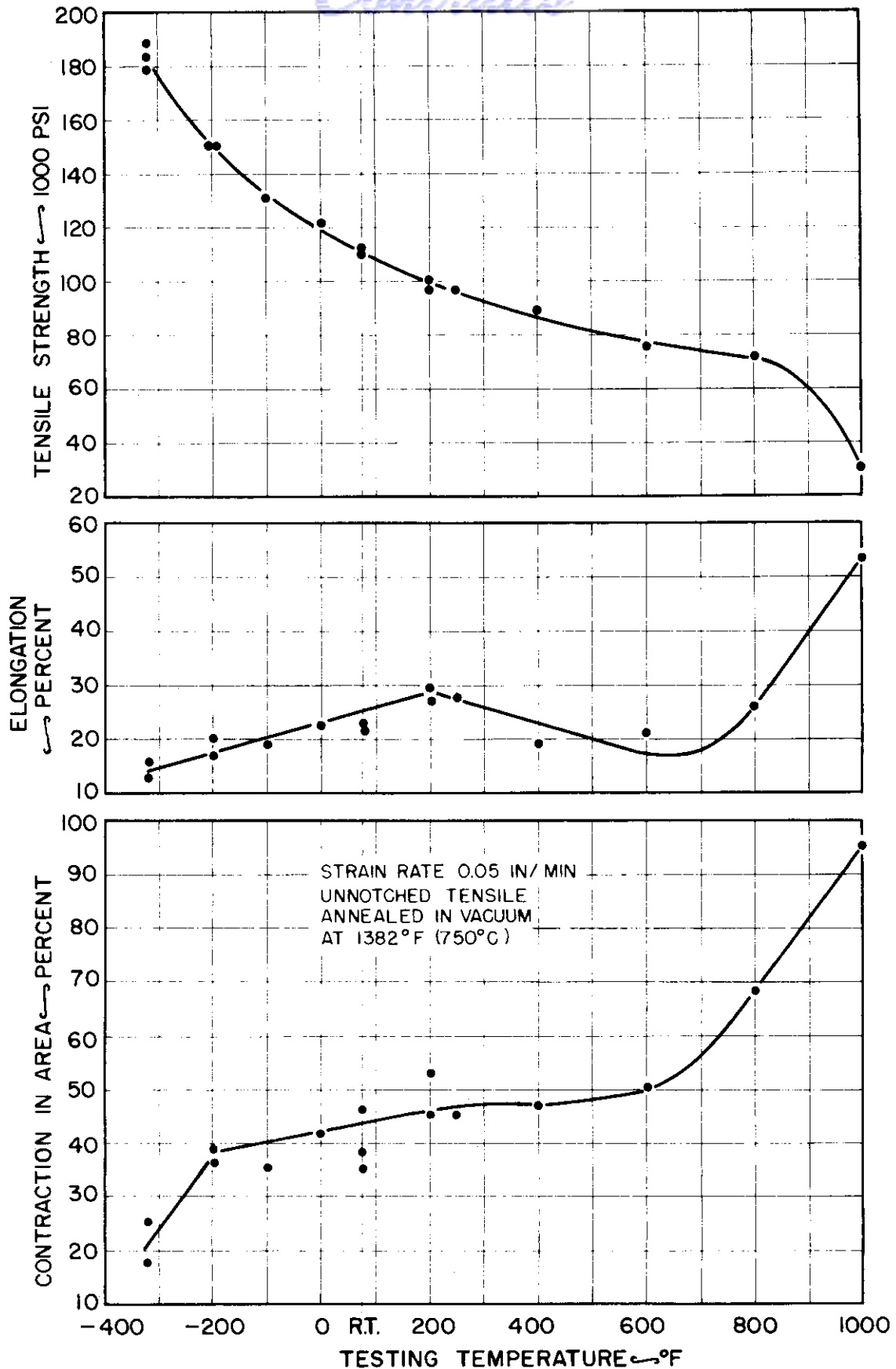


FIG. 47: UNNOTCHED TENSILE PROPERTIES vs. TESTING TEMPERATURE FOR THE TITANIUM-540 PERCENT MANGANESE ALLOY.

Controls

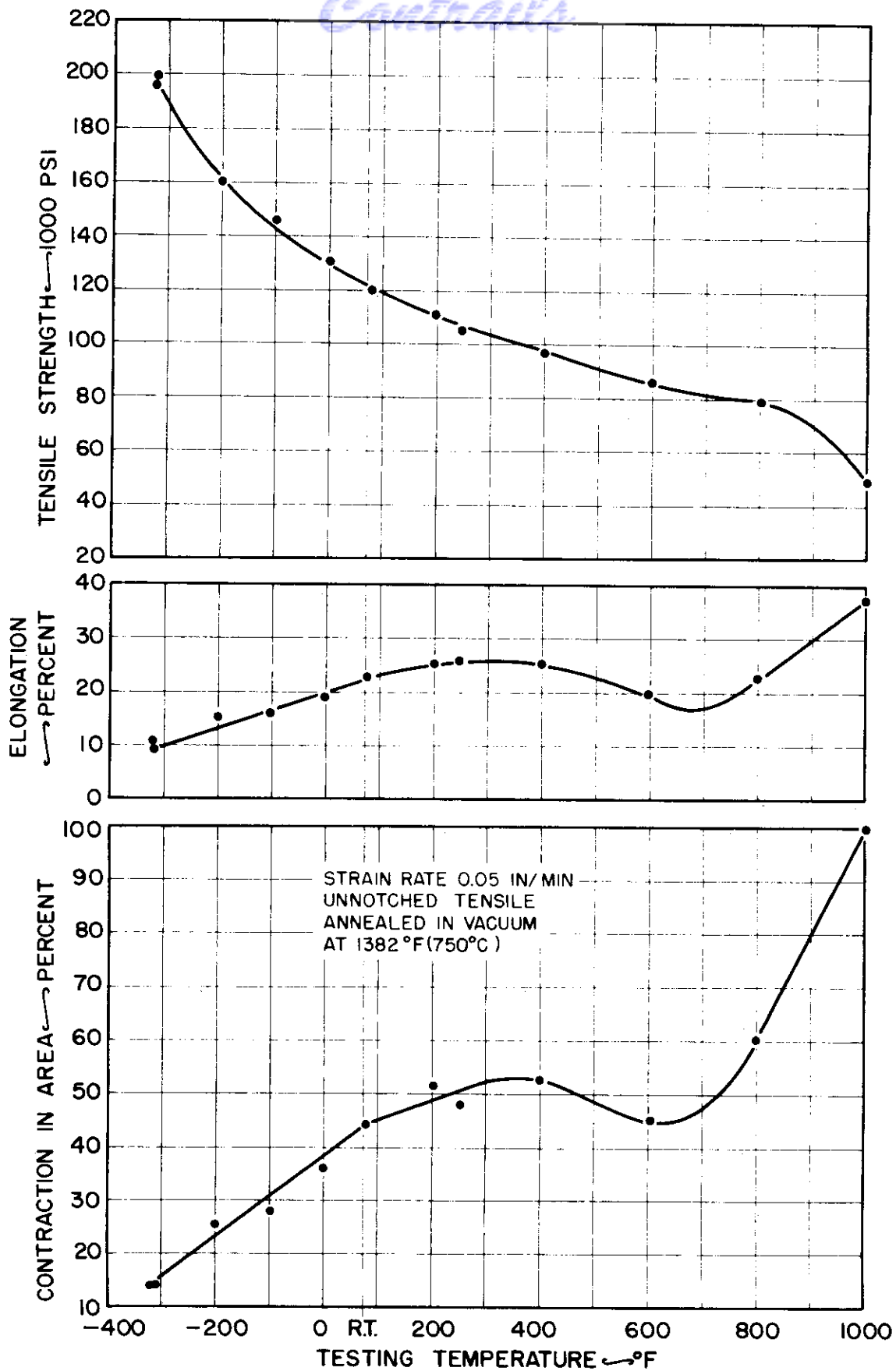


FIG.48 UNNOTCHED TENSILE PROPERTIES vs. TESTING TEMPERATURE FOR THE TITANIUM-5.75 PERCENT MANGANESE ALLOY.

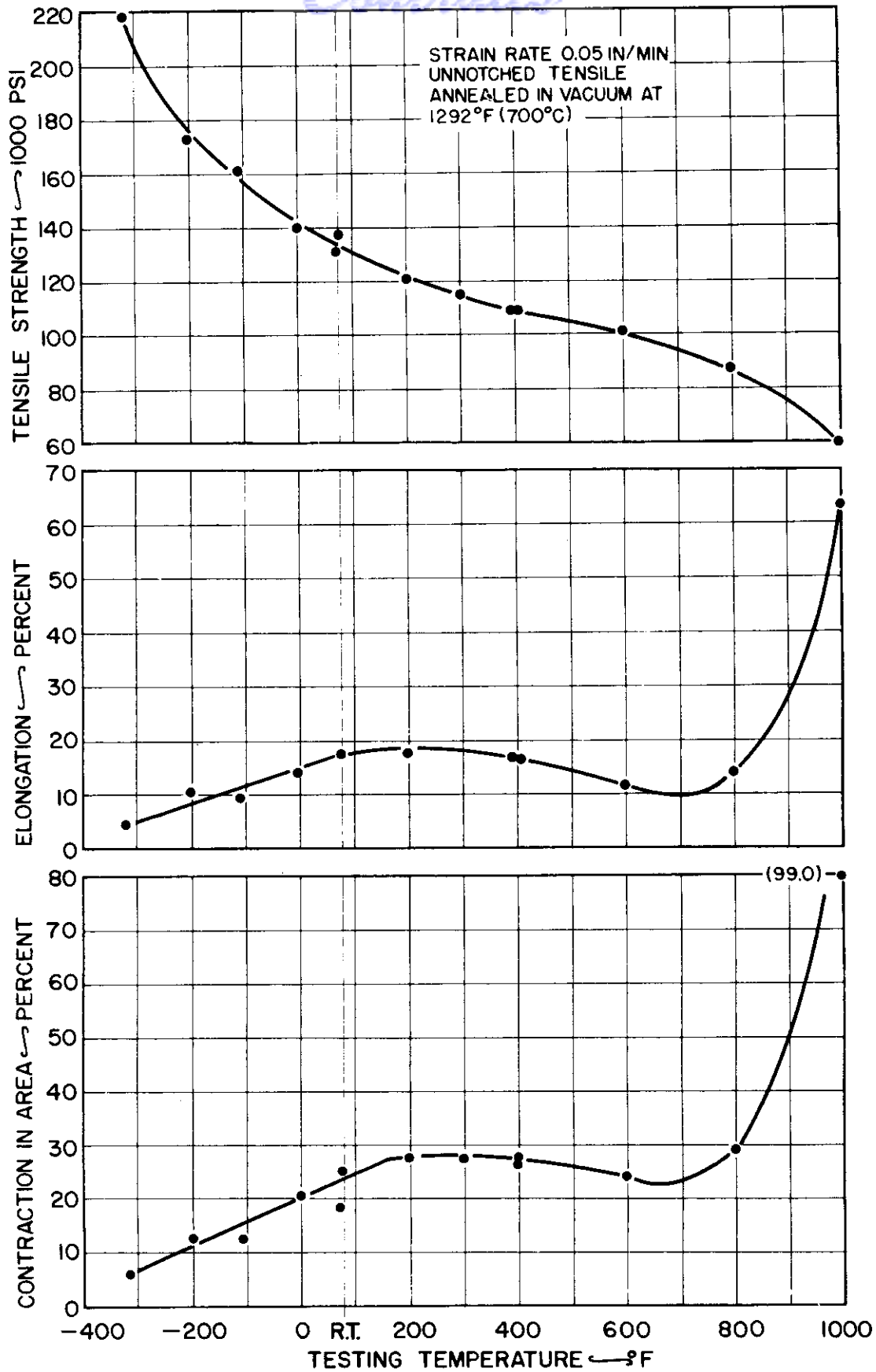


FIG.49: UNNOTCHED TENSILE PROPERTIES vs. TESTING TEMPERATURE FOR THE TITANIUM-8.0 PERCENT MANGANESE ALLOY.

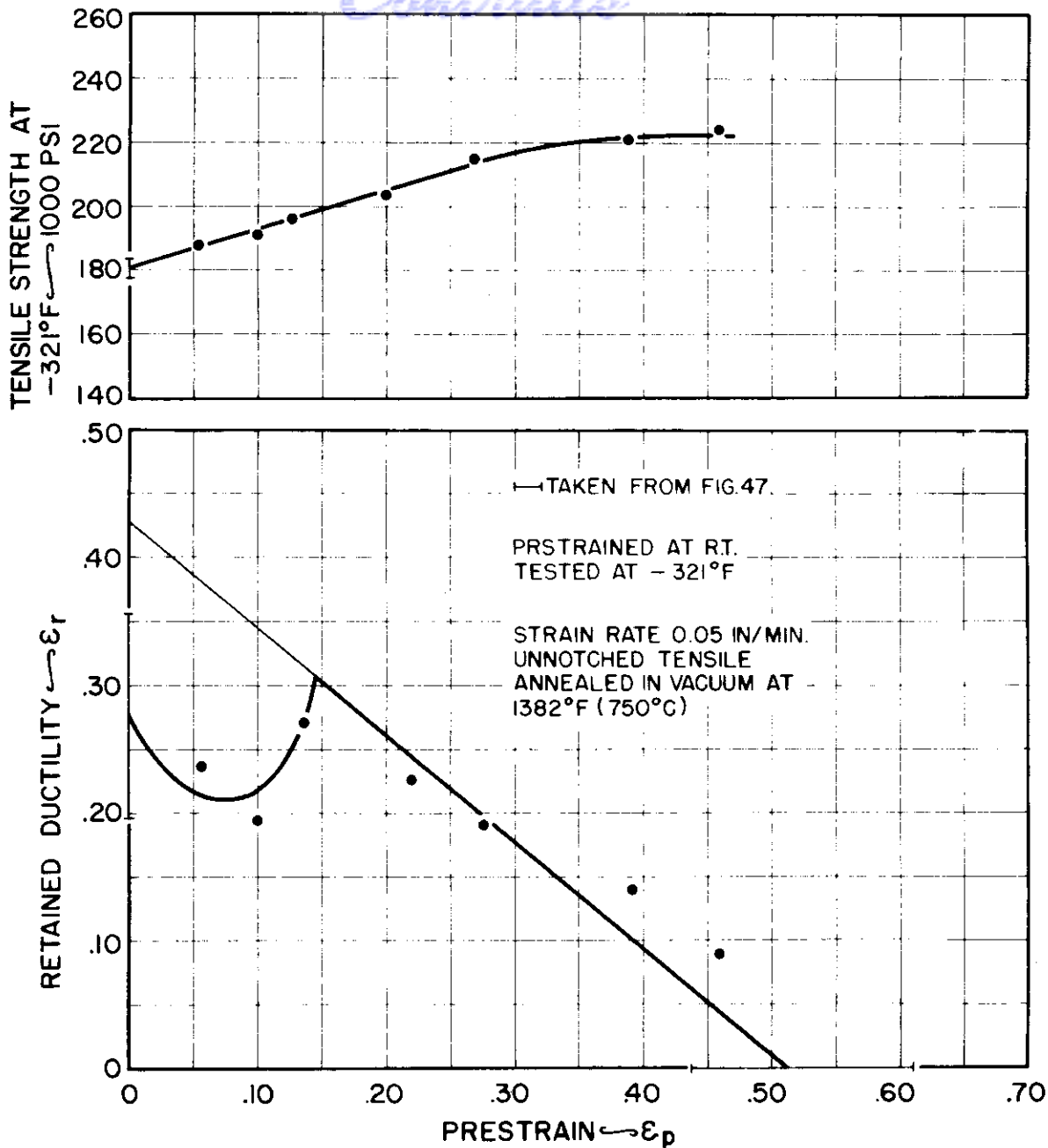


FIG. 50: RHEOTROPIC BEHAVIOR OF THE TITANIUM-5.40 PERCENT MANGANESE ALLOY.

Controls

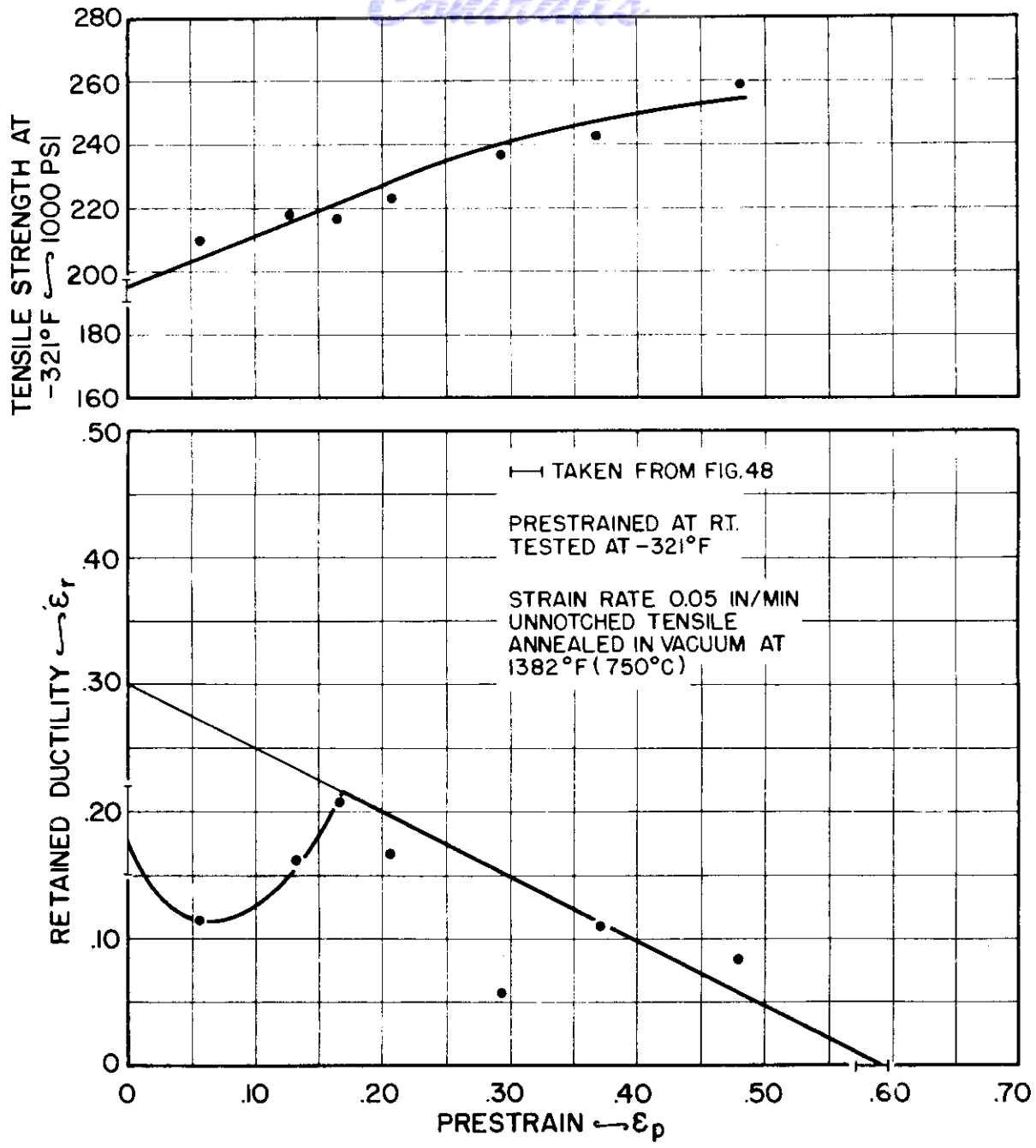


FIG.5 I: RHEOTROPIC BEHAVIOR OF THE TITANIUM-5.75 PERCENT MANGANESE ALLOY.

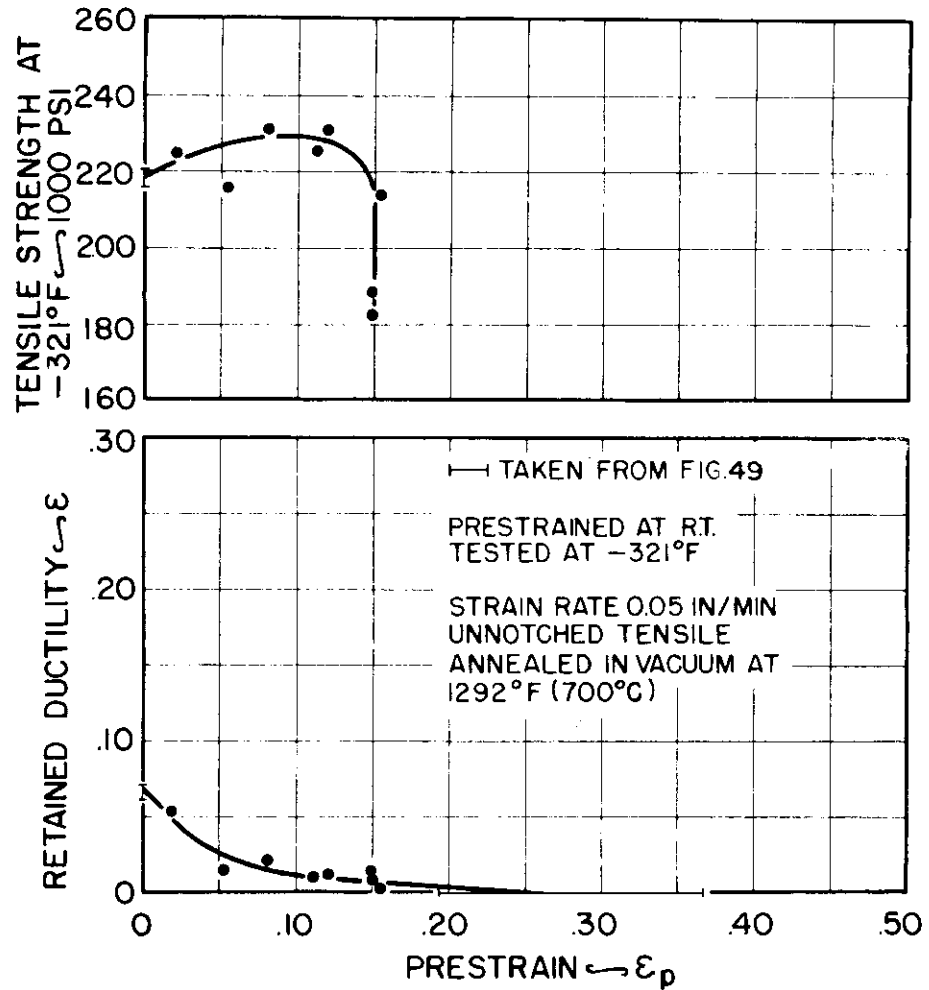


FIG.52 RHEOTROPIC BEHAVIOR FOR TITANIUM—8.0 PERCENT MANGANESE ALLOY.

TENSILE AND RHEOTROPIC BEHAVIOR OF A COMMERCIAL
AND AN EXPERIMENTAL ALLOYINTRODUCTION

In addition to investigating the mechanical properties of the interstitial and substitutional alloys, the tensile and rheotropic behavior of an alpha-beta commercial alloy (Ti 140A) and an experimental alloy (3-Mn complex) were also investigated. The Ti 140A in the "as-received" condition was quite high in hydrogen. Consequently, a brief investigation of the effect of hydrogen level on the tensile properties of this alloy had to be conducted before the mechanical properties of the alloy, in the absence of hydrogen, could be defined. Because of the current interest in the effect of hydrogen, these test results are described below in some detail along with the tensile and rheotropic behavior of the alloys.

MATERIAL AND PROCEDURE

The Ti 140A was purchased from the Titanium Metals Corporation as 3/4 inch diameter rods in the annealed and ground condition. As shown below, the hydrogen content of this material was quite high so that specimens were tested in both the "as-received" and vacuum annealed condition. Rough machined specimens of the alloy

were vacuum annealed at 1200°F for four hours.* Vacuum annealing did not change the microstructure of the alloy which is shown in Fig. 53-a.

The 3-Mn complex alloy was supplied by the Battelle Memorial Institute. The alloy was heat treated according to information supplied by Battelle to two different strength levels before testing. The heat treatment consisted of quenching from 1380°F after a two hour anneal, followed by artificial aging at 800°F for 48 hours to develop the higher strength level, while aging at 895°F for 24 hours was employed to produce the lower strength level. The microstructure of the alloys at the two strength levels is shown in Figs. 53-b and c. The nominal composition of the alloys are shown in Table III.

TABLE III
NOMINAL COMPOSITIONS OF THE COMMERCIAL
AND EXPERIMENTAL ALLOYS, PERCENT

	<u>Ti 140A</u>	<u>3 Mn-Complex</u>
Fe	1.5-2.5	1
Cr	1.5-2.5	1
Mo	1.5-2.5	1
Mn	-	3
V	-	1

* At less than 5×10^{-5} mm Hg.

Continued

The test procedures used in this phase of the investigation were the same as those described in Part I for the titanium-nitrogen alloys, with the exception of the techniques for the high strain rate tests. The tests at 100 in/min movement of the test machine head were conducted on a tube drawing bench which was adapted for tensile straining, while the tests at 19,000 in/min used a guillotine type drop hammer that was adapted for tensile straining.

RESULTS AND DISCUSSION

Ti 140A Alloy

The tensile properties of two rods of Ti 140A in the "as-received" (annealed and ground) condition were determined as a function of testing temperatures as shown in Fig. 54 by the solid circles and crosses. The wide differences in ductility of these two rods at temperatures just below ambient and the shape of the ductility depression suggested that these specimens were hydrogen embrittled. Hydrogen analyses were made by the Battelle Memorial Institute on four pieces of the rod whose properties are shown in Fig. 54 as crosses in order to determine the hydrogen distribution within a single rod. The analyses found on these four specimens, taken at widely spaced intervals within the single supplied rod, were 280, 270, 269, and 270 ppm., indicating that the hydrogen content within a single "as-received" rod was quite uniform.

One of the broken test bars used in the series that showed the severest embrittlement (solid circles) was also analyzed for hydrogen by the Battelle Memorial Institute. The hydrogen content of the rod from which this specimen was taken was assumed to be quite uniform, not only because of the constant hydrogen distribution found in the first rods, but also because all the specimens whose data are shown as solid circles in Fig. 54 were machined from a single rod, and these data show practically no scatter. The hydrogen content for this material was found by Battelle to be 310 ppm.

A reduction of the hydrogen content from 310 ppm. to approximately 270 ppm. produced a much shallower depression in ductility as a function of testing temperature on these slow strain rate tests, Fig. 54. The ductility recovery at low temperatures, however, was still apparent even with the lower hydrogen alloy.

Test bars of a third rod were vacuum annealed at 1200°F for four hours. The hydrogen analyses supplied by Battelle on two vacuum annealed broken test bars were 170 and 92 ppm. Decreasing the hydrogen content by vacuum annealing eliminated the slow strain rate ductility depression that had been found at temperatures slightly below ambient, Fig. 54.

In steels, hydrogen not only produces a minimum in the ductility-testing temperature curve at slow strain rates, but at increased strain rates the magnitude of the depression is attenuated and

Centrad

elevated to higher testing temperatures until eventually, when the strain rate is sufficiently high, the depression is completely eliminated. Since the slow strain rate ductility-testing temperature curves found for this alpha-beta alloy were so much like those found in hydrogen charged steels, the ductility of the alloy was also determined as a function of testing temperature at higher strain rates. Only a limited amount of each of these rods was available -- consequently, specimens were prepared from the highest hydrogen rod (310 ppm.) for testing at a single high strain rate (19,000 in/min), while other specimens from the rod with an intermediate hydrogen content (270 ppm.) were prepared for testing at the single intermediate strain rate of 100 in/min.

The material with the highest hydrogen content continued to show a ductility depression as a function of testing temperature at the highest strain rate, but this minimum was mild and displaced to a higher testing temperature, Fig. 55. Since a ductility minimum was found even at this high strain rate for the high hydrogen alloy, the ductility-testing temperature curve was also obtained on vacuum annealed specimens at a strain rate of 19,000 in/min as shown in Fig. 56. As was the case for slow strain rate deformations, vacuum annealing again eliminated the ductility depression.

The material with the intermediate hydrogen content no longer displayed a ductility-testing temperature minimum at a strain rate

of 100 in/min, at least, not at testing temperatures below +300°F,

Fig. 57.

Brown and Baldwin (21) characterized the shape of the hydrogen produced ductility depression in steel as a function of testing temperature and strain rate by describing the slope of the two surfaces that produced the depression on a three dimensional chart, Fig. 58.

One of these surfaces was described by the equations:

$$\left(\frac{\partial \epsilon}{\partial \dot{\epsilon}}\right)_T > 0 \quad ; \quad \left(\frac{\partial \epsilon}{\partial T}\right)_{\dot{\epsilon}} < 0 \dots\dots\dots [6]$$

while the other was defined by the pair of equations,

$$\left(\frac{\partial \epsilon}{\partial \dot{\epsilon}}\right)_T > 0 \quad ; \quad \left(\frac{\partial \epsilon}{\partial T}\right)_{\dot{\epsilon}} > 0 \dots\dots\dots [7]$$

The authors pointed out that a description of this figure in three dimensions is essential before an acceptable theory for the mechanism of hydrogen embrittlement is possible.

The hydrogen embrittlement concept wherein the diffusion rate of hydrogen is competitive with the rate at which the material is being deformed as suggested by the planar pressure theory of Zapffe and his co-workers (22), or the diffusion controlled extension of Orowan's theory on delayed fracture in glass by Petch and

Conclusions

Stables (23), suggest surfaces of the type given by equations [6]. Surfaces of the type given by equations [7] are rationalized by de Katensky (24) on the basis that the solubility of hydrogen in the metal (as opposed to that collected in the voids) increases with testing temperature; hence, surfaces described by equations [7] as well as by equations [6] should be expected.

Plotting the ductility data obtained in this investigation on alpha-beta Ti 140A as a function of both testing temperature and strain rate produced the same type of surfaces that Brown and Baldwin found for steel, Figs. 59 and 60. This suggests that hydrogen embrittlement in alpha-beta titanium is produced by the same mechanism that produces embrittlement in hydrogen charged steels; these data are consistent with a competitive rate theory as the mechanism for hydrogen embrittlement.

The suggestion that hydrogen produces embrittlement in alpha-beta titanium by the same mechanism by which steel is hydrogen embrittled is supported by data recently presented by Kotfila and Erbin on the 3-Mn complex titanium alloy, Fig. 61 (25). Although these authors investigated only three temperatures at each of three strain rates, they appear to be consistently developing surfaces that would be described by equations [6] and [7] when their hydrogen content was sufficiently high (200 and 300 ppm.).

Data collected by G. A. Lenning, C. M. Craighead and R. I. Jaffee

Corrections

at Battelle Memorial Institute (26) on a number of different alpha-beta alloys indicate the existence of surfaces of the type described by equation [7], but the ductility recovery at low temperatures described by equation [6] has not been found.

Hydrogen embrittlement in these alpha-beta alloys is also quite different from that found (27) in alpha alloys. This latter class of alloys appears to produce titanium hydrides which elevate the transition temperature of the metal and result in behaviors much like that described in Part I of this report for titanium-nitrogen alloys.

Two series of slow notch tests were also conducted on the Ti 140A, the first series utilizing vacuum annealed specimens, and the second series employing specimens in the "as-received" condition*, Fig. 62. The notch ductilities found in these two test series were identical.** Lt. G. T. Hahn suggested that since notches restrict deformation to such a limited volume of metal, notch tests even at moderate strain rates (in terms of axial specimen travel) must be considered as high strain rate deformations (28).

After defining the dependence of ductility on testing temperature

* One of the broken test bars in the "as-received" condition, and one as vacuum annealed, both with nominal notch depths of ten percent were analyzed for hydrogen. Battelle reported the former bar to have 265 ppm. while the latter bar had 83 ppm. as shown in Fig. 62.

** The differences in notch strength of the two test series in Fig. 62 result because the vacuum annealed rod was somewhat harder than the hydrogen bearing rod.

for Ti 140A with a low hydrogen content, specimens of this material were prestretched at room temperature and subsequently tested at -321°F in order to determine whether or not it would exhibit a rheotropic recovery. As shown in Fig. 63, the low temperature ductility deficiency of this alloy can be alleviated by super-transition temperature prestraining.

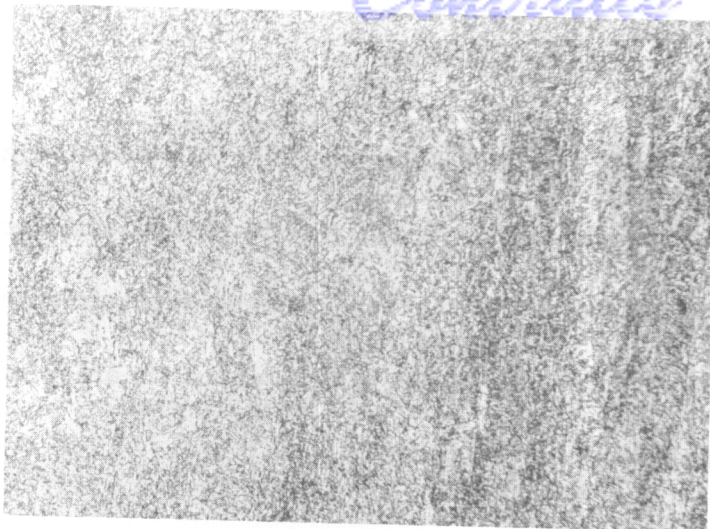
3 Mn-Complex Alloy

The 3 Mn-Complex alloy heat treated to two different strength levels, was tested over a range of temperatures in order to define its tensile property-testing temperature relations after two different aging operations. As shown in Fig. 64, increasing the strength level of the alloy produced embrittlement by elevating the transition temperature. The ductility of the alloy at the high strength level scattered so severely that it was not possible to determine conclusively whether or not a rheotropic recovery of this metal was possible. This was indeed unfortunate, since such a recovery of this extremely high strength titanium alloy might produce satisfactory ductilities along with enormous tensile strengths.

Room temperature prestraining did not produce a rheotropic recovery of the alloy at -321°F when it was heat treated to the lower strength level of 180,000 psi, Fig. 65.

CONCLUSIONS

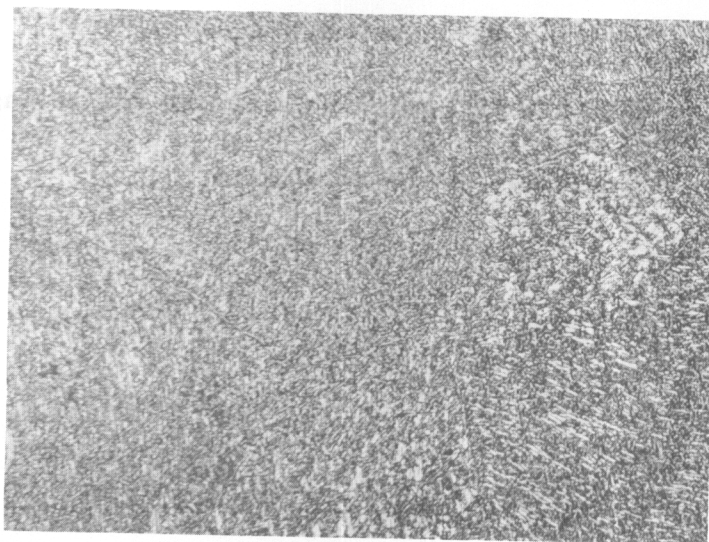
1. Hydrogen embrittlement in alpha-beta Ti 140A is characterized by ductility-testing temperature-strain rate surfaces similar to those previously presented to describe hydrogen embrittlement in steel. This behavior is consistent with present theories of the mechanism of hydrogen embrittlement.
2. The behavior of alpha-beta alloys is markedly different from that previously described for hydrogen embrittled alpha alloys.
3. Notch tests at a moderate strain rate did not detect the presence of hydrogen in Ti 140A.
4. Rheotropic recovery was possible in vacuum annealed Ti 140A.
5. The 3-Mn Complex did not display rheotropic brittleness at a strength level of 180,000 psi. Heat treating this alloy to a higher strength level (220,000 psi) caused excessive scattering so that rheotropic studies could not be conducted.



A
TI 140 A
VACUUM ANNEALED AT
1200° F (650°C) WATER
QUENCH



B
3 Mn COMPLEX
VACUUM ANNEALED AT
1380° F (750°C) WATER
QUENCH AGED 24 HRS
AT 895° F (480°C)



C
3 Mn COMPLEX
VACUUM ANNEALED AT
1380° F (750°C) WATER
QUENCH AGED 48 HRS
AT 800° F (425°C)

250X
ELECTROLYTIC POLISH AND ETCH

FIG.53: MICROSTRUCTURE OF VACUUM ANNEALED TI 140 A AND
3 Mn COMPLEX ALLOYS.

Controls

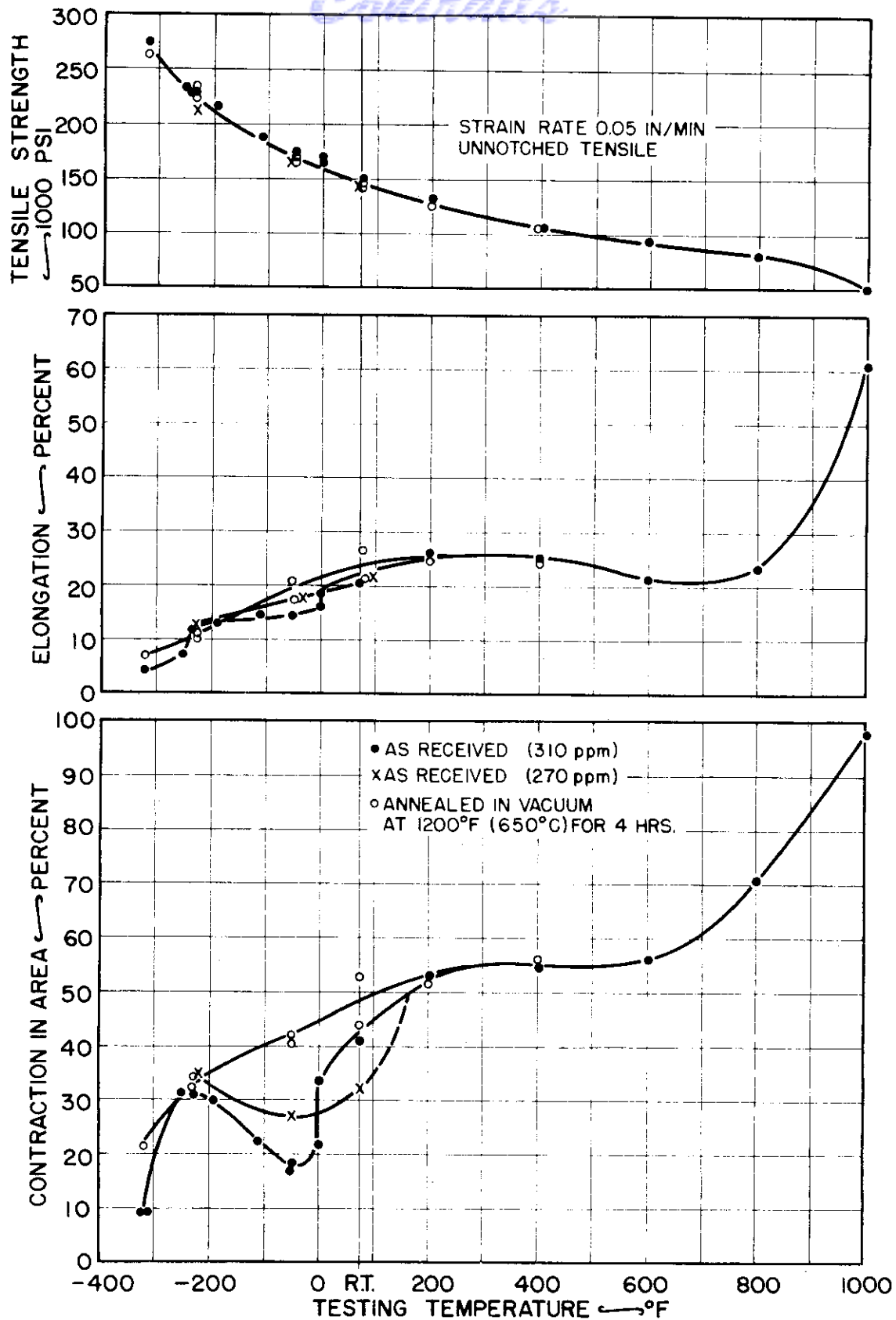


FIG.54: EFFECT OF HYDROGEN LEVEL ON THE TENSILE PROPERTIES OF TI 140A AT A STRAIN RATE OF 0.05 IN/MIN.

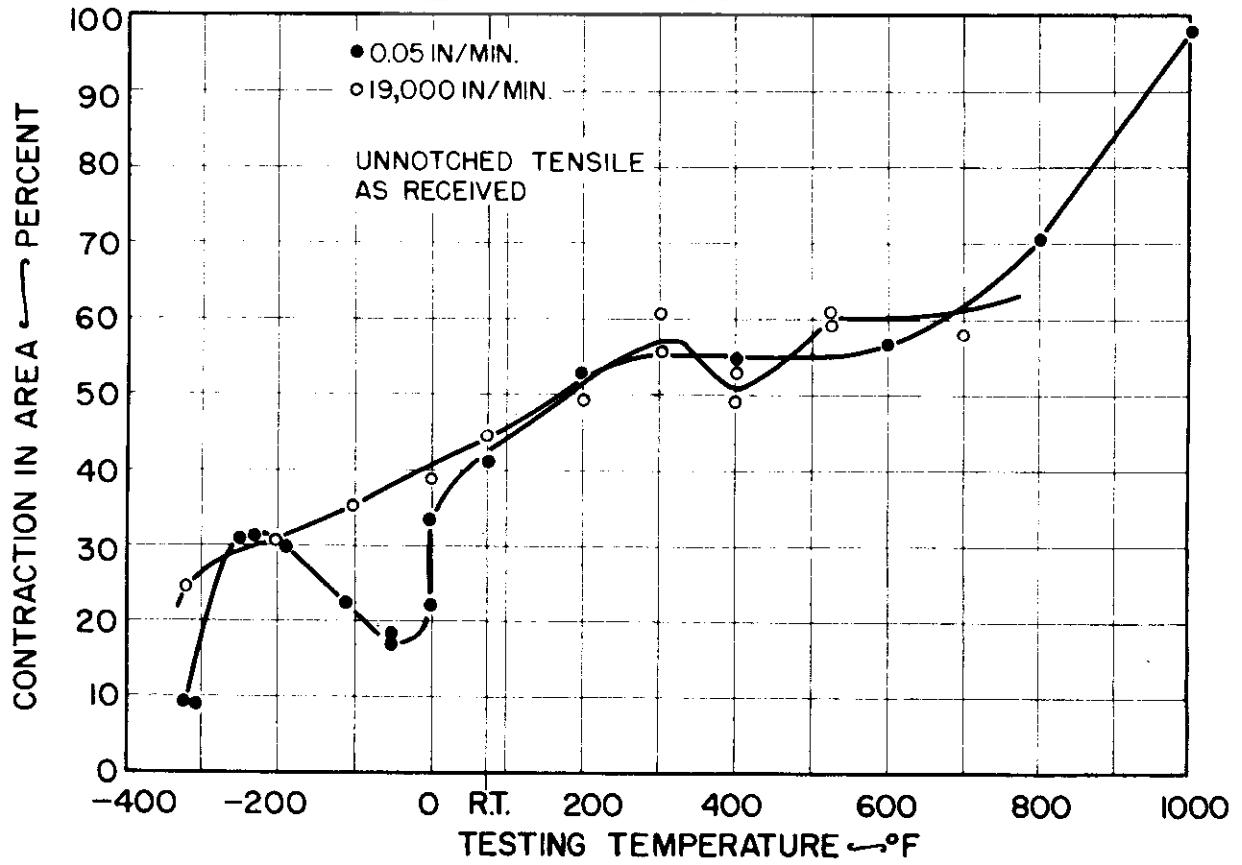


FIG.55: EFFECT OF STRAIN RATE ON THE DUCTILITY OF TI 140A WITH 310 ppm HYDROGEN.

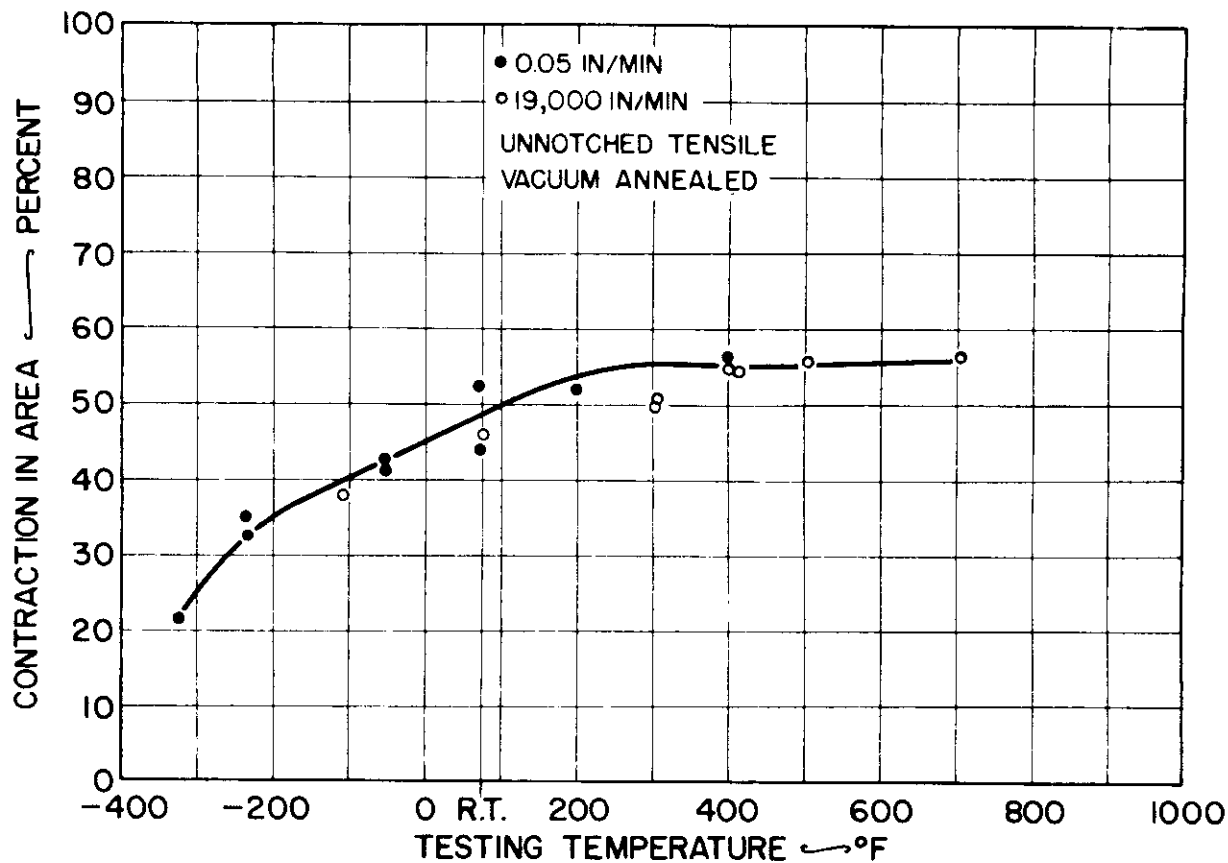


FIG.56: EFFECT OF STRAIN RATE ON THE DUCTILITY OF VACUUM ANNEALED TI 140A.

Contrails

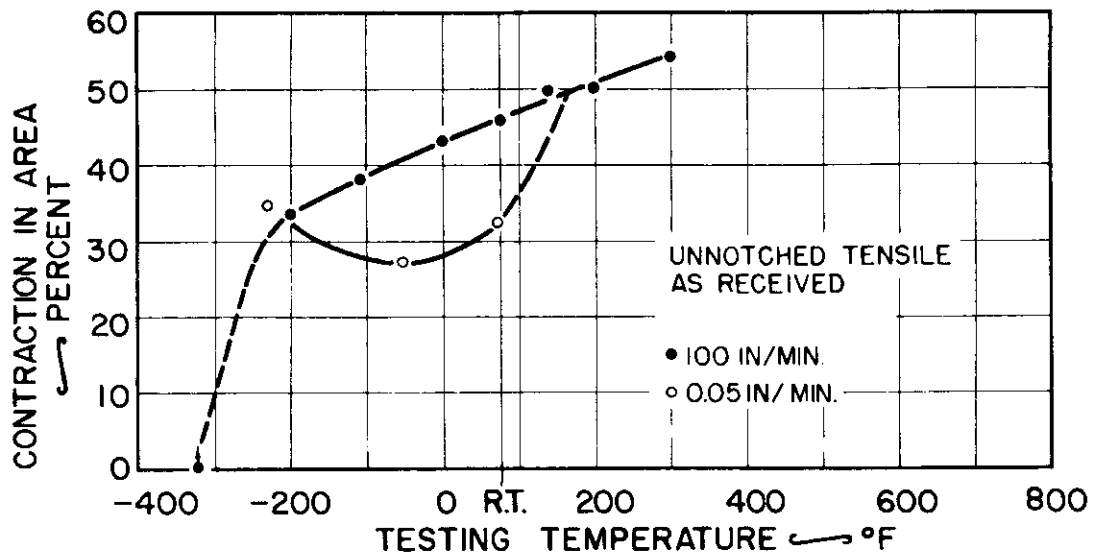


FIG.57: EFFECT OF STRAIN RATE ON THE DUCTILITY OF TI 140A WITH 270 ppm OF HYDROGEN.

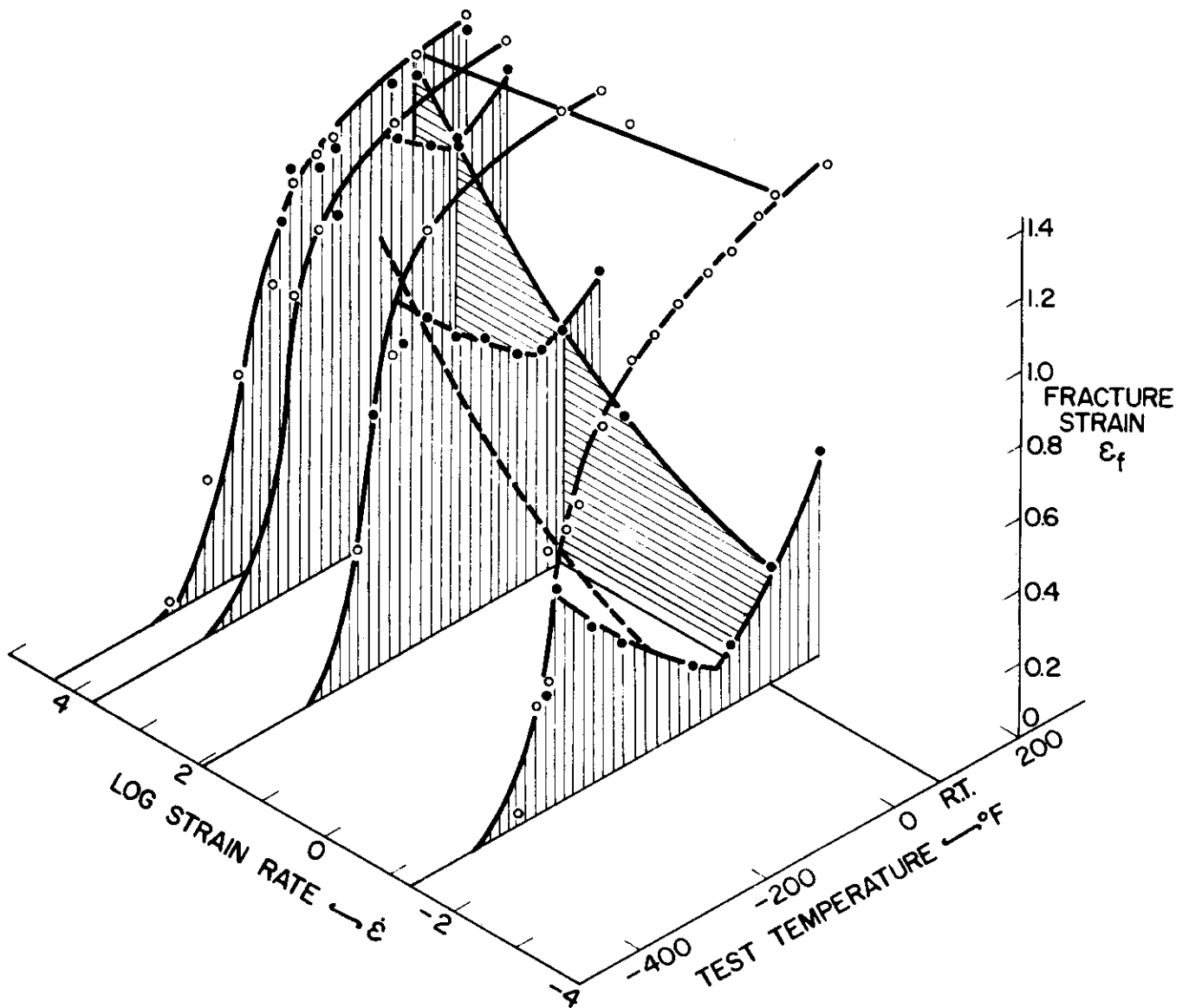


FIG.58 : FRACTURE STRAIN OF SPHERODIZED SAE 1020 STEEL WITH AND WITHOUT HYDROGEN EMBRITTLEMENT AS A FUNCTION OF TEMPERATURE AND STRAIN RATE (BROWN AND BALDWIN (21)).

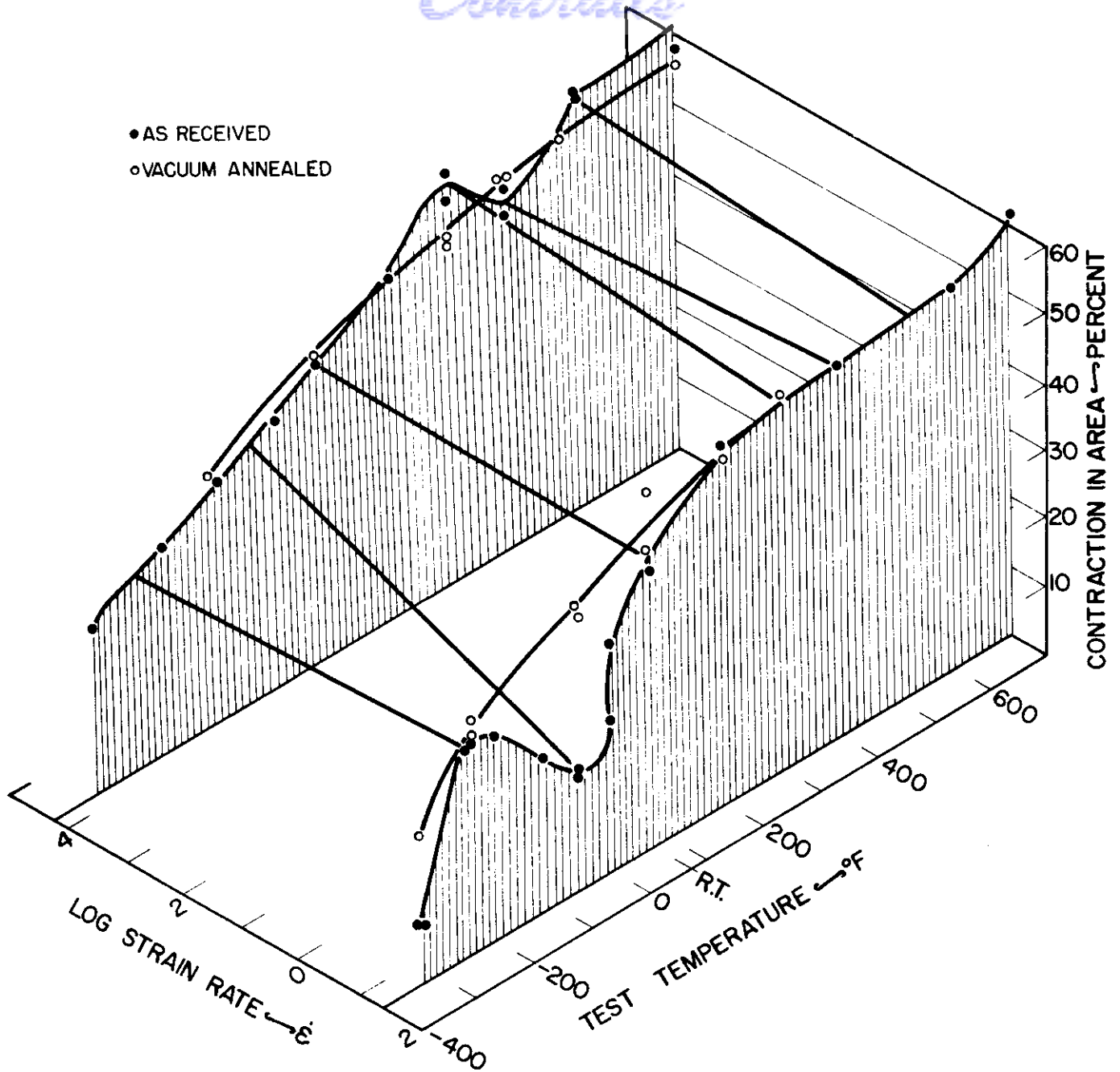


FIG.59 DUCTILITY OF TI 140 A IN THE AS RECEIVED (310ppm OF HYDROGEN) AND VACUUM ANNEALED CONDITION vs. TESTING TEMPERATURE AND STRAIN RATE.

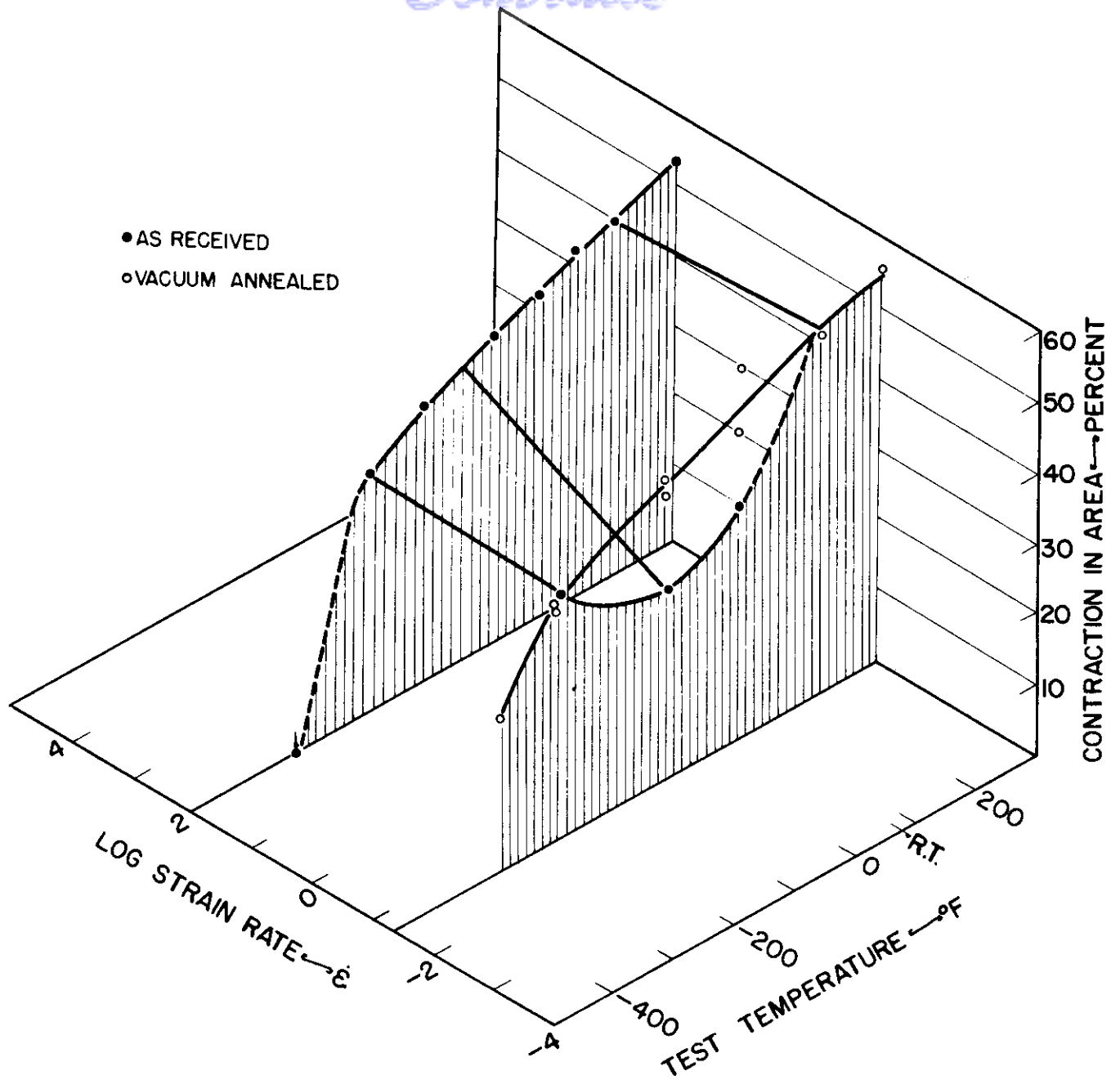


FIG.60.DUCTILITY OF TI 140 A IN THE AS RECEIVED(270 ppm OF HYDROGEN) AND VACUUM ANNEALED CONDITION vs. TESTING TEMPERATURE AND STRAIN RATE.

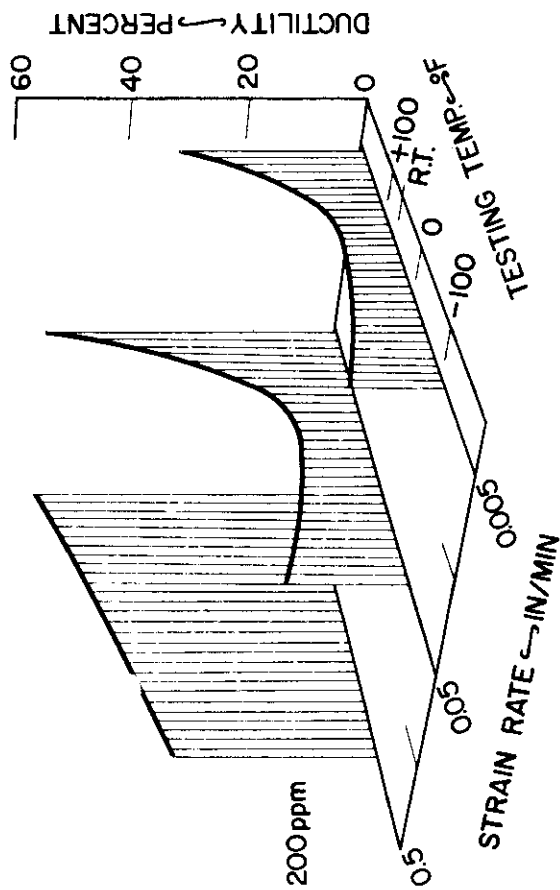
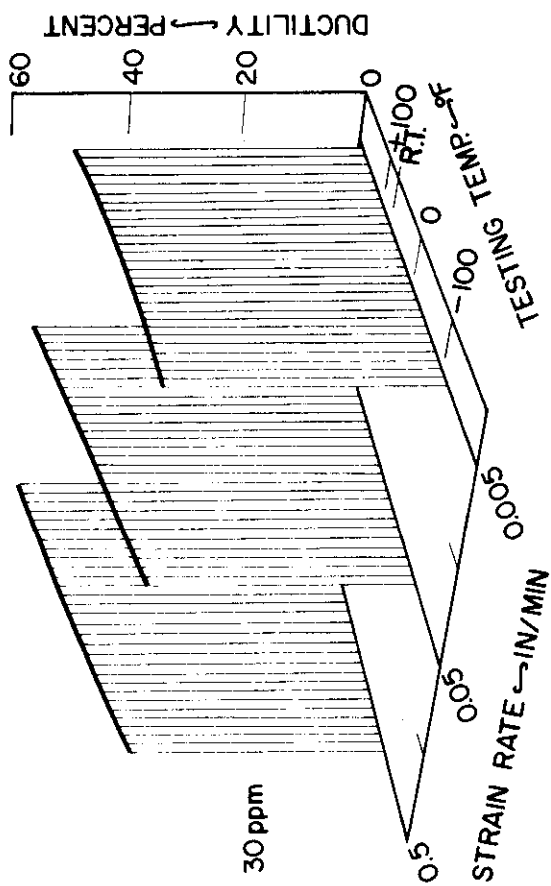
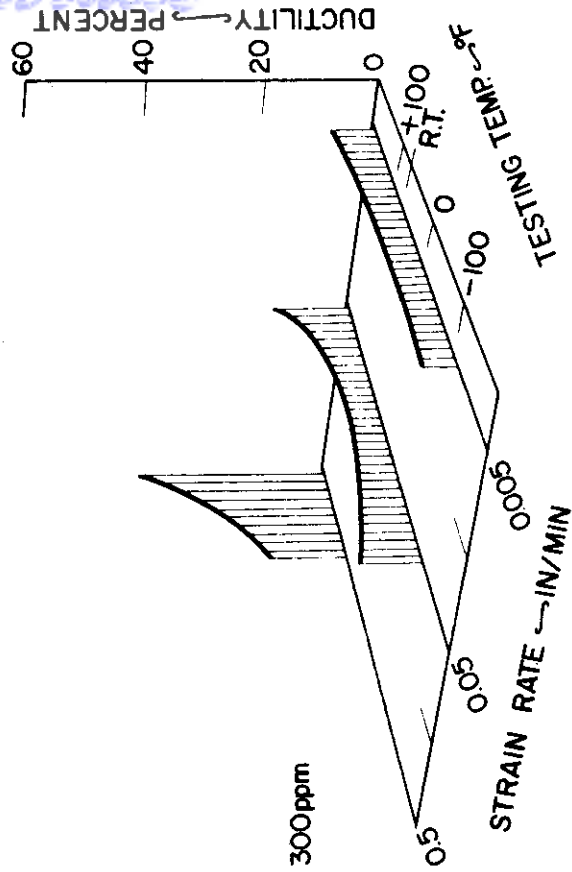
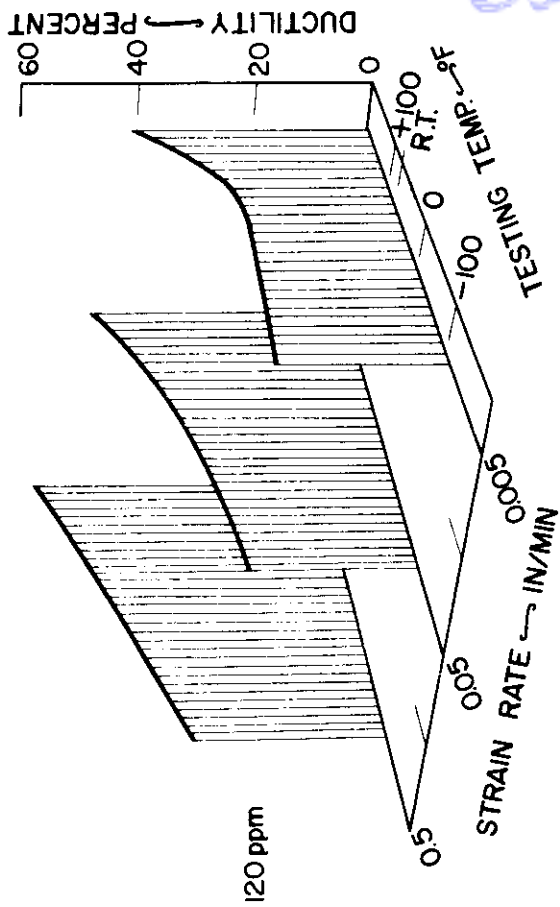


FIG. 6.1. EFFECT OF HYDROGEN LEVEL ON THE DUCTILITY OF 3Mn-COMPLEX ALLOY AT A VARIETY OF TESTING TEMPERATURES AND STRAIN RATES (KOTFILA AND ERBIN) (25).

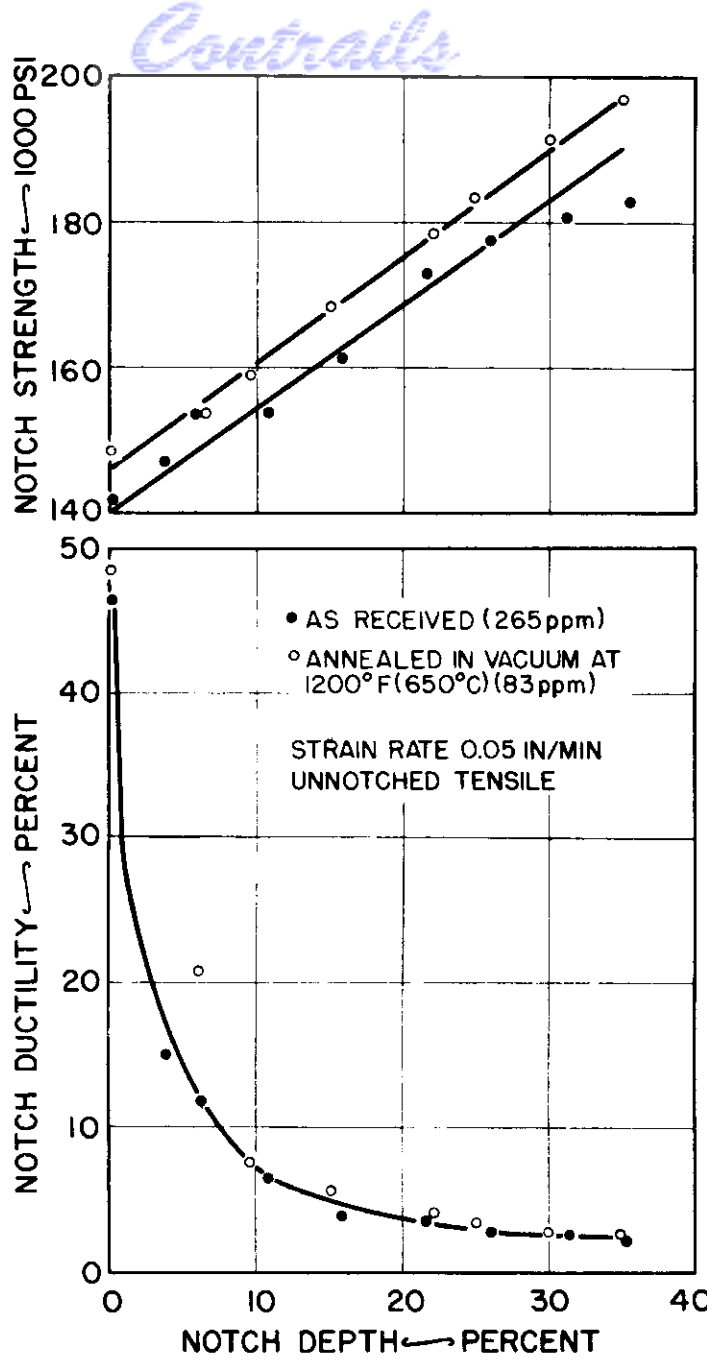


FIG.62 ROOM TEMPERATURE NOTCH PROPERTIES OF TI 140 A WITH A HIGH AND LOW HYDROGEN CONTENT.

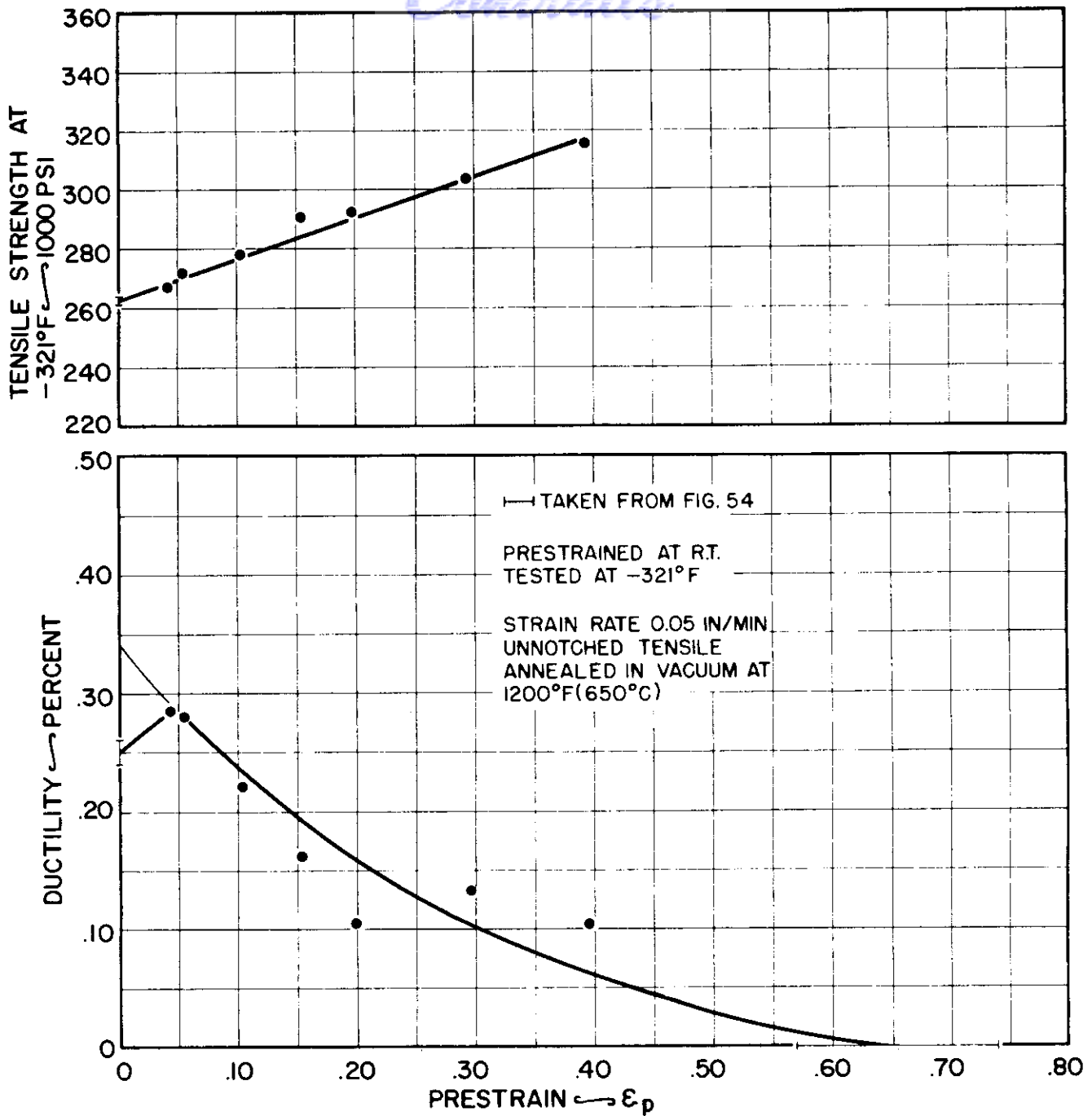


FIG.63:RHEOTROPIC BEHAVIOR OF THE TI 140A ALLOY.

Controls

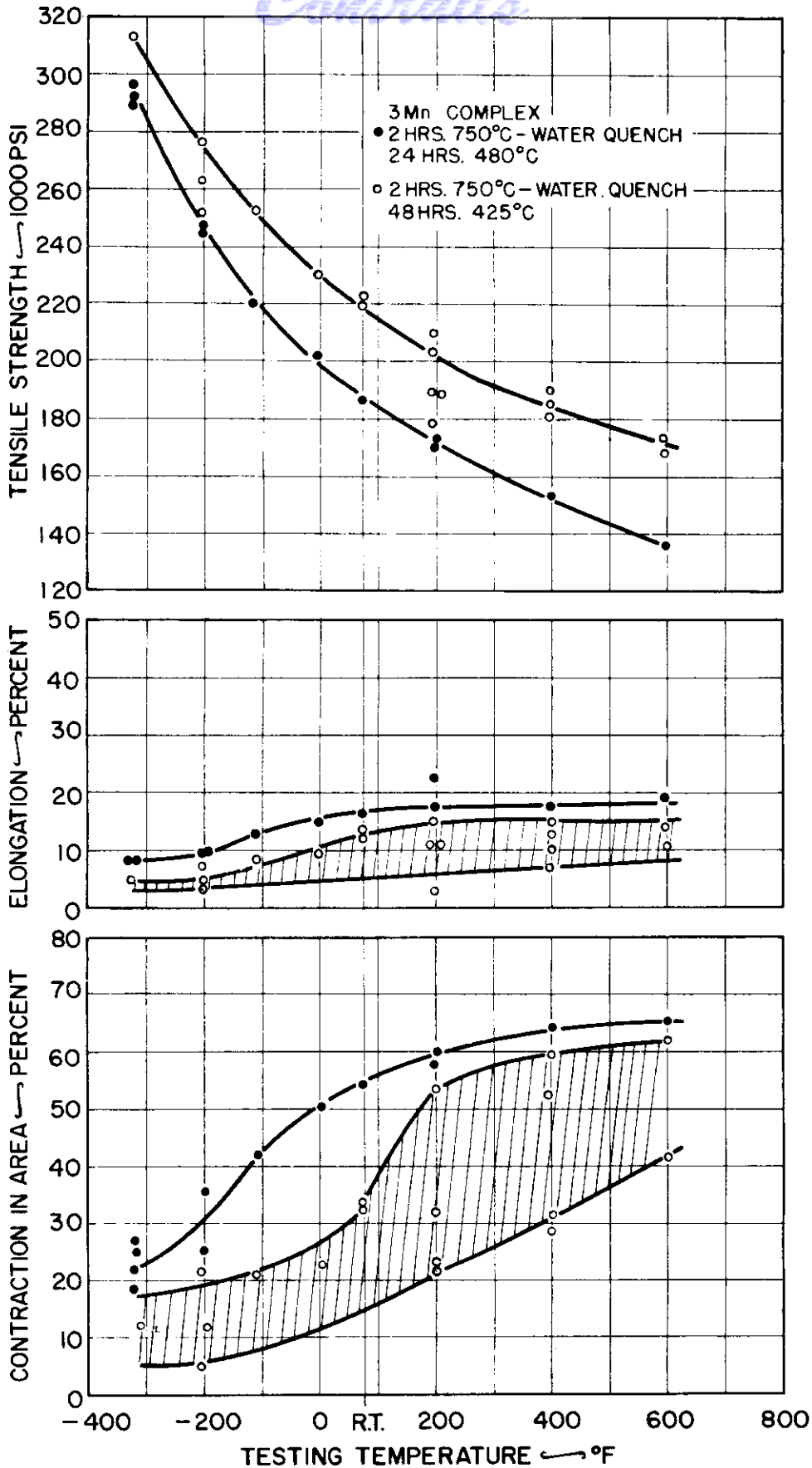


FIG.64 UNNOTCHED TENSILE PROPERTIES vs. TESTING TEMPERATURE FOR THE 3Mn-COMPLEX ALLOY.

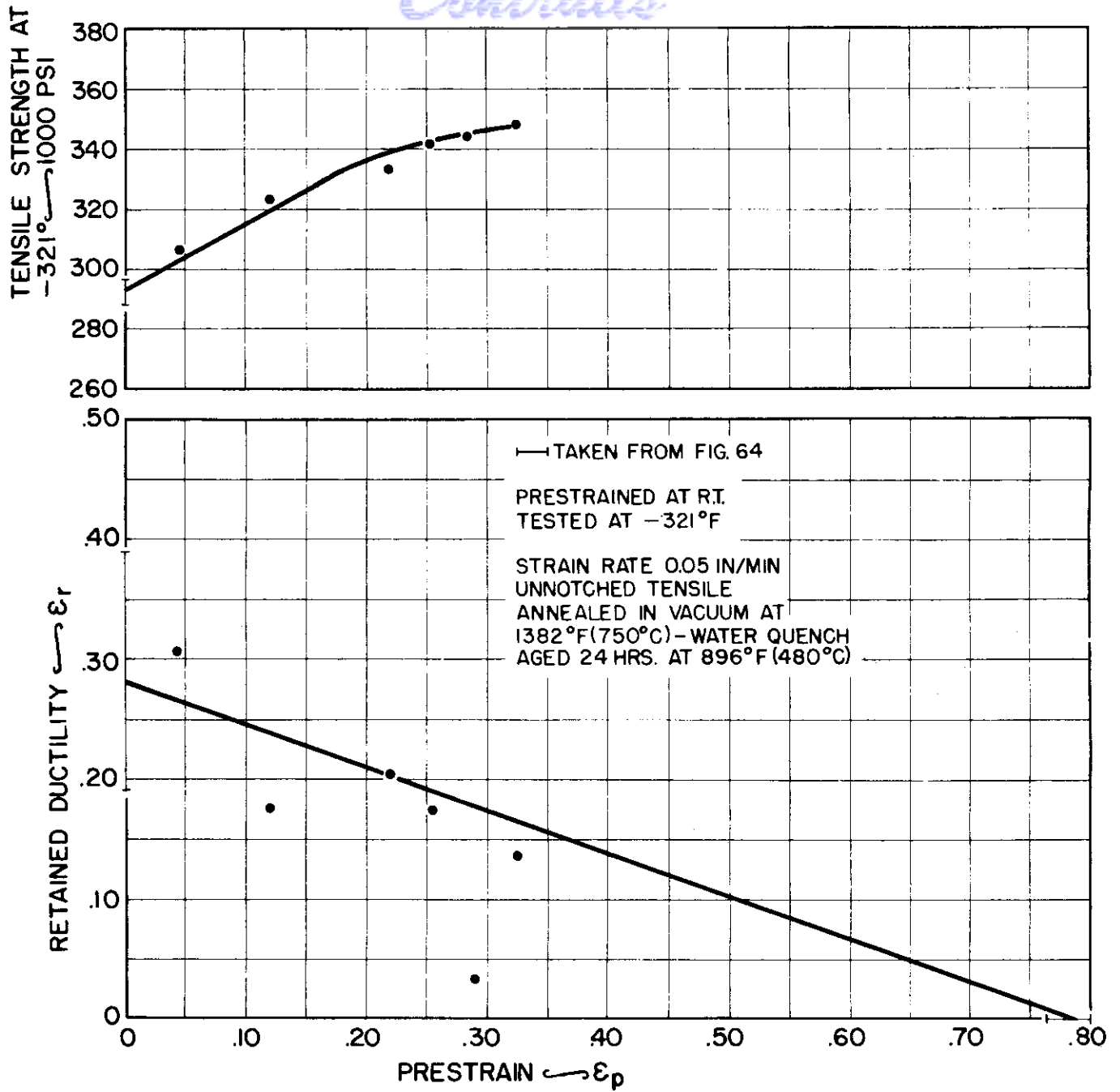


FIG. 65: RHEOTROPIC BEHAVIOR OF THE 3Mn-COMPLEX ALLOY.

TENSILE AND RHEOTROPIC BEHAVIOR OF COMMERCIAL
UNALLOYED MOLYBDENUM

INTRODUCTION

Molybdenum appears to be unique among structural materials in that it becomes more brittle rather than more ductile when recrystallized. This presumably unique embrittlement has been labeled "recrystallization embrittlement."

A considerable effort has been expended in the last five to ten years in an attempt to explain and eventually eliminate this type of brittleness. Work on this subject was tacitly based on the assumption that recrystallization embrittlement is a property peculiar to metals which are molybdenum base.

Actually, recrystallization embrittlement appears to be a behavior that might be expected in all non-face-centered cubic metals and it seems to be nothing more than another manifestation of rheotropic brittleness, as described in the previous parts of this report. The importance of correlating these two types of brittleness is obvious -- it would mean that any techniques developed for the elimination of one of these might be applicable in eliminating the other.

Consequently, this investigation was undertaken in an attempt to show that recrystallization brittleness is one type of rheotropic

brittleness.

Contrails

MATERIAL and PROCEDURE

The material was purchased as unalloyed commercial molybdenum from the Climax Molybdenum Company as 3/4 inch diameter hot rolled arc cast bars. Two of the rods were recrystallized by the supplier, one rod to a fine grain size (by annealing for one hour at 2200°F), and the other to a coarse grain structure (by annealing for two hours at 3100°F). The microstructures of the "as-rolled", and two recrystallized bars are shown in Fig. 66a, b, and c.

The testing procedures were identical with those described above in Part I of this report for the slow strain rate tests, and in Part III for the high strain rate tests.

RESULTS and DISCUSSION

Specimens of the "as-rolled" rod were tested over a temperature range from -100 to +1200°F at three strain rates in order to define the transition temperature of the material, as shown in Fig. 67. The recrystallized, fine and coarse grained specimens were also tested at one high and one slow strain rate in order to find the effect of recrystallization on the transition temperature, Figs. 68 and 69. Recrystallizing, even to produce a fine grained structure, produced an appreciable elevation of the transition temperature (from approximately 0°F to +100°F on slow testing), while producing a

Continued

coarse grained structure elevated the transition even more (to about +400°F on slow testing). A similar elevation of transition temperature was found on testing at a high strain rate.

According to the description previously given to rheotropic embrittlement, the transition temperature elevation resulting from the recrystallizing heat treatment would have been expected.

The hot rolled rods were sufficiently cold worked at the finish rolling temperature to produce a rheotropic recovery, and this recovery was overcome by the recrystallization anneal. The fact that the deformation given to the molybdenum in rolling is cold work, is attested to by the "as-rolled" grain structure in Fig. 66a.

Rheotropic recovery would not predict the further elevation of transition temperature produced by the grain coarsening anneal. This, although not a rheotropic effect, is in keeping with the general metallurgical rule that coarse grains lead to less ductile performance.

Because only the ductility loss experienced by the metal on first recrystallizing can be considered as a rheotropic brittleness phenomenon, additional tests were conducted only on fine grained specimens.

A group of these specimens were prestrained various amounts in tension at +400°F after which these test bars were subsequently stretched to failure at room temperature. As shown in Fig. 70,

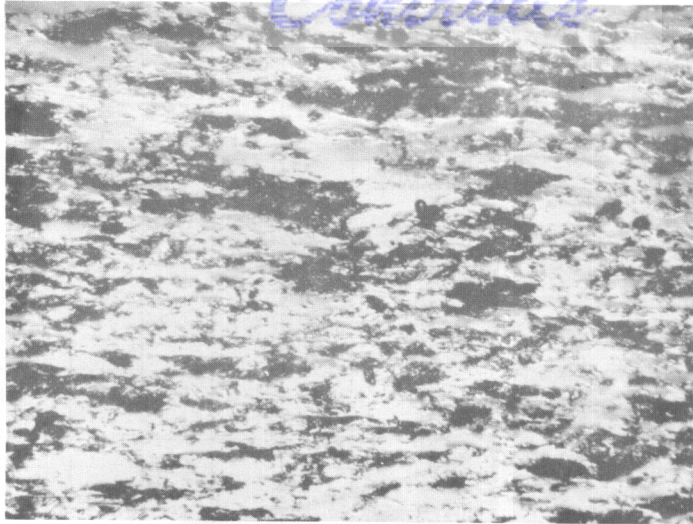
Contrails
prestretching the equiaxed specimens produced a rheotropic recovery even at rather small strains. This ductility improvement was possible even though the grains were still essentially equiaxed after a prestrain of $\epsilon = 0.2$.

Other specimens were stretched to an ϵ of approximately 0.4 at a variety of temperatures followed by testing at room temperature. Here again, prestraining at super-transition temperatures produced a rheotropic recovery, Fig. 71.

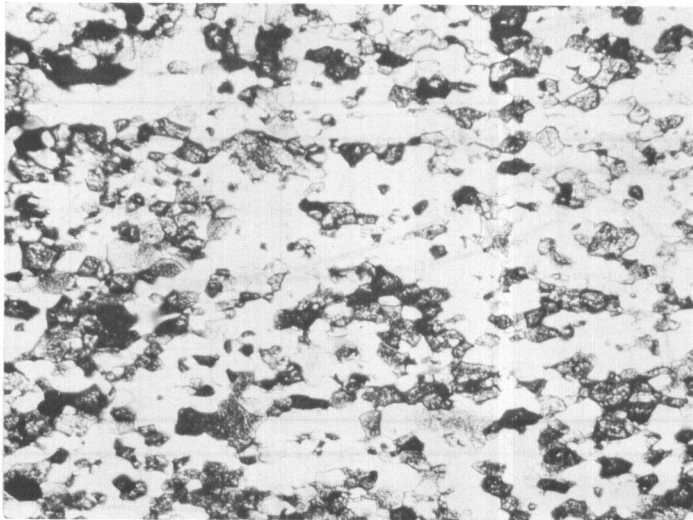
CONCLUSIONS

1. Recrystallization embrittlement in commercial unalloyed molybdenum is a manifestation of rheotropic embrittlement although the additional embrittlement produced by grain coarsening probably is not.

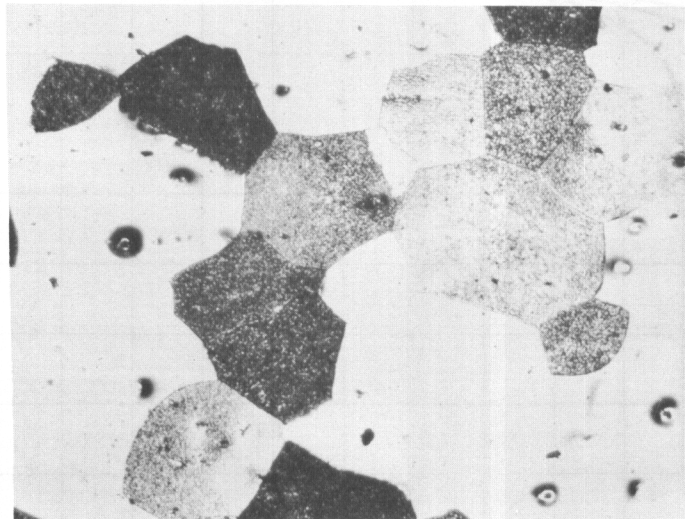
Contrails



A
UNALLOYED
MOLYBDENUM
AS ROLLED



B
EQUIAXED
RECRYSTALLIZED
(FINE GRAIN)
UNALLOYED
MOLYBDENUM



C
EQUIAXED
RECRYSTALLIZED
(COARSE GRAIN)
UNALLOYED
MOLYBDENUM

250X

ELECTROLYTIC POLISH AND ETCH

FIG.66: MICROSTRUCTURES OF UNALLOYED MOLYBDENUM.

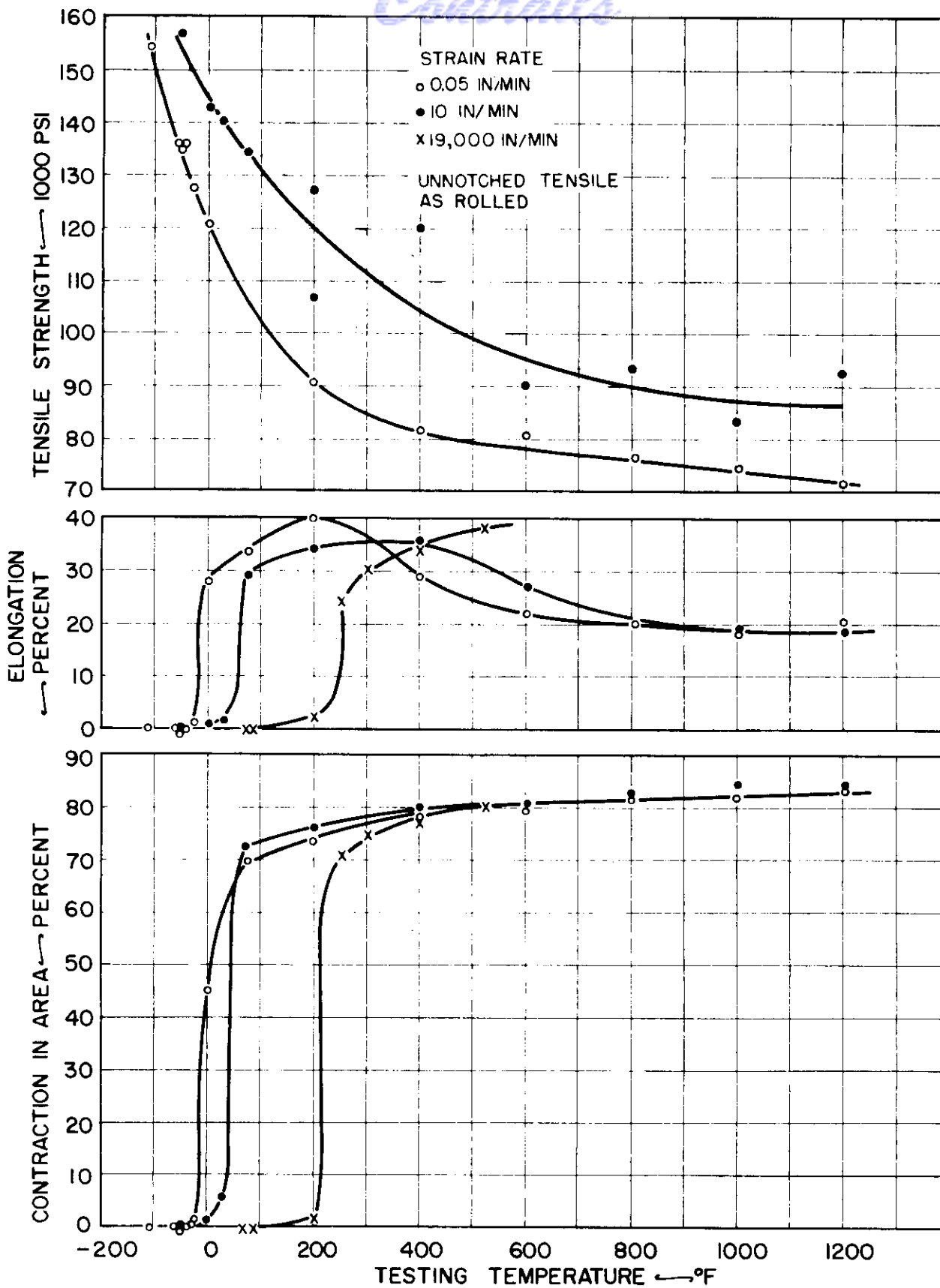


FIG.67: UNNOTCHED TENSILE PROPERTIES vs. TESTING TEMPERATURE FOR UNALLOYED MOLYBDENUM.

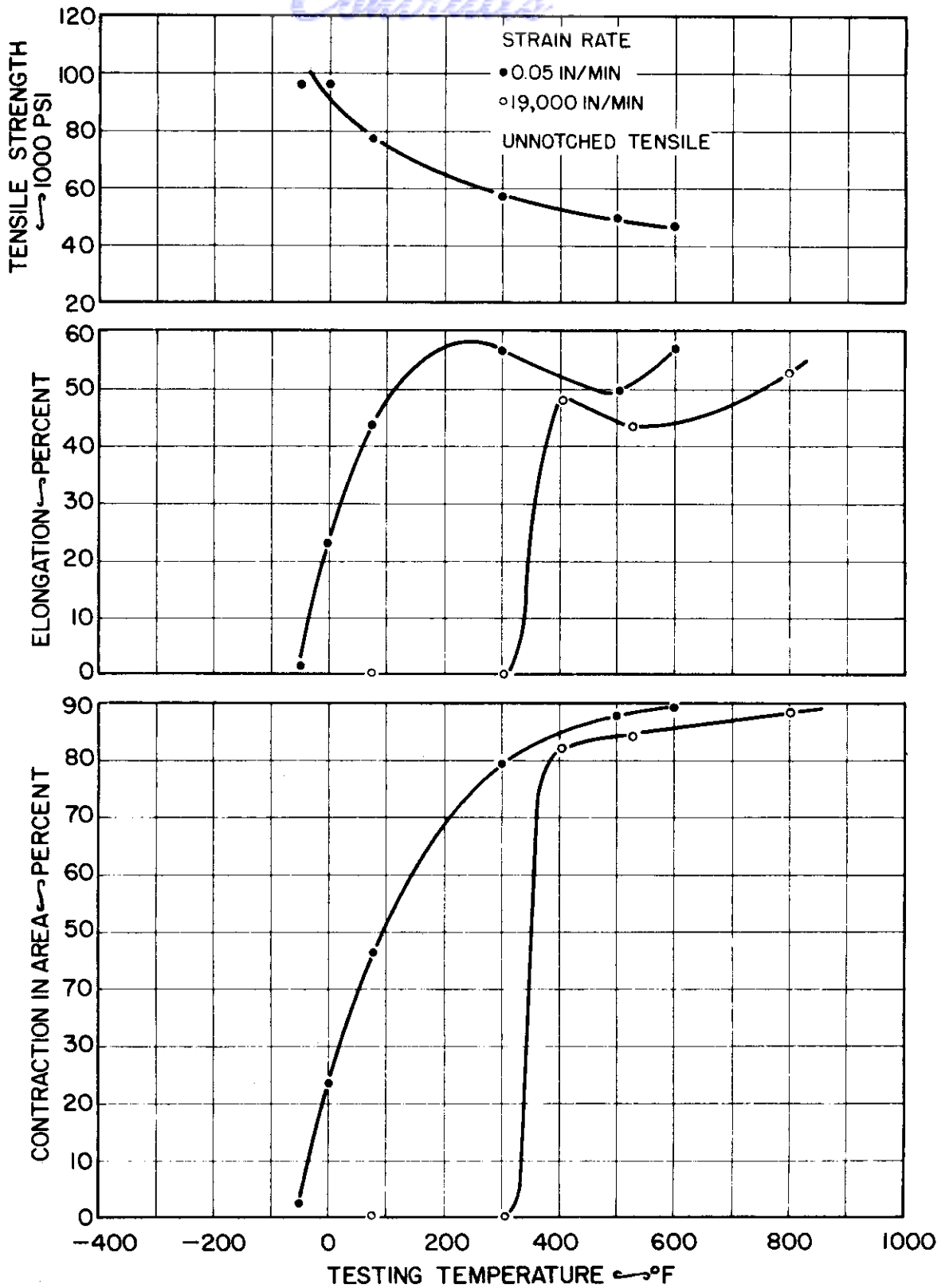


FIG.68: UNNOTCHED TENSILE PROPERTIES vs. TESTING TEMPERATURE FOR EQUIAXED RECRYSTALLIZED (FINE GRAIN) UNALLOYED MOLYBDENUM.

Contrails

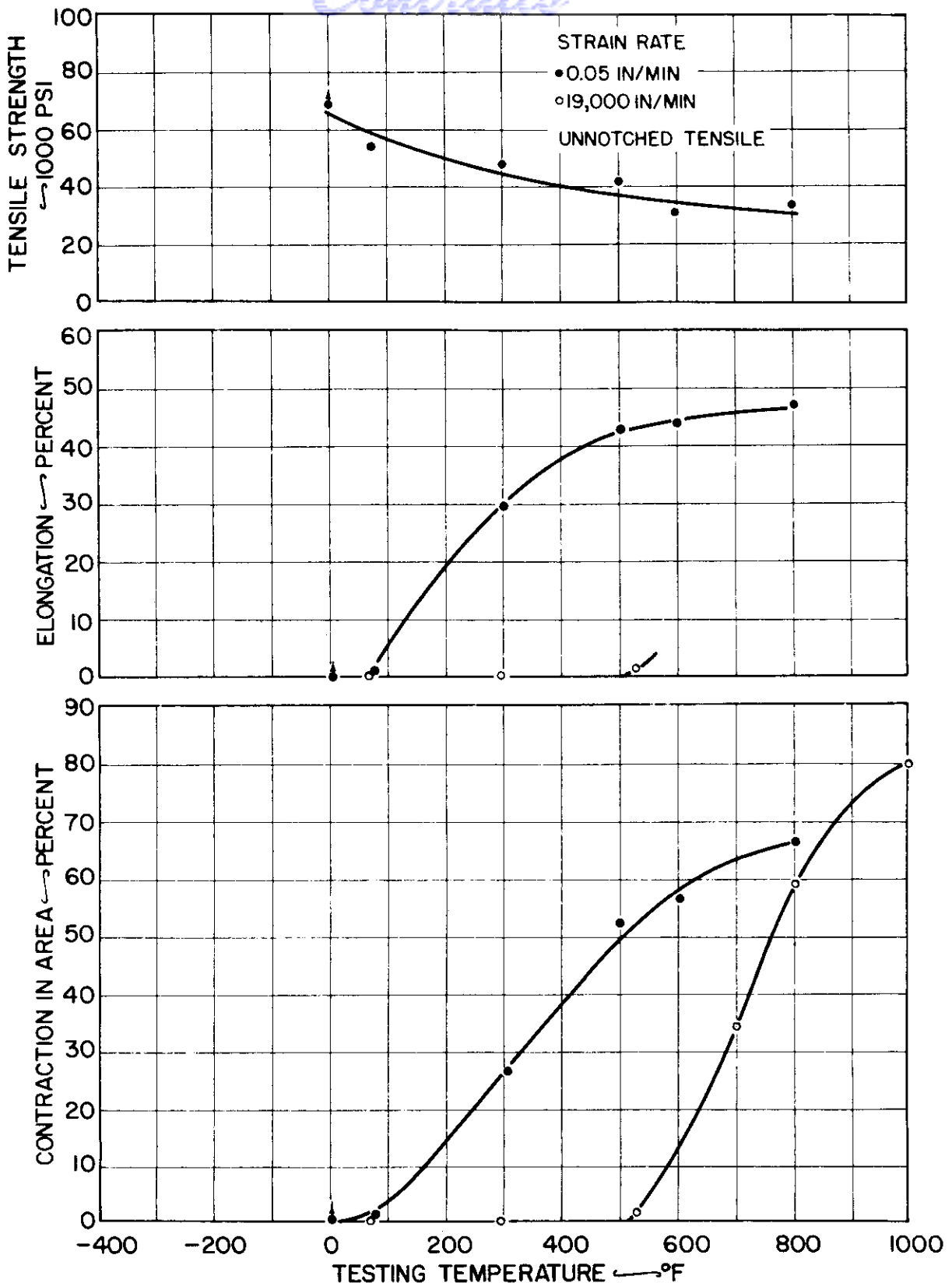


FIG.69: UNNOTCHED TENSILE PROPERTIES vs. TESTING TEMPERATURE FOR EQUIAXED RECRYSTALLIZED (COARSE GRAIN) UNALLOYED MOLYBDENUM.

Controls

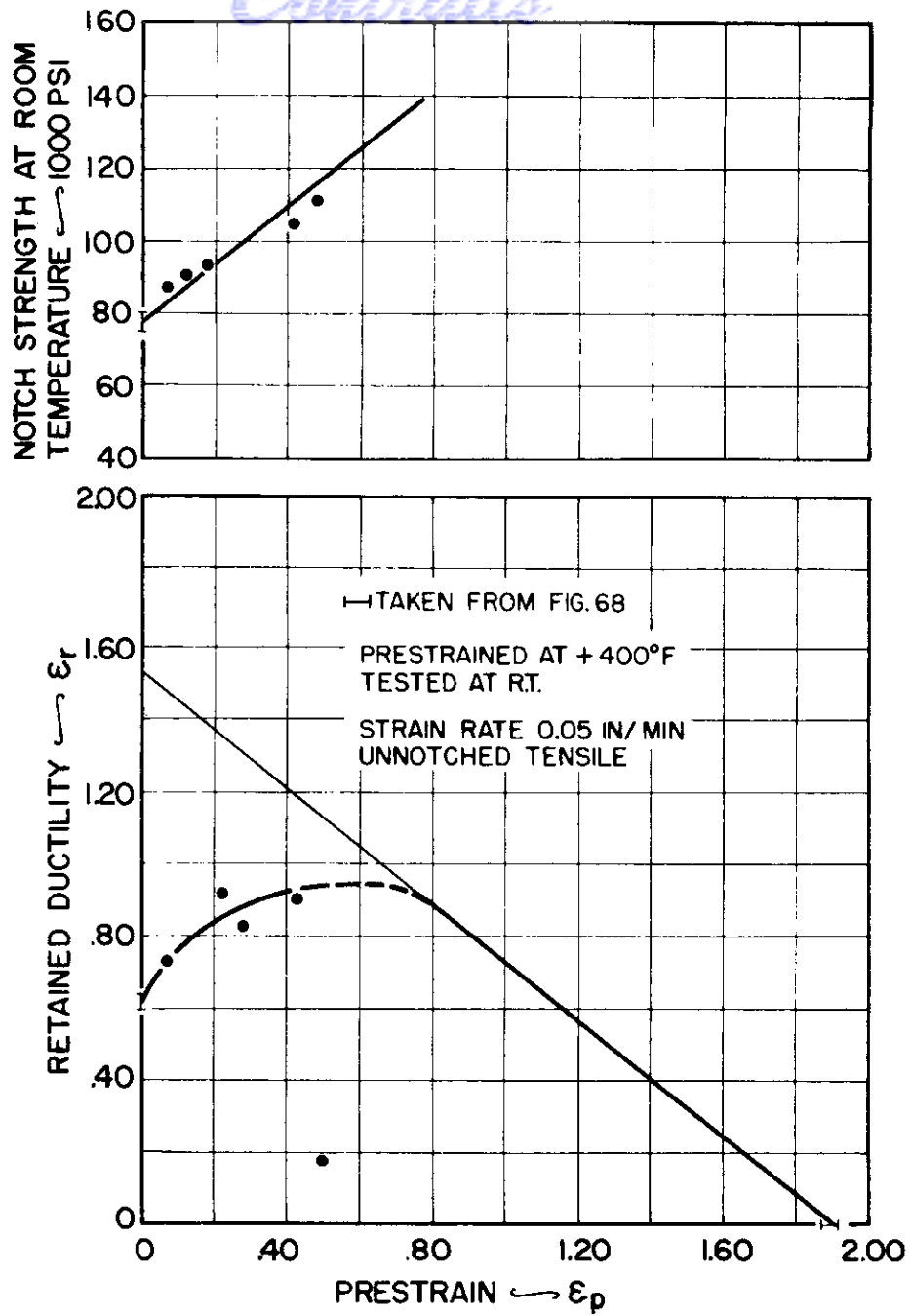


FIG.70:RHEOTROPIC BEHAVIOR OF EQUIAXED RECRYSTALLIZED (FINE GRAIN) UNALLOYED MOLYBDENUM.

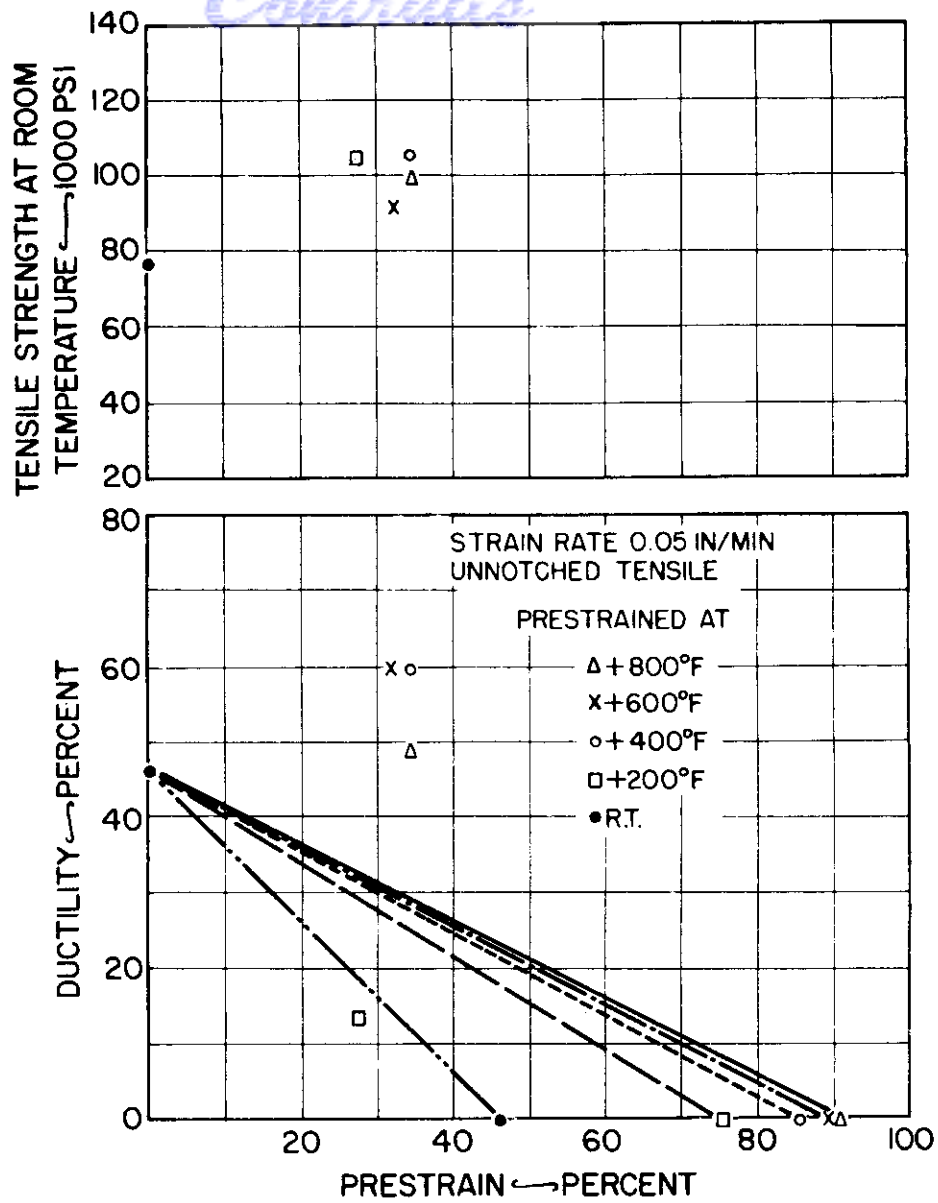


FIG.71: RHEOTROPIC BEHAVIOR OF EQUIAXED RECRYSTALLIZED (FINE GRAIN) UNALLOYED MOLYBDENUM PRESTRAINED AT A VARIETY OF TEMPERATURES AND TESTED AT ROOM TEMPERATURE.

Centraids
BIBLIOGRAPHY

1. R. I. Jaffee and I. E. Campbell, "The Effect of Oxygen, Nitrogen and Hydrogen on Iodide Refined Titanium" Trans. AIME, 185, 646-654 J. of Metals (Sept 1949) TP2681E.
2. W. L. Finlay and J. A. Snyder, "Effects of Three Interstitial Solutes (Nitrogen, Oxygen and Carbon) on the Mechanical Properties of High-Purity Alpha Titanium," Trans AIME, 188, 277-286, J. of Metals (Feb 1950) TP2759E.
3. R. I. Jaffee, H. R. Ogden and D. J. Maykuth, "Alloys of Titanium with Carbon, Oxygen and Nitrogen," Trans AIME V 188, 1261-1266 J. of Metals (Oct 1950) TP 2955E.
4. D. R. Luster, W. W. Wentz, and J. P. Catlin, "Effect of Strain Rate on the Mechanical Properties of Titanium-Base Materials," WADC Tech Report 53-71 Sept 1953.
5. E. J. Ripling and W. M. Baldwin, Jr., "Rheotropic Embrittlement of Steel," Trans. ASM V. 43 1951.
6. E. J. Ripling and W. M. Baldwin, Jr., "Rheotropic Brittleness: General Behaviors," Proceedings ASTM V. 51 1951.
7. E. J. Ripling, "Rheotropic Embrittlement" Bul ASTM, No. 186, Dec 1952 p. 37 T. P. 179.
8. E. J. Ripling and G. Tuer, "Apparatus for Tensile Testing at Sub-Zero Temperatures", Product Engineering, V. 20, No. 1, 1949, p. 103.
9. Z. Jeffries, "Effect of Temperature, Deformation and Grain Size on the Mechanical Properties of Metals," Trans. AIME, V. 60, 1919.
10. W. P. Sykes, "Effect of Temperature, Deformation, Grain Size and Rate of Loading on Mechanical Properties of Metals," Trans. AIME, V. 64, 1920.
11. L. Seigle and R. M. Brick, "Mechanical Properties of Metals at Low Temperatures: A Survey," Trans. ASM V. 40, 1948.
12. E. R. Parker, "High Temperature Properties of Refractory Metals", Trans. ASM, V. 42, 1950.

- Control*
13. A. S. Kalish and F. J. Dunkerley, "The Low Temperature Properties of Tin and Tin-Lead Alloys", AIME Metals Tech., Sept. 1948, T. P. 2442.
 14. E. J. Ripling, "The Factors Influencing the Ductility and Toughness of Magnesium and Its Alloys", First Phase Report, Frankford Arsenal, Contract No. DA-33-019-ORD-1360, July, 1954.
 15. W. M. Baldwin, Jr., "Private Communication."
 16. F. Rosi, F. Perkins and L. L. Seigle, "Effect of Temperature on Slip and Twinning in Titanium" Minutes on Titanium Symposium on Diffusion and Mechanical Behavior Under the Auspices of the Metallurgical Advisory Committee on Titanium June 9 and 10, 1954.
 17. E. J. Ripling, "Notch Sensitivity of Steels", "Symposium on the Effect of Temperature on the Brittle Behavior of Metals, with Particular Reference to Low Temperatures," ASTM Special Tech. Pub. No. 158, 1953.
 18. H. L. Wain, F. Henderson and S. T. M. Johnstone, "A Study of the Room Temperature Ductility of Chromium", Commonwealth of Australia, Dept. of Supply, Research and Development Branch, A.R.L./MET. 1, 1954.
 19. F. Erdmann-Jesnitzer and W. Hofman, "Some Observations on the Impact Bending Strength and Notch Bar Toughness of Zinc Alloys", Zeitschrift für Metallkunde, V. 35, 1943.
 20. E. J. Ripling, "Notch Sensitivity of Face-Centered Cubic Metals", to be published.
 21. J. T. Brown and W. M. Baldwin, Jr., "Hydrogen Embrittlement of Steel," Trans. AIME, Vol. 200 (1954), p. 294.
 22. C. A. Zapfée and C. E. Sims, "Hydrogen Embrittlement, Internal Stress and Defects in Steel", Trans. AIME, Vol. 145 (1941), p. 225.
 23. N. J. Petch and P. Stables, "Delayed Fracture of Metals Under Static Load", Nature, Vol. 169 (1952), p. 842.
 24. F. De Kazinczy, "Discussion of Reference 21", Trans. AIME, Vol. 200 (1954), p. 1327.

Contrails

25. R. J. Kotfila and E. F. Erbin, "Hydrogen Embrittlement of a Titanium Alloy", Metal Progress, Vol. 66, No. 4 (Oct. 1954), p. 128.
26. G. A. Lenning, C. M. Craighead and R. I. Jaffee, "The Effect of Hydrogen on the Mechanical Properties of Titanium and Titanium Alloys", Third Summary Report to Watertown Arsenal by Battelle Memorial Institute, Contract No. DA-33-019-ORD-938.
27. G. A. Lenning, C. M. Craighead and R. I. Jaffee, "Constitution and Mechanical Properties of Titanium-Hydrogen Alloys", Trans. AIME, Vol. 6, p. 367, Journal of Metals (March, 1954).
28. G. T. Hahn, "Private Communication."